

**National Technical University of
Ukraine
“Igor Sikorsky Kyiv Polytechnic
Institute”**

VERTICAL WIND TURBINE

Thesis Advisor: DMYTRO ZINCHENKO

**BY
BERKAN TURAN**

9.12.2020

Contents

1. OVERVIEW OF STRUCTURES OF WIND GENERATORS	10
1.1 Propeller Type Wind Turbines	11
1.1.1. The Theory Of A Real Windmill	13
1.1.2. An Example Of The Design Of Propeller-Type Generators.....	19
1.2. Wind Turbines With A Vertical Axis.....	22
2. PROJECT PART- AERODYNAMIC DESIGN OF A VERTICAL AXIS TURBINE.....	28
2.1. General Principles	28
2.2. Aerodynamic Design Of The Working Surface Profile Of The Wind Turbine	34
2.2.1. Analysis Of Existing Wing Profiles And Their Characteristics.....	34
2.2.2. Development Of A Profile Of A Working Surface Of The Wind Turbine .	39
2.2.3. Calculation Of Aerodynamic Characteristics Of The Proposed Profile.....	42
2.3. Aerodynamic Design Of The Working Surface Of The Wind Turbine	50
2.3.1. Method Of Calculating The Aerodynamic Characteristics Of The Working Surface Of The Wind Turbine With The Proposed Profile	50
2.3.2. Estimated Model Of The Working Surface Of The Wind Turbine	52
2.3.3. The Results Of The Calculation	55
3. DESIGN PART. DEVELOPMENT OF WINDOW GENERATOR WORKING STRUCTURE	60
3.1. Wind Turbine Torque	60
3.2. Aerodynamic Loads	65
3.3. Analysis Of The Strength Of The Blade Structure.....	74
3.4. Assembly Of The Blade.....	77
4. TECHNOLOGICAL PART	83
4.1. Laser Cutting	83
4.1.2 Principle Of Operation, Structure And Characteristics Of Co2 Laser	88
4.1.3 Interaction Of Laser Radiation With Polymers.....	92
4.2. Bonding Wood.....	101
5. OCCUPATIONAL HEALTH AND SAFETY IN EMERGENCIES.....	112

5.1 Introduction	112
5.2 Safety Of Wind Turbine Operation.	113
5.2.1 Safety During Installation Of The Wind Turbine	113
5.2.2 Measures To Reduce The Level Of Vibration During Operation Of The Wind Turbine	115
5.2.3 Measures To Ensure Electrical Safety During Operation Of The Wind Turbine.....	115
5.2.4 Protection Of The Wind Generator From Lightning Strikes.....	117
5.2.5 Ensuring Fire Safety During Operation Of The Wind Turbine.....	118
5.2.6 Hazards That May Occur Under The Influence Of Meteorological Environmental Conditions	119
5.3. Characteristics Of Air And Meteorological Conditions.....	119
5.3.1 Characteristics Of Air And Meteorological Conditions In The Working Area Of The Project Developer, As A Factor That Determines The Choice Of Methods And Means Of Their Normalization	119
5.3.2 Determining The Category Of Visual Work Of The Computer User, Choosing The Optimal Distance From The Computer To The User's Eyes.....	120
5.4. Conclusion.....	121

Figure 1. Average daily consumption at the entrance to a 108-apartment house with electric stoves.	7
Figure 2 Average electricity consumption for Turkey.	8
Figure 3 Turkey's economic potential is about 50,000 MW of wind power.	8
Figure 4 Wind energy potential on the territory of Turkey.	9
Figure 5 General view, section and structural elements of a typical windmill .	12
Figure 6. Scheme of a propeller-type windmill	13
Figure 7 Scheme of propeller-type windmill forces.	14
Figure 8 Components of wind turbine capacity	16
Figure 9 Appearance of the EuroWind 500 wind turbine.....	19
Figure 10 Dependence of EuroWind 500 wind turbine power on wind speed.	20
Figure 11 Autonomous provision of the object (with batteries). The facility is powered only by the wind turbine	21
Figure 12 Hybrid autonomous system - sun-wind	21
Figure 13 Ancient Persian mill with a wind guide Wall	22
Figure 14 Darrieus rotor wind turbines	23
Figure 15 Savonius wind generator	23
Figure 16 Aerodynamic Forces Affecting the H-Rotor Darrieus Wind Turbine .	24
Figure 17 Vector diagram of the wind turbine.....	25
Figure 18 The scheme of forces of a working surface	29
Figure 19 Experimental dependences of the aerodynamic characteristics of the NACA0012 wing in the process of circular purge.....	30
Figure 20 Experimental dependences of aerodynamic characteristics of wings with different profiles in the process of circular purge.....	32
Figure 21 Influence of viscosity parameter Re on bearing properties of work surface profile	33
Figure 22 Contours of existing profiles.	35
Figure 23 Bearing properties of wing profiles. $M = 0.15$. $Re = 100000$	36
Figure 24 Polar aerodynamic profiles. $M = 0.15$. $Re = 100000$	37
Figure 25 Instantaneous characteristics of aerodynamic profiles. $M = 0.15$. $Re = 100000$	38
Figure 26 Comparison of bearing properties of aerodynamic profiles. $M = 0.15$. $Re = 150000$	39
Figure 27 Ideology of wind generator profile construction.....	40
Figure 28 Characteristic load distribution on the wind turbine profile.	41
Figure 29 Components of the work of pressure forces.....	46
Figure 30 Aerodynamic characteristics of the designed profile	47
Figure 31 Range of settlement cases.	49

Figure 32 Calculation scheme of the basic method.	52
Figure 33 Calculated model of the work surface	53
Figure 34 General view of the work surface.	54
Figure 35 Typical cross section of the work surface.....	55
Figure 36 Dependence of the coefficient of aerodynamic force on the angle of attack	56
Figure 37 Dependence of the relative position of the center of application of aerodynamic force on the value of the coefficient of aerodynamic force.	57
Figure 38 Vortex veil blade wind turbine. Critical angle of attack.....	57
Figure 39 Aerodynamic characteristics of the blade with circular blast.....	58
Figure 40 Determining the angle of installation of the working blade of the wind turbine.....	61
Figure 41 Calculation scheme for determining the angle of installation of the working blade of the wind turbine.	61
Figure 42 Calculation scheme for determining the total torque of the wind turbine blades.	62
Figure 43 Dependence of the torque of the wind turbine blade on the angle of rotation.	64
Figure 44 Dependence of the coefficient S_u of the normal component of the aerodynamic load of the blade elements of the wind generator in terms of span. $\alpha = 25, V = 17\text{m} / \text{s}$	66
Figure 45 Dependence of the coefficient C_x of the tangential component of the aerodynamic load of the elements of the wind turbine blades on the scope...	67
Figure 46 Dependence of the bending moment of the aerodynamic load M_x of the wind turbine blade on the scope. $\alpha = 25, V=17\text{m/s}$	70
Figure 47 The dependence of the bending moment of the aerodynamic load M_Y of the wind turbine blade on the scope. $\alpha = 25, V=17\text{m/s}$	71
Figure 48 Dependence of the tangential component of the aerodynamic load Q_X of the wind turbine blade on the scope. $\alpha = 25, V=17\text{m/s}$	71
Figure 49 Distribution of the coefficient of pressure W_{ed} on the chord of the blade. $\alpha = 25, V=17\text{m/s}$	73
Figure 50 The power circuit of the blade	74
Figure 51 Power wooden construction.....	79
Figure 52 Components of a blade design.....	80
Figure 53 General view of the blade.....	81
Figure 54 Laser Machine.....	84
Figure 55 Laser cutting of plastic	85
Figure 56 Pos-materials.....	86

Figure 57 Installation of laser cutting of TRUMATIC LC-3030.....	88
Figure 58 Lower vibrational levels of the ground electronic state of CO ₂ and N ₂ molecules (for simplicity of drawing, rotational levels are not shown here)	89
Figure 59 Schematic representation of a CO ₂ laser with late gas flow	91
Figure 60 Cutting acrylic glass	94
Figure 61 Foamed PVC sheets	95
Figure 62 Scheme of experimental optical-acoustic installation:.....	97
Figure 63 Optical-acoustic diagram	98
Figure 64 Optical-acoustic diagram	98
Figure 65 Scheme of the experimental setup:	99
Figure 66 Determination of the optimal distance from the lens to the sample	100
Figure 67 Dependence of the width of the cut on the speed of the laser for plexiglass and vinyl.....	100
Figure 68 Dependence of the width of the cut on the speed of movement of the laser for carbon fiber	101
Figure 69 The main types of gluing wood	102
Figure 70 Clamps:	109
Figure 71 Pneumatic hose press (vaima)	110
Figure 72 Wind Turbine Work Safety.....	114
Figure 73 Grounding scheme of three-phase network with voltage up to 1000V.....	116
Figure 74 computer user positions	121

INTRODUCTION

The search for additional energy sources with the rapid development of consumer needs of modern civilization is becoming one of the priorities of developers. Access to renewable energy resources can significantly increase the autonomy of the human community. Wind energy has been used by mankind for a long time to solve energy problems - sailing ships, windmills and other means are well known from history.

Thus, the energy needs of the elementary part of society, on average, do not exceed the level of 100... 200 kW per month. The maximum consumer power for a private house does not exceed 5 kW / h. As derived from the statistics shown in Fig.1. daily distribution of electricity consumption for an apartment building according to [1] with electric stoves has clearly defined maximums:

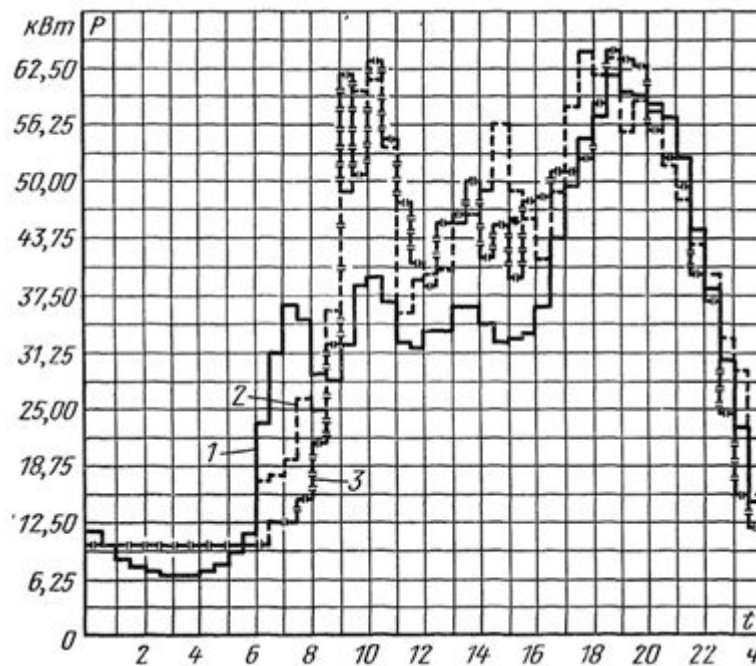


Figure 1. Average daily consumption at the entrance to a 108-apartment house with electric stoves.

1 - working day, 2 - Saturday, 3 – Sunday

The distribution of average relative consumption in% of electricity in Turkey during the day according to [2] is shown in Figure 2. Characteristically, the relative distribution of speed during the day coincides with the graph in Fig.2.

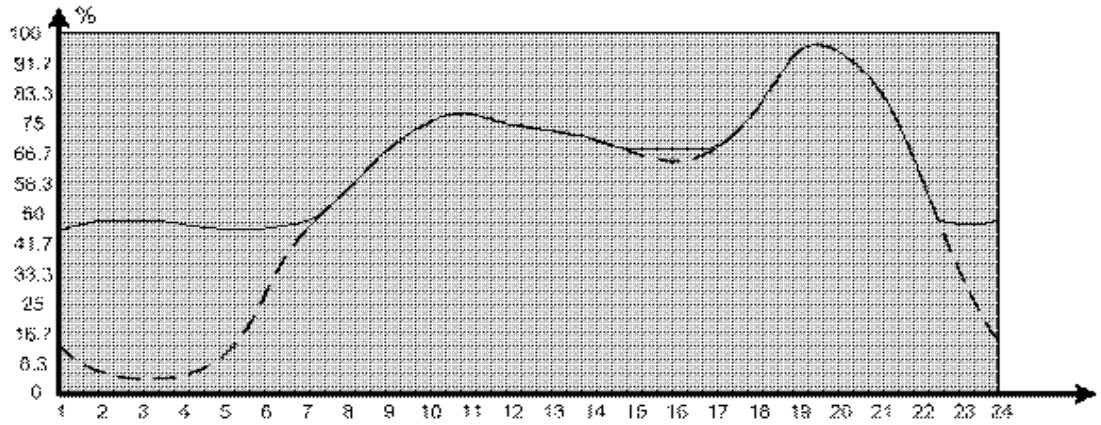


Figure 2 Average electricity consumption for Turkey.

Below, in Figure 3. Locations that use the most wind energy in Turkey.

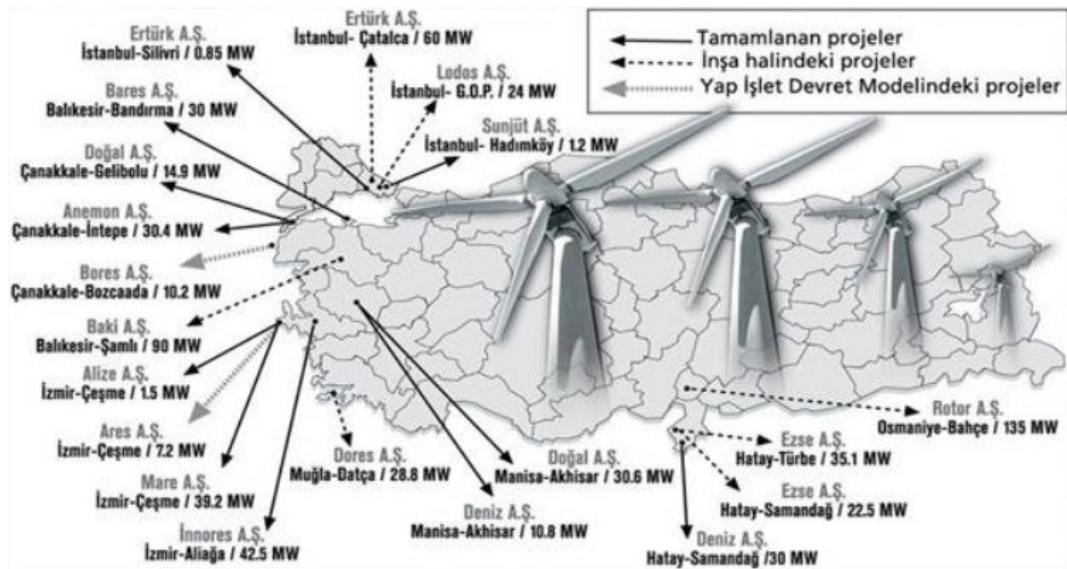


Figure 3 Turkey's economic potential is about 50,000 MW of wind power.

Housing and residential use of autonomous energy not common in Turkey.

Therefore, the usage areas of wind energy are also limited compared to other energy sources. wind energy in Turkey is generally not to meet the energy needs of homes and is used for local needs. For example, energy needs for agriculture in certain regions are met by wind turbines. Water pumps, grain milling systems are often powered by energy from wind turbines. On the other hand, the electrical energy required for operations such as logistics and storage in industrial enterprises is also met by wind power plants. It is generally used in lighting systems in residential and residential areas.

Turkey is used most classical biomass energy and hydraulic energy from renewable sources. Utilizing geothermal energy ranks third, but its use is

limited. While the use of solar energy is low, the use of wind energy is increasing.

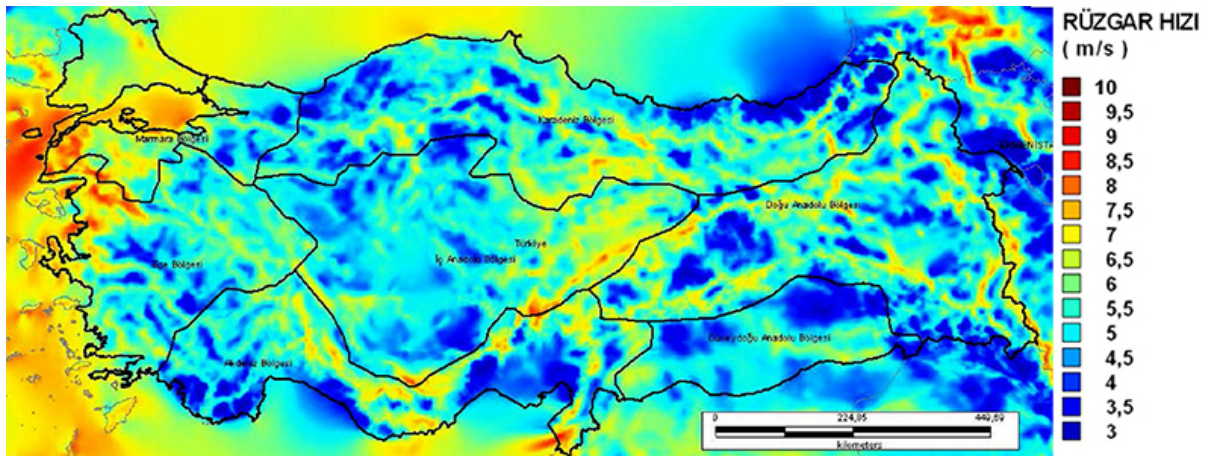


Figure 4 Wind energy potential on the territory of Turkey.

Today, the rapid development of wind energy is caused by the technical simplicity of generator sets, increased efficiency. electric current generators. However, wind turbines of the classical propeller scheme have significant limitations on wind speed - this makes it impossible to produce energy in conditions of its maximum concentration.



To solve this problem, my work proposes a project of a generator created by several vertical wing elements. At the same time, there is almost no restriction in wind speed, and the shape of the wing and the type of profile will allow to use the units of already existing light aircraft to solve this problem.

The paper considers and proposes the use of fixed mechanization of the generator blade, evaluates the feasibility of using a variant of layout with one axis of rotation, and with several.

The basic geometrical parameters of the vortex generator based on a typical consumer power of 2 kW are obtained.

1. OVERVIEW OF STRUCTURES OF WIND GENERATORS

Wind energy is inexhaustible. For centuries, man has tried to use wind energy to maximum advantage. Wind farms are being built that perform various functions: water and oil pumps, power plants. As the practice and experience of many countries have shown, the use of wind energy is extremely profitable. After all, as you know, the wind is free - this is the first time. And, secondly, it is very environmentally friendly, because electricity is obtained from wind energy, and not by burning carbon fuel, the combustion products of which are dangerous to humans.

Wind generator (wind turbine) - a device for converting the kinetic energy of wind into electricity.

Wind turbines can be divided into two categories:

- Industrial
- home (for private use).

Industrial are established by government agencies or large energy companies. As a rule, they are combined into a network. The result is a real power plant. Its main difference from traditional (thermal, nuclear) - the complete absence of raw materials and waste. The only basic requirement is a high average annual wind level. The capacity of modern industrial wind turbines reaches 8 MW.

The task of a rotary wind power plant is to convert the energy of the wind flow into electrical energy. The station includes a special mechanical device, an electric current generator, wind turbine and generator control devices (automatic), as well as facilities for their installation and maintenance. For efficient operation, everything in the wind farm must be high quality and reliable - engine, generator, blades, mast, mast fasteners, inverter, controller, battery.

WPP is a complex of technical devices used to convert the kinetic energy of the wind flow into mechanical energy of the generator rotor rotation. A wind power plant consists of one or more wind power plants, a storage or backup

device and systems for automatic control and regulation of wind turbine operating modes.

The kinetic energy of wind is converted into mechanical energy by a mechanical device, after which the electric generator converts it into electrical energy.

The wind is characterized by the following indicators:

- Average monthly and average annual speed (in accordance with gradations in size and external characteristics on the Beaufort scale)
- Maximum speed in a rush (a very important indicator of the stability of the wind farm)
- the direction of the winds ("wind rose", the frequency of changing directions and wind strength)
- Turbulence (internal structure of the air flow, creates velocity gradients in the horizontal and vertical plane);
- Gusty (change in wind speed per unit of time);
- The density of the wind flow (depends on atmospheric pressure, temperature and humidity).

1.1 Propeller Type Wind Turbines

Undoubtedly, one of the oldest models of propeller-type wind energy generators is a well-known windmill in the world. Appearance and structural components are shown below in Fig.5.:

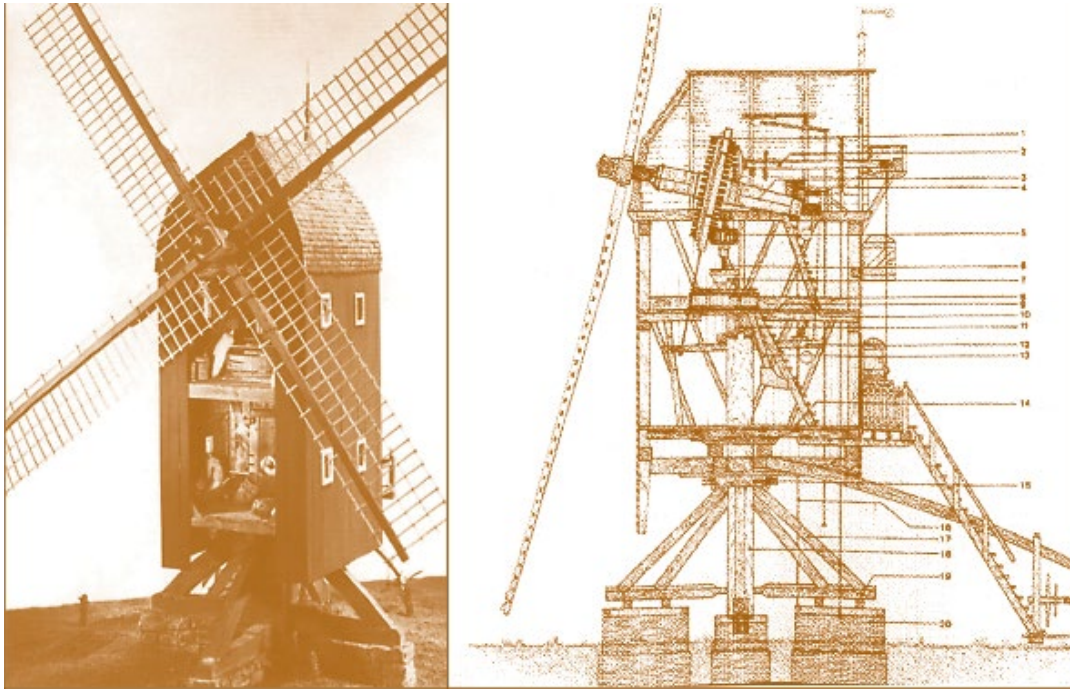


Figure 5 General view, section and structural elements of a typical windmill

Types of sailing wings: a - the most ancient type with a two-sided wing (about 1600): 1 - wedges; 2 - cut end; 3 - max; b - the traditional form of the old Danish type (one support ledge is brought forward): 1 - the canvas of the sail, which is removed; 2 - support shelf; 3 - leading edge; 4 - end bar; 5 - longitudinal ties; 6 - rail; c - a wing with louvers and an air brake: 1 - louvers; 2 - brake louvers d - a wing with louvers and a shield: 1 - louvers; 2 - shield

To date, the appearance of models of propeller-type wind energy generators has changed significantly, but the physical foundations of its functioning remain. At the heart of this is a propeller, autorotue under the action of the incoming air. To determine the features of this type of generator, consider the basic principles of its theory.

1.1.1. The Theory Of A Real Windmill

Select from the blades of the windmill two concentric circles with radii r and $r + dr$ annular surface $dF = 2nrdr$. This ring on the wings will cut segments of length dr , which are called elementary blades

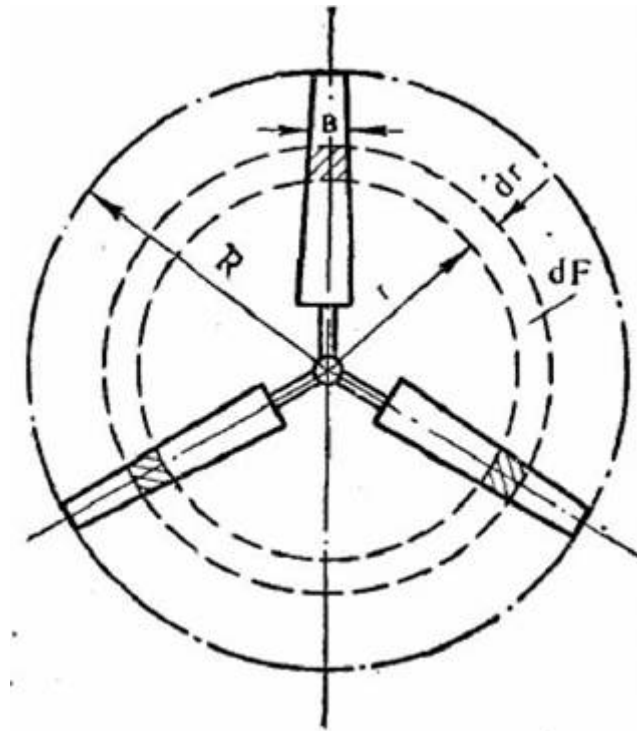


Figure 6. Scheme of a propeller-type windmill

The first connection equation:

$$W = \sqrt{V_1^2 + (-\omega r - u_1)^2}, \quad (1.1)$$

where:

Y is the lifting force of the wing, directed perpendicular to the flow;

X is the force of resistance of the wing (frontal resistance of the wing), directed downstream;

β is the angle between the plane of rotation of the windmill and the direction of air flow reaching the wing;

i- - the number of blades of the windmill.

Due to the rotation of the windmill in the $x - x$ plane, the air flow hits the windmill not with wind speed V , but with relative speed W , consisting geometrically of wind speed V and circumferential speed south, where y is the angular velocity and r is the distance of the blade element from the axis. wind wheel rotation.

The flow velocity incident on the element of the blade, in relative motion is equal to:

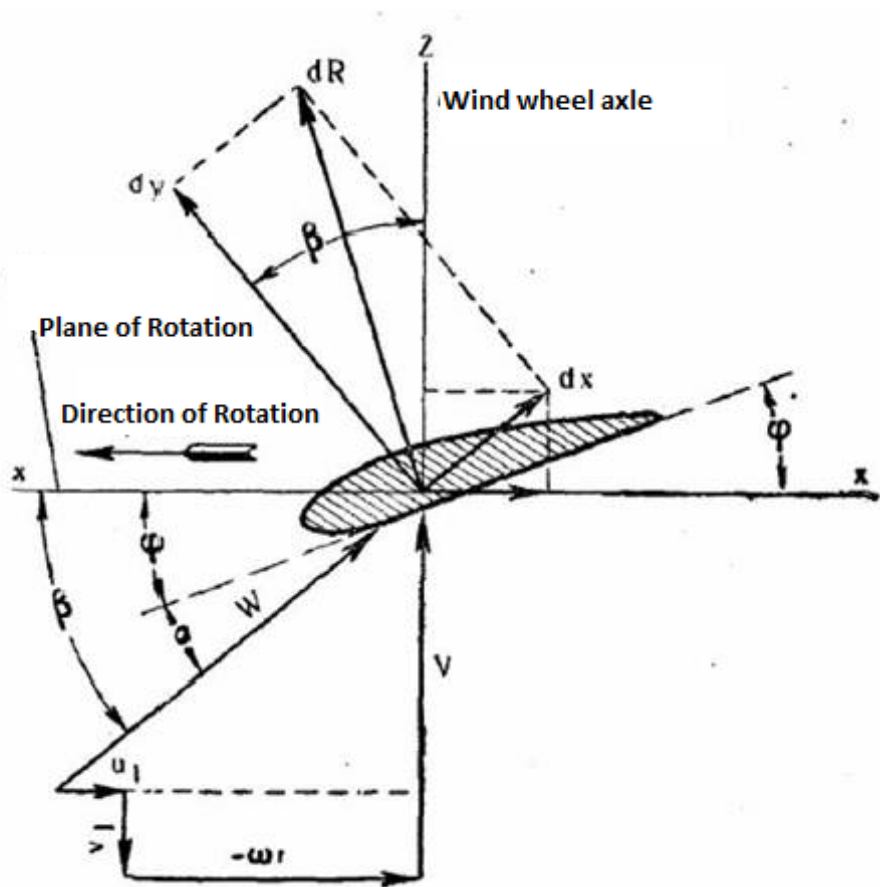


Figure 7 Scheme of propeller-type windmill forces.

where: $V = V - v$ - wind speed in the plane of the windmill

The speed ω is formed as a reaction from the torque developed by the blades. This speed has the opposite direction of the moment; its value is taken as the average for the entire zone in which the blades operate. In fact, this speed in front of the wind wheel is zero and immediately behind the mill is equal to ω .

Because the law of variation of this speed is unknown, then, as a first approximation, it is taken equal to:

Hi and 1 are the final expression for the first constraint equation:

$$ibC_y = 8\pi \frac{e}{(1+e)(1+e)^2} \frac{1}{(z_u + \mu)\sqrt{1+z_u^2}} \quad (1.2)$$

$$\xi = 4e \frac{1-e}{1+e} \frac{1-\mu z_u}{z_u + \mu} \frac{z}{1-e} \quad (1.3)$$

Z =

$$\frac{C_x}{C_y} = \mu -$$

reverse wing quality

$$\frac{v_1}{V} = e$$

Since the expression $4e(1-e)/(1+e)$ is an ideal wind utilization factor, we can write:

$$\xi = \xi_i \frac{1-\mu z_u}{z_u + \mu} \frac{z}{1-e} = \xi_i \eta, \quad (1.4)$$

$$\eta = \frac{1-\mu z_u}{z_u + \mu} \frac{z}{1-e} \quad (1.5)$$

Called the relative efficiency of an elementary wind turbine. With a large number of modules, you can roughly read (second coupling equation):

The main parameters of wind turbines:

Rated power P_{NOM} [W, kW] - power developed by the wind turbine at the calculated wind speed;

Estimated wind speed V_P [m / s] - see determination of rated power;

Wind turbine diameter D [m]

For exotic types of wind turbines other dimensions, based on which the area of the wind turbine is calculated;

Energy production per month WM [kW • H] - a value that depends on the average wind speed; Average power PSR [kW] - power, with continuous maintenance of which, energy production per month will be equal to the real.

Wind turbine power is equal to: $P_{BЭY} = \eta \cdot P_T$

η : the efficiency of the generator and transmission (usually equal to 0.8 - 0.9);

P_T : Wind turbine power

Turbine power is: $P_T = \xi \cdot P_{II}$

ξ : the coefficient of the vitrification table. It differs fundamentally from efficiency in that the "lost" power, in general, is not a loss, but remains in the flow. According to various theories, the maximum value of the coefficient of the vitrified rim of an ideal device is 0.59 - 0.68. In this case, the flow must completely stop, which already contradicts its presence. The real winding ratio of a well-designed turbine is 0.4-0.55; P_{II} - power of the wind flow passing through the area around the wind turbine.

The flow capacity is calculated by the formula:
$$P_{II} = \frac{\rho \cdot V^3}{2} S$$

ρ : Air density (standard value 1.225 kg / m³);

V - Speed of undisturbed wind flow;

$S = \pi \cdot D^2 / 4$ - Streamlined area;

These dependences are enough to match such parameters of wind turbines as rated power, diameter and estimated wind speed. But no less important are the expected energy production and average power of the wind turbine. These

values can be calculated quite accurately, knowing the diagram of the distribution of wind speeds for the period of interest. To compare different wind turbines with each other, you can do with a less accurate theoretical calculation.

When calculating the monthly energy production, the following assumptions are made: - wind power at a wind speed below the estimated cube of the wind speed:

$$P = P_{HOM} \cdot (V/V_P)^3;$$

- power of the wind turbine at a wind speed above the design value is equal to the nominal (limited by the control system or generator power);

- the distribution of wind speeds over time obeys Gauss's law

$$p = A \cdot e^{-\pi \cdot A^2 (V - V_0)^2}$$

V_0 - average wind speed;

A - parameter depending on V_0 . The table shows the A values determined by M. M. Pomortsev on the basis of statistical data.

$V_0, \text{ m/c}$	3	4	5	6
A	0.228	0.185	0.165	0.15

Thus, the average power of the wind turbine, depending on its design speed and average wind speed will be:

$$P_{CP} = \int_0^{\infty} P_{HOM} \left(\frac{V}{V_P} \right)^3 A \cdot e^{-\pi \cdot A^2 (V - V_0)^2} dV \quad (1.9)$$

1.1.2. An Example Of The Design Of Propeller-Type Generators

The EuroWind 500 wind generator is shown in fig.9

Generator performance: 0-700 watts

Initial wind speed: 2 m / s

Nominal wind speed: 9 m / s

Total weight of the wind generator: 134 kg



Figure 9 Appearance of the EuroWind 500 wind turbine

This wind turbine is perfect for a classic Ukrainian country house, where the owners are not often. It provides alarm, lighting, charging for mobile phones, laptops, players, and other portable devices.

The EuroWind 500 wind turbine is ideal for autonomous maintenance of field pumps, autonomous refrigeration systems, street lighting lamps, surveillance cameras and other single energy-dependent systems.

Wind turbine performance:

Monthly energy production is 120 kW per month at an average wind speed of 6 m / s

Generator performance 0-700 watts

Voltage of the wind generator is 24 Volts

Maximum current 30 Amps

Recommended batteries 2 pcs. 12V 200Ah

Voltage after the inverter 220 Volts 50 Hz

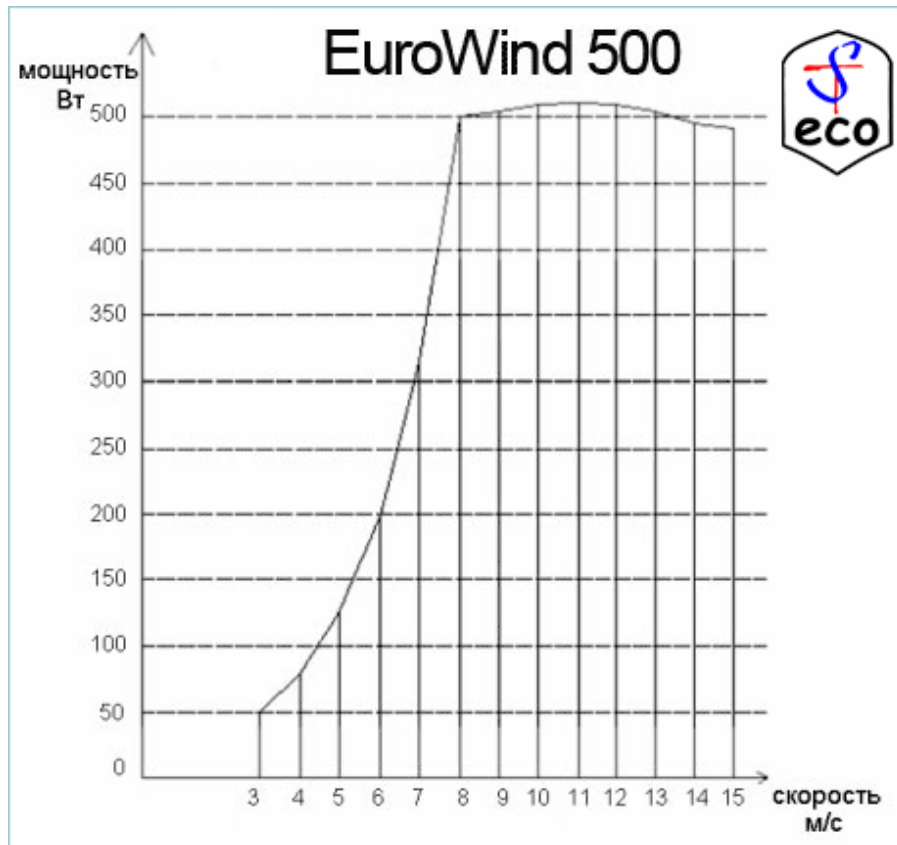


Figure 10 Dependence of EuroWind 500 wind turbine power on wind speed

Characteristics of the wind generator:

Number of blades 3 pcs.

The diameter of the rotor is 2.5 meters

FRP blade material (composite material - fiberglass)

Type of PMG wind turbine (on permanent magnets)

Hurricane wind protection AutoFurl (automatic)

Mast height 6 meters

AIC charge controller (automatic)

Operating temperature from -40 to +60 C

Here are some popular schemes of operation of wind turbine systems with the consumer. These are just some examples, so other schemes of work are possible. In each case, an individual project is developed, which is able to solve the task before us.

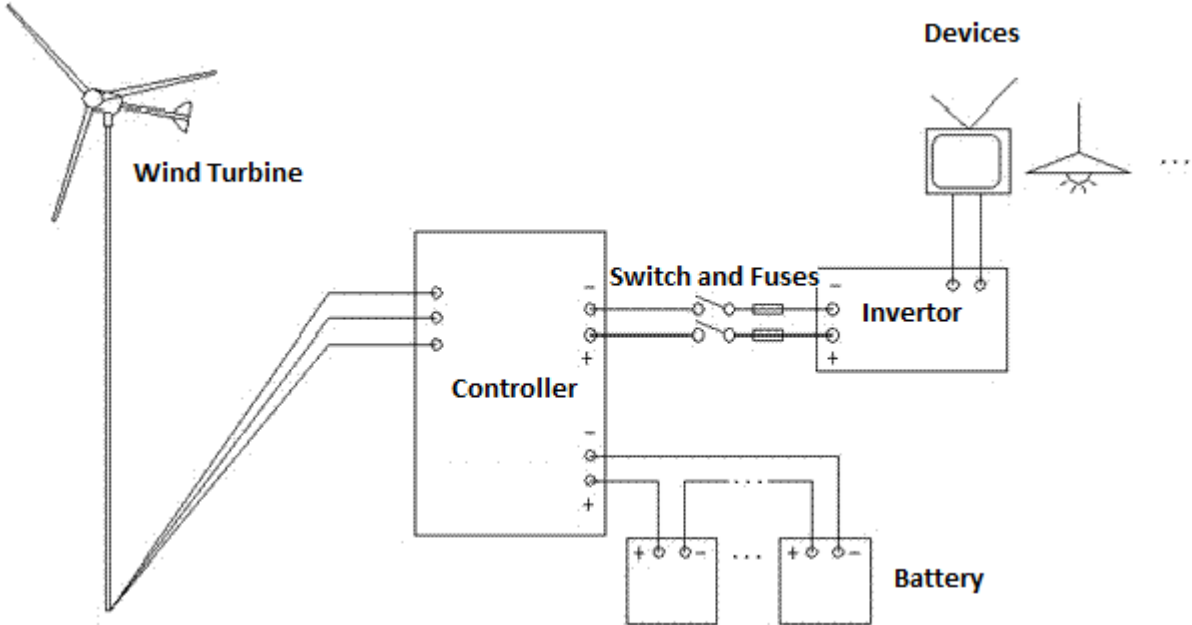


Figure 11 Autonomous provision of the object (with batteries). The facility is powered only by the wind turbine

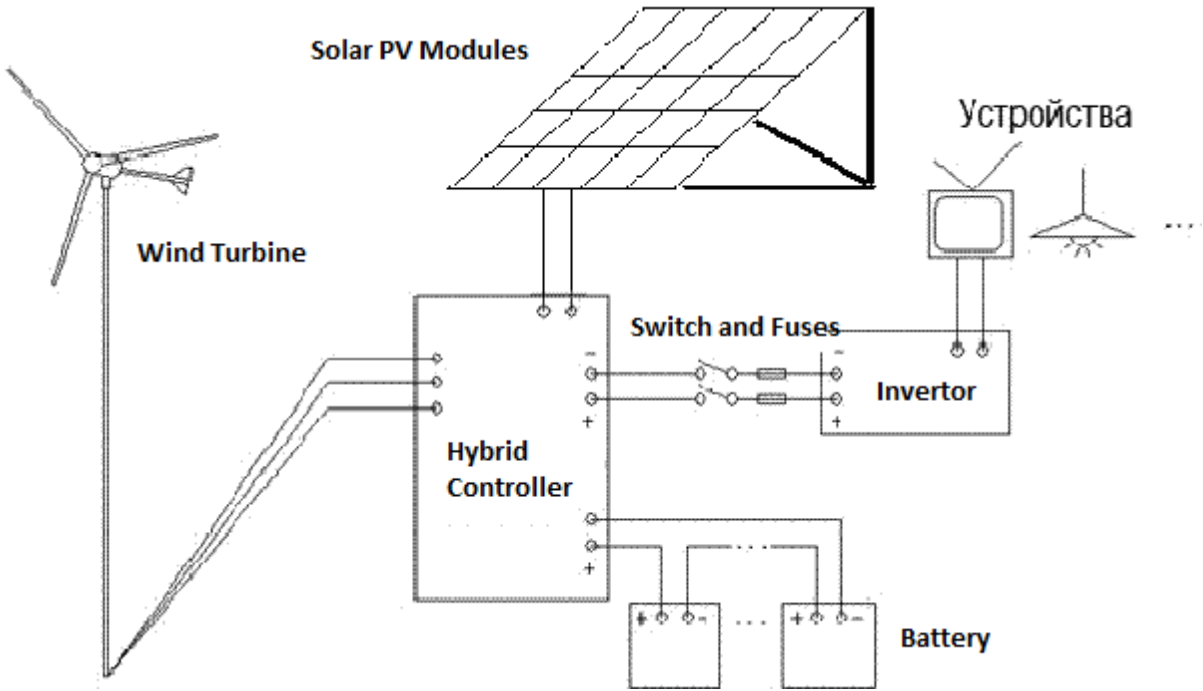


Figure 12 Hybrid autonomous system - sun-wind

1.2. Wind Turbines With A Vertical Axis

Vertical axis wind turbines are also well known in human history. Appearance below in Fig.13. :



Figure 13 Ancient Persian mill with a wind guide Wall

Today, the appearance of models of wind energy generators with a vertical axis has also changed significantly, but the physical foundations of its operation have remained. It is basically an air propeller that rotates under the action of incoming air. To determine the features of this type of generators, consider the basic principles of his theory.

There are two types of wind turbines with a vertical axis of rotation: the Savonius rotor and the Darrieus rotor.

Darrieus rotor wind turbines do not require much space, do not require guidance systems (independent of wind direction), are easy to install. The disadvantages include the fact that they have a low coefficient of utilization of wind energy (approximately 0.05 for the classical Darrieus rotor, with a practical coefficient of 0.45-0.47 for classical horizontal-axial windmills with a theoretical maximum of 0.593), poor self-starting (requires pre-acceleration of the rotor), low mechanical strength, more noise during operation.

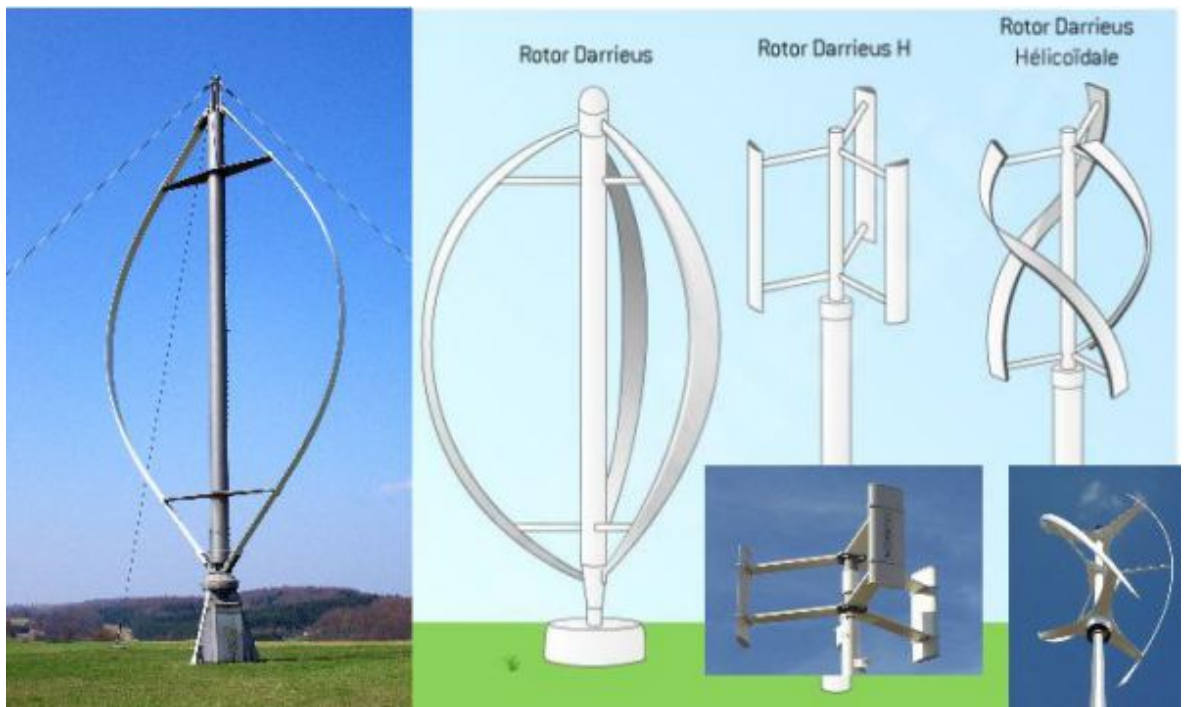


Figure 14 Darrieus rotor wind turbines

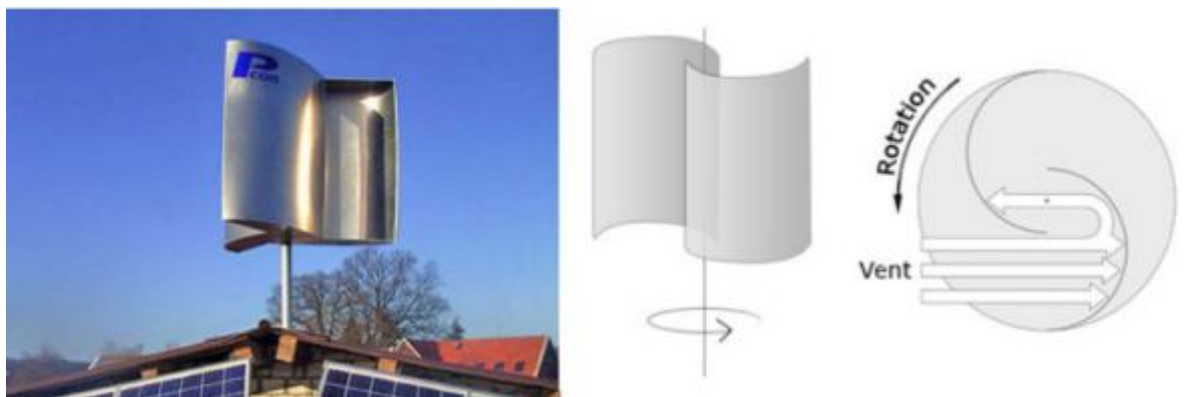


Figure 15 Savonius wind generator

The Savonius wind generator also has a low utilization factor of wind energy in comparison with usual wind generators, bigger material consumption, but has an advantage in work with winds of any directions.

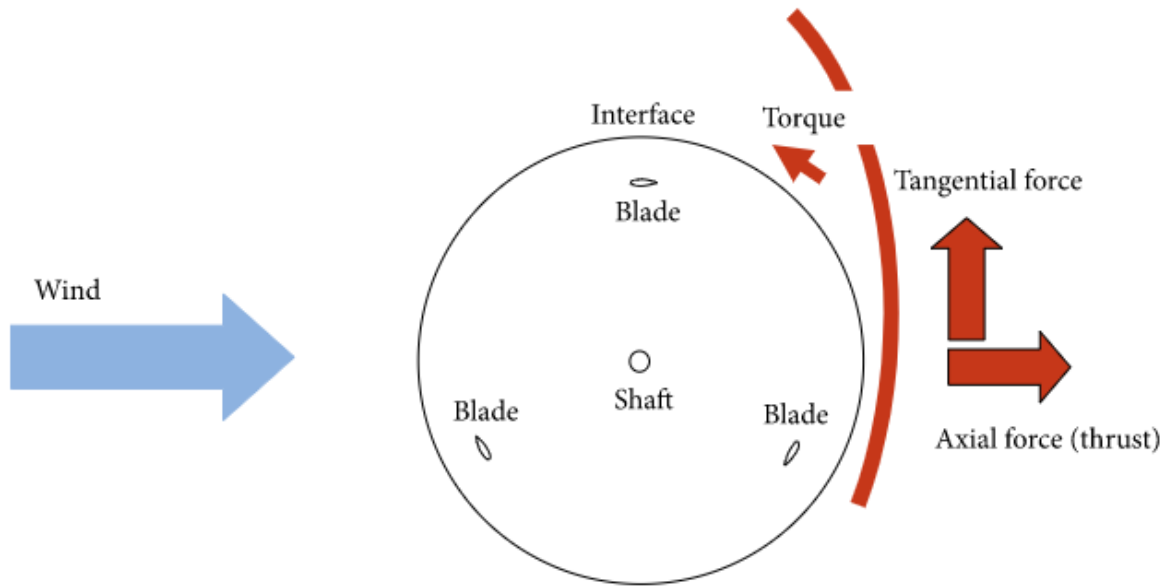


Figure 16 Aerodynamic Forces Affecting the H-Rotor Darrieus Wind Turbine

Systems of equations:

$$\begin{aligned}
 F_{\Sigma 1} &= F_{\max} \sin(\omega t + \alpha_{an} + \varphi_n), \\
 F_{\Sigma 2} &= F_{\max} \sin(\omega t + \alpha_{an} + \varphi_n - 2\pi / 3), \\
 F_{\Sigma 3} &= F_{\max} \sin(\omega t + \alpha_{an} + \varphi_n - 4\pi / 3), \quad (1.10)
 \end{aligned}$$

$$F_{R1} = k_F^R S_n \rho V_e^2 \cos \varphi_{,n}$$

$$\begin{aligned}
 F_{R1} &= F_{\max}^R \sin(\omega t + \varphi_n + \varphi_n), \\
 F_{R2} &= F_{\max}^R \sin(\omega t + \varphi_n + \varphi_n - 2\pi / 3), \\
 F_{R3} &= F_{\max}^R \sin(\omega t + \varphi_n + \varphi_n - 4\pi / 3), \quad (1.11)
 \end{aligned}$$

$$F_{m1} = \frac{F_{R1} \cos \angle(F_m, F_n) - F_{a1}}{\sin \angle(F_m, F_n)}.$$

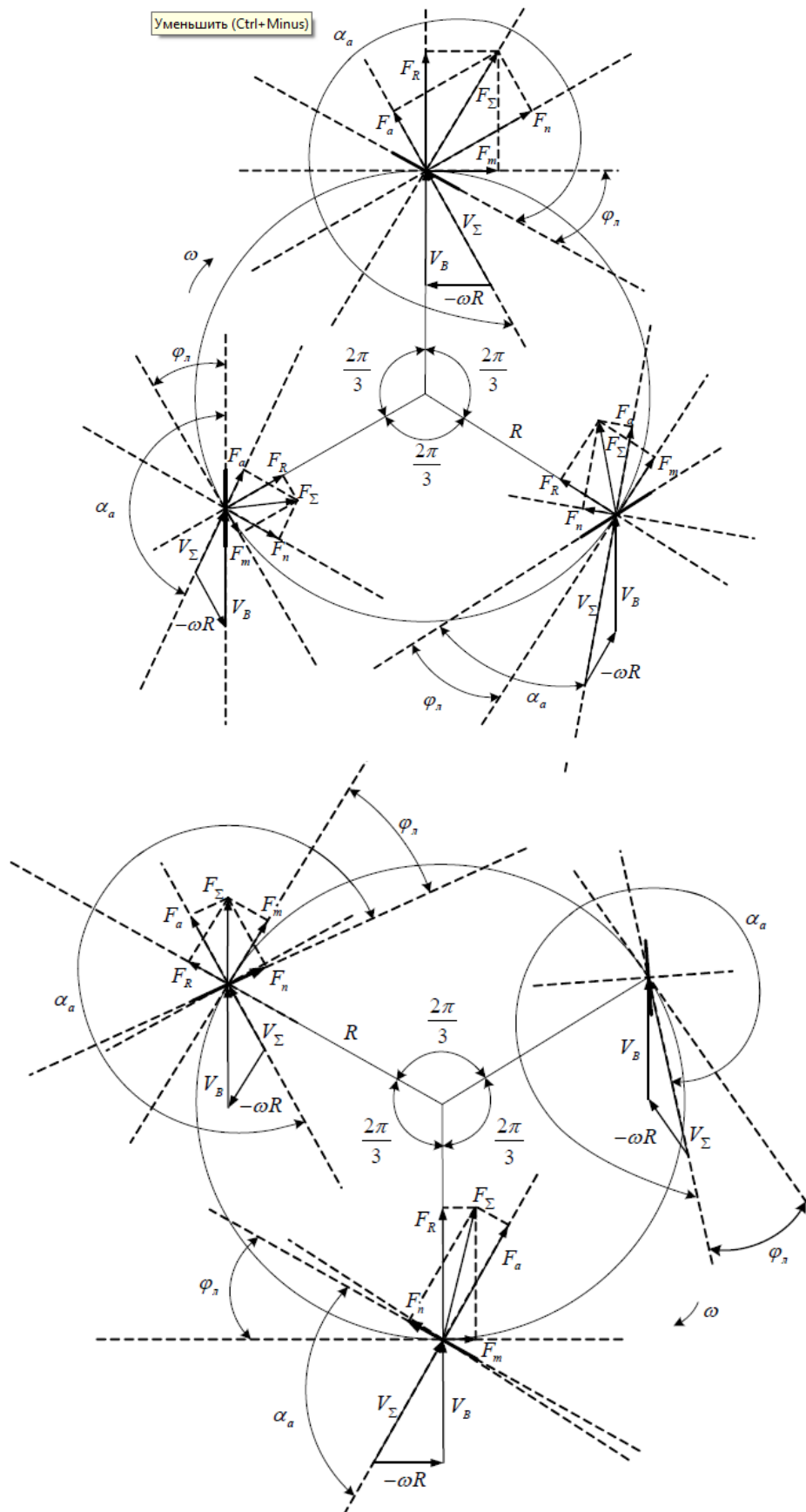


Figure 17 Vector diagram of the wind turbine

$$\begin{aligned}
F_{m1} &= F_{\max}^m \sin(\omega t + \varphi_n + \varphi_n - \pi / 2), \\
F_{m2} &= F_{\max}^m \sin(\omega t + \varphi_n + \varphi_n - \pi / 2 - 2\pi / 3), \\
F_{m3} &= F_{\max}^m \sin(\omega t + \varphi_n + \varphi_n - \pi / 2 - 4\pi / 3).
\end{aligned} \tag{1.12}$$

$$F_{\max}^m = \frac{F_{m1}}{\sin(\varphi_{\text{II}} + \varphi_{\text{I}} - \pi / 2)}, \tag{1.13}$$

Total moment:

$$M_{o\delta}^{\delta} = F_m^{\delta} R = \frac{F_{\max}^m}{\sqrt{2}} R, \tag{1.14}$$

Conclusions on the section:

1. The wind generator as a machine for the transformation of wind energy is an efficient device with a detailed theory;
2. The propeller-type wind turbine has a significant limitation of energy production, determined by the maximum wind speed. This is justified, first of all, by the increase in air velocity along the blade swing, and the manifestation of the aerodynamic phenomenon of compressibility, which begins to manifest itself with a velocity value of 0.7 air velocity.
3. The efficiency of the propeller wind turbine significantly depends on the coincidence of the wind speed direction with the propeller axis. Because in vivo wind usually has the ability to change direction frequently, the issue of tracking the direction of the propeller axis for high-power products is solved by automation. The presence of a lateral component of the speed significantly reduces the efficiency. propeller, and the periodic change of wind direction is a factor of additional oscillations of the wind turbine blade, which reduces the operating range of the wind turbine in terms of wind speed and total life of the device.
4. The wind generator with a vertical axis has no restrictions on aerodynamics in the process of rotation, its maximum speed is limited only by the requirements of structural strength.
5. The wind generator with a vertical axis has no restrictions on the direction of the wind and does not require additional equipment for adjustment, which greatly simplifies and reduces the cost of product design.
6. To solve this problem, the most appropriate way is to develop a wind turbine with a vertical axis of rotation.

2. PROJECT PART- AERODYNAMIC DESIGN OF A VERTICAL AXIS TURBINE

2.1. General Principles

A wind turbine is by definition a machine that converts the kinetic energy of the translational motion of the wind into the kinetic energy of the rotational motion of the armature of the generator.

The kinetic energy of rotational motion according to the laws of theoretical mechanics is defined as:

$$E_k = \frac{1}{2} I_z \omega^2 \quad (2.1)$$

I_z - the moment of inertia of the body relative to the axis of rotation;

ω - the angular velocity of rotation.

The condition for the presence of balanced motion is the absence of angular acceleration ε and the constancy of the value of the angular velocity ω . In this case, the torque M_Z , which is defined as:

$$M_z \frac{d\varphi}{dt} = J_z \omega \frac{d\omega}{dt} \quad (2.2)$$

Will be equal in value to the product of the moment of inertia of the wind turbine and the angular velocity.

Thus, there is a clear connection between the kinetic energy E_K and the external moment of the aerodynamic forces M_Z acting on the working surfaces.

The greater the value of the external moment of the aerodynamic forces M_Z acting on the working surface during rotation, the greater the kinetic energy will be realized.

The moment of aerodynamic forces M_Z acting on the axis of rotation from one working surface of the wind turbine is the product of the value of the aerodynamic force R_a and the arm between the axis of rotation and the center of pressure h_R .

$$M_Z = R_a * h_R \quad (2.3)$$

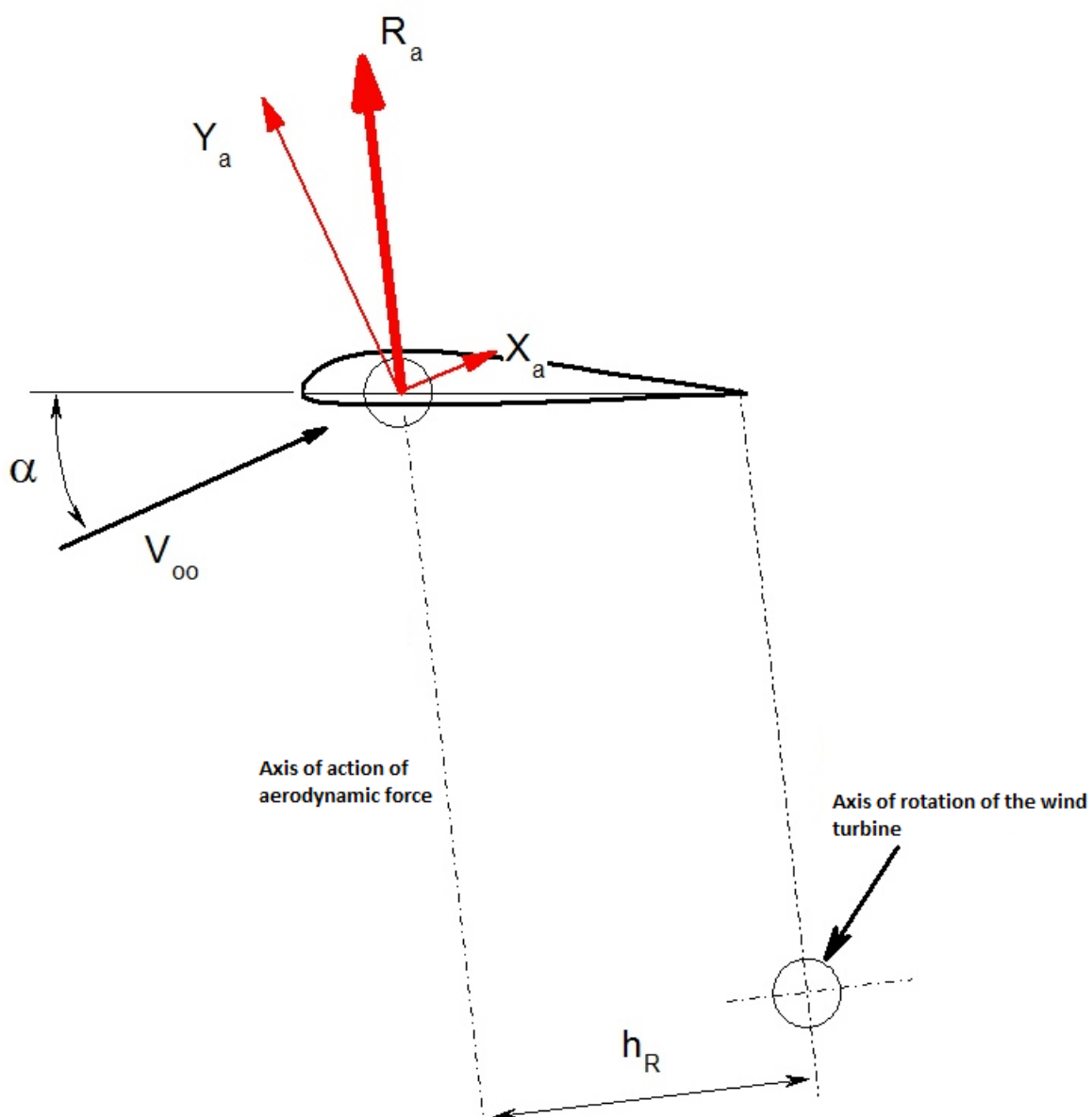


Figure 18 The scheme of forces of a working surface

The total aerodynamic force R_a acting on the working surface of the wind turbine is the aerodynamic force of the wing element and depends on the wind speed V_{∞} and the angle of attack α .

$$R_a = 0.5 * c_{Ra} * \rho * (V_{\infty})^2 * S$$

$c_{Ra} = (c_{Ya}^2 + c_{Xa}^2)^{0.5}$ – the coefficient of total aerodynamic force equal to the vector sum of the coefficients of lifting force c_{Ya} and drag c_{Xa} of the working surface of the wind turbine in the speed coordinate system;

ρ -the density of air;

S - work surface area

The values of the coefficients of lifting force c_{Ya} and frontal resistance c_{Xa} of the working surface of the wind turbine are functions of the angle of attack α , and have a characteristic appearance for classical profiles. In the presence of the implementation of continuous flow aerodynamic profile is able to realize the maximum value of the aerodynamic force Ra_{MAX} , after which there is a separation of air flow from the upper or lower surfaces of the wing.

The typical dependences of the aerodynamic characteristics c_{Ya} and c_{Xa} obtained during the purging of a wing compartment with an aerodynamic profile in the range of angles of attack from 0 to 360 are shown below in Fig. 19.:

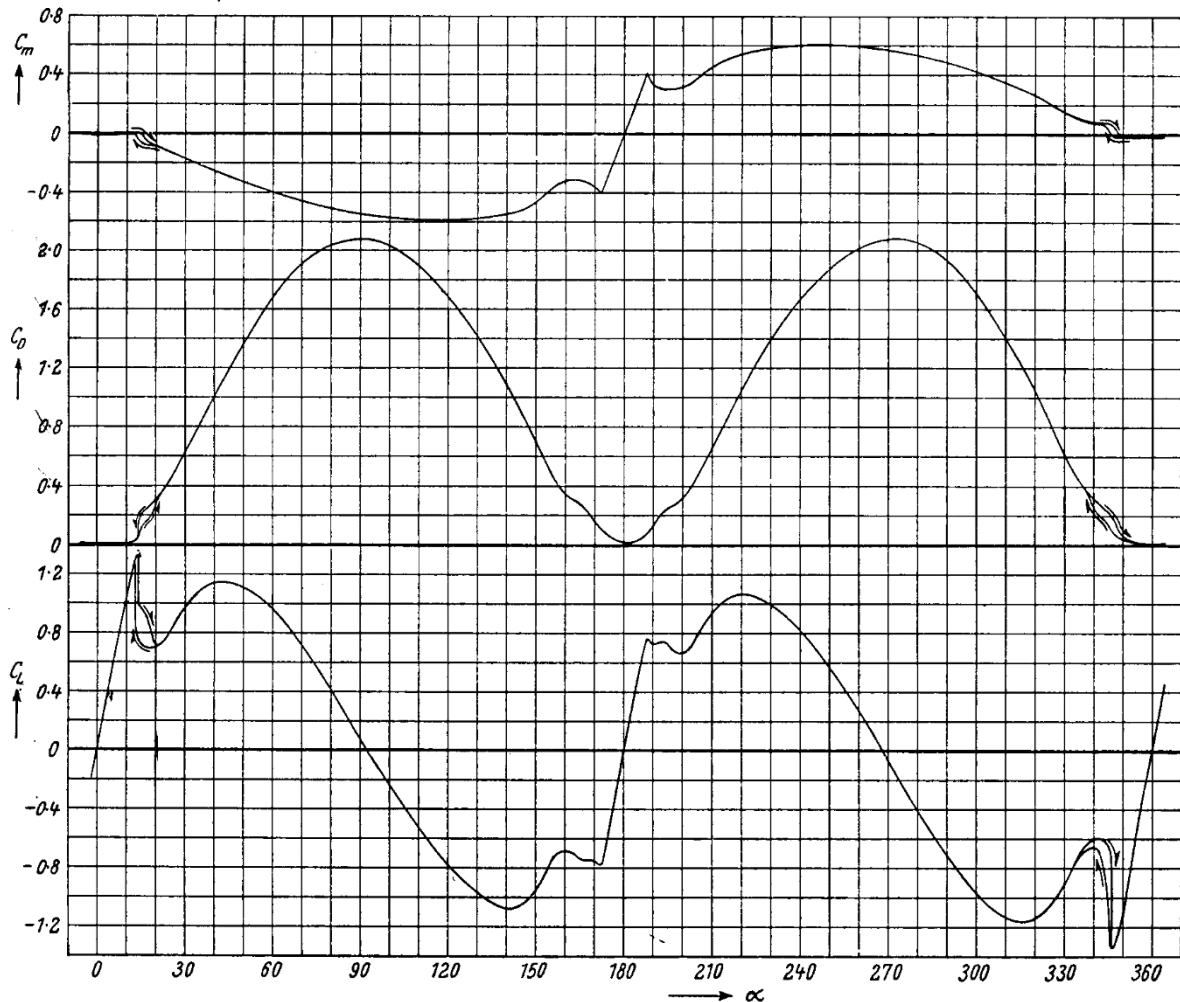


Figure 19 Experimental dependences of the aerodynamic characteristics of the NACA0012 wing in the process of circular purge

From the given graph it is visible that maxima of values of aerodynamic characteristics correspond to possibility of realization of the maximum value of a twisting moment from a working surface of the wind generator.

As derived from the analysis of Fig.18. and additional results of circular purge of the profiles shown in Fig.19, in the range of angles of attack $200 < \alpha < 3200$, corresponding to the detachable flow aerodynamic characteristics are almost the same. This makes it possible to use for aerodynamic calculation of the working surface of the wind turbine these experimental results to determine the torque from the working surface at angles corresponding to the detachable flow.

RAF-34

M-12

Gottingen-429

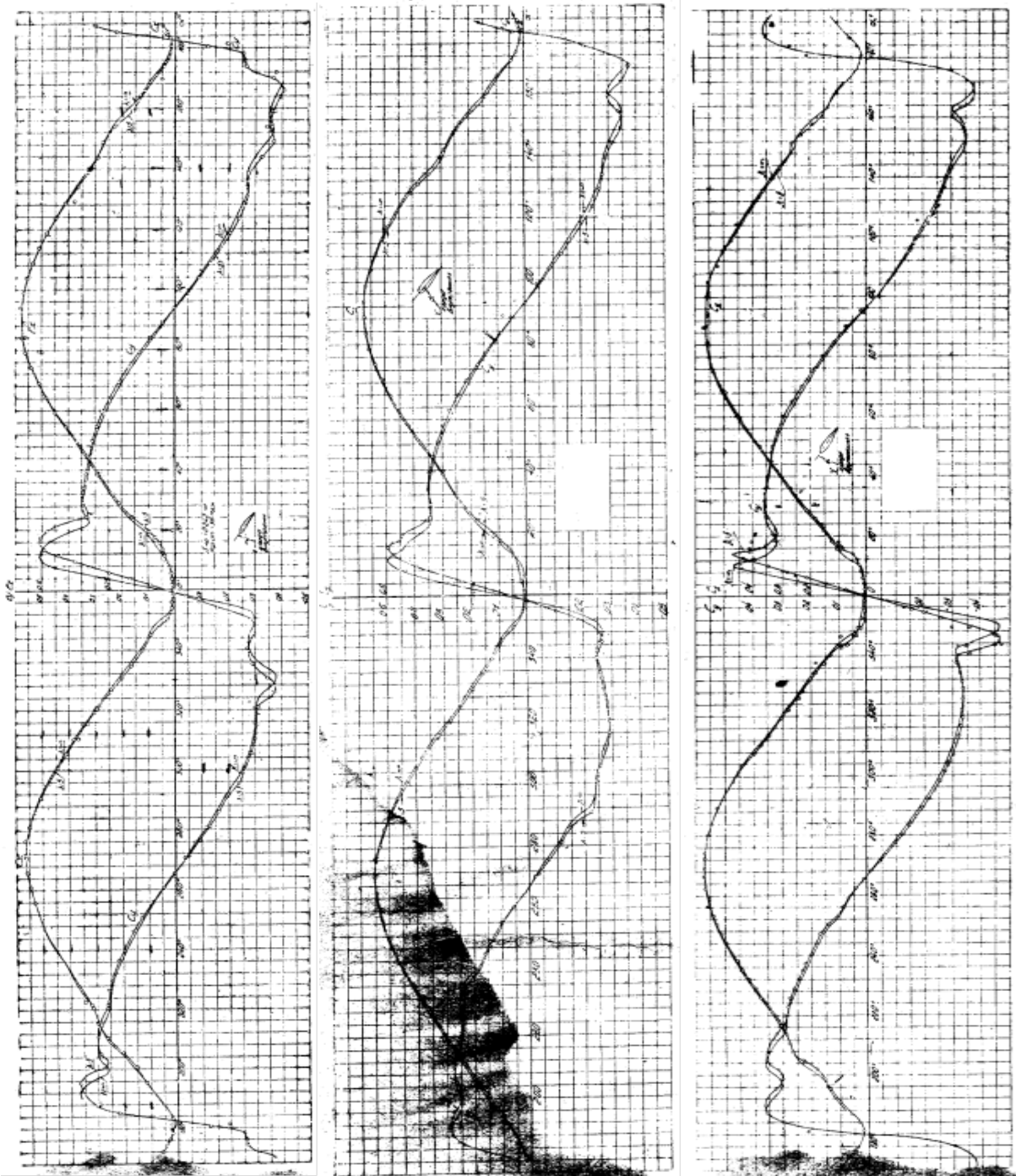


Figure 20 Experimental dependences of aerodynamic characteristics of wings with different profiles in the process of circular purge.

Obviously, it is advisable to consider the factors that affect the value of the components of aerodynamic force. A typical effect of the viscosity parameter Re

on the bearing properties of the profile of the working surface of the wind turbine is shown below in Fig.21:

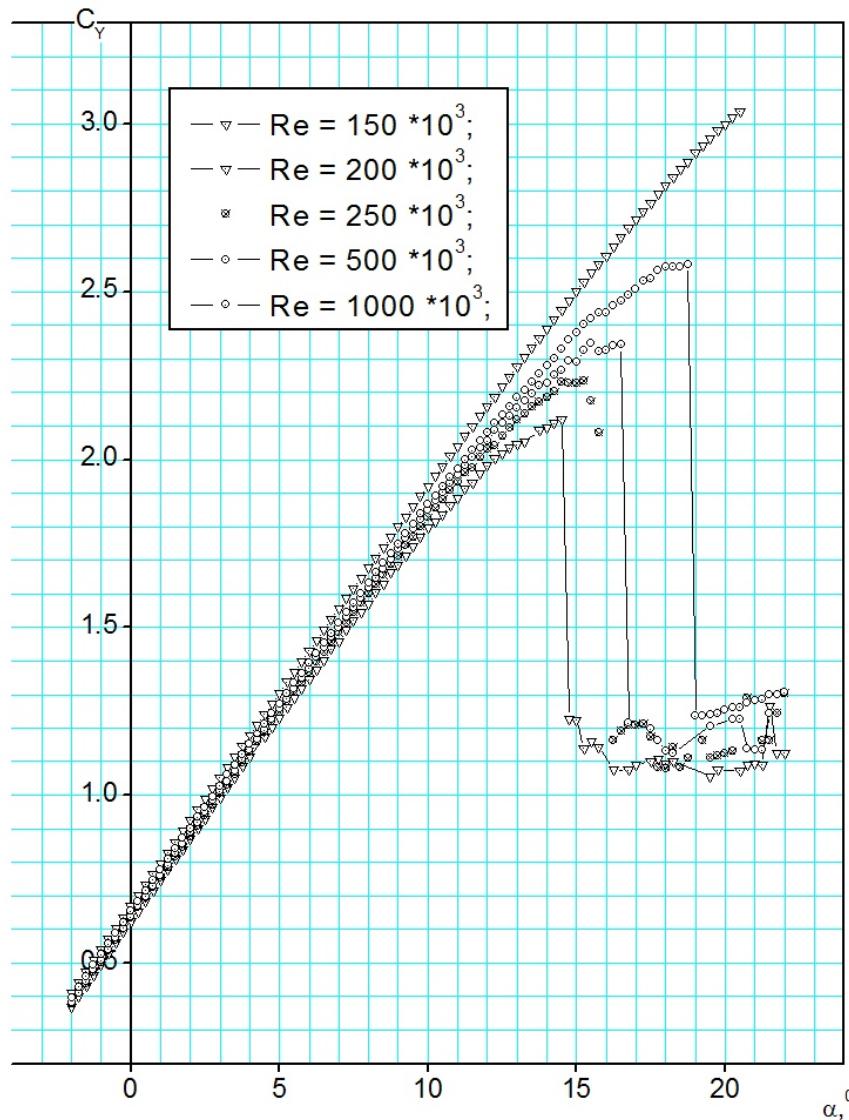


Figure 21 Influence of viscosity parameter Re on bearing properties of work surface profile

The influence of the compression phenomenon can be neglected, because the operating wind speed usually does not exceed 0.1... 0.15 speed of sound.

As derived from the analysis of formulas (2.3), (2.4), the maximum efficiency of the wind turbine and its competitiveness will be achieved provided that the maximum possible load-bearing properties of the working surface at the lowest possible speed and viscosity parameter Re.

$$Re = V_{\infty} * b / \nu \quad (2.5)$$

V_{∞} - the speed of the oncoming flow (wind speed);

b - characteristic size (for a wind turbine - wing chord)

v - the kinematic viscosity of the flow

That is, first of all it is expedient to design such profile of a working surface of the wind generator which would provide from a condition of manufacturability of a design the maximum possible components of aerodynamic force. To solve this problem, we compare the aerodynamic characteristics of different types of aerodynamic profiles when flowing at low speed.

2.2. Aerodynamic Design Of The Working Surface Profile Of The Wind Turbine

2.2.1. Analysis Of Existing Wing Profiles And Their Characteristics

The results of calculating the aerodynamic characteristics of various profiles, incl. and with elements of mechanization. The calculation was carried out according to the method on the software of the Antonov State Enterprise. As follows from the above dependences, the largest values of the components of the aerodynamic force at low wind speeds can be realized on the profile with the slats installed - the value of the maximum value of the lift for this case is 30% higher than in the CLARK Y profile, which is widespread in aircraft modeling. The dependence of the longitudinal moment coefficient C_m on the lift force coefficient C_y , shown in Fig. 2.8, demonstrates the minimum value and constancy of the value of the derivative $C_m^{C_y}$.

As a basic profile for the mechanized wing, a typical symmetrical profile is adopted, which is installed on the stabilization and control bodies of general purpose aircraft.

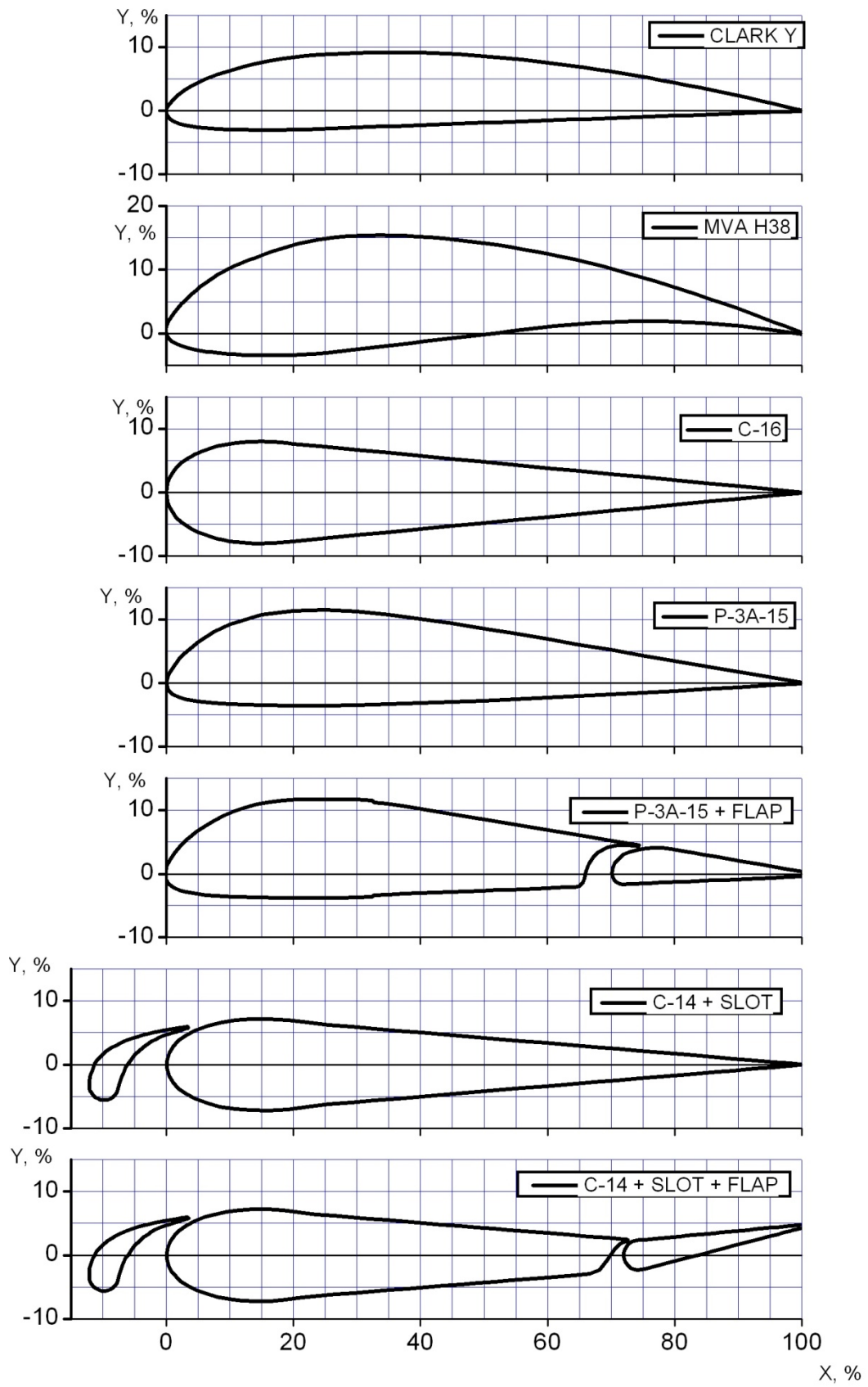


Figure 22 Contours of existing profiles.

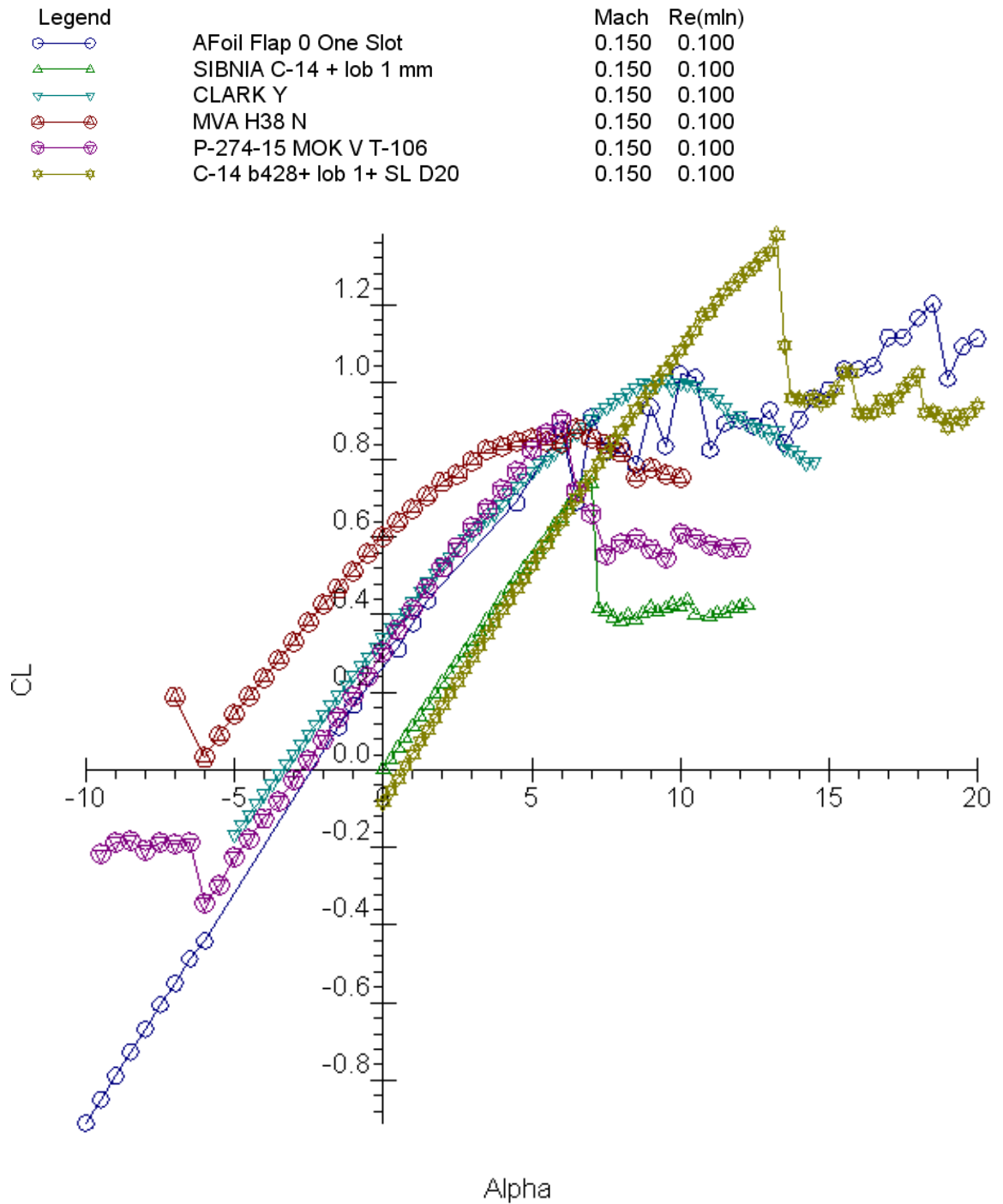


Figure 23 Bearing properties of wing profiles. $M = 0.15$. $Re = 100000$.

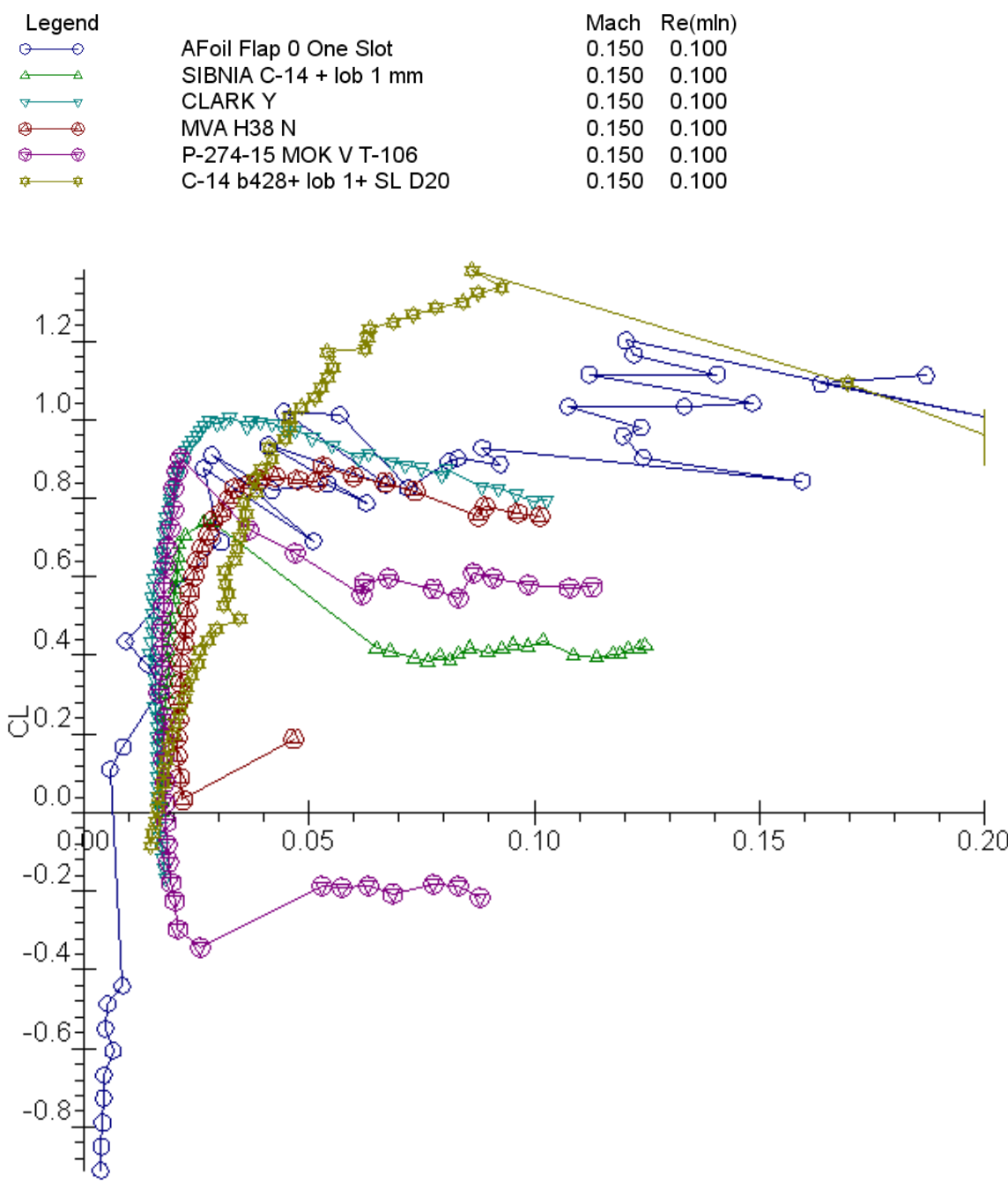








Figure 24 Polar aerodynamic profiles. M = 0.15. Re = 100000.

Legend		Mach	Re(mIn)
	Afoil Flap 0 One Slot	0.150	0.100
	SIBNIA C-14 + lob 1 mm	0.150	0.100
	CLARK Y	0.150	0.100
	MVA H38 N	0.150	0.100
	P-274-15 MOK V T-106	0.150	0.100
	C-14 b428+ lob 1+ SL D20	0.150	0.100

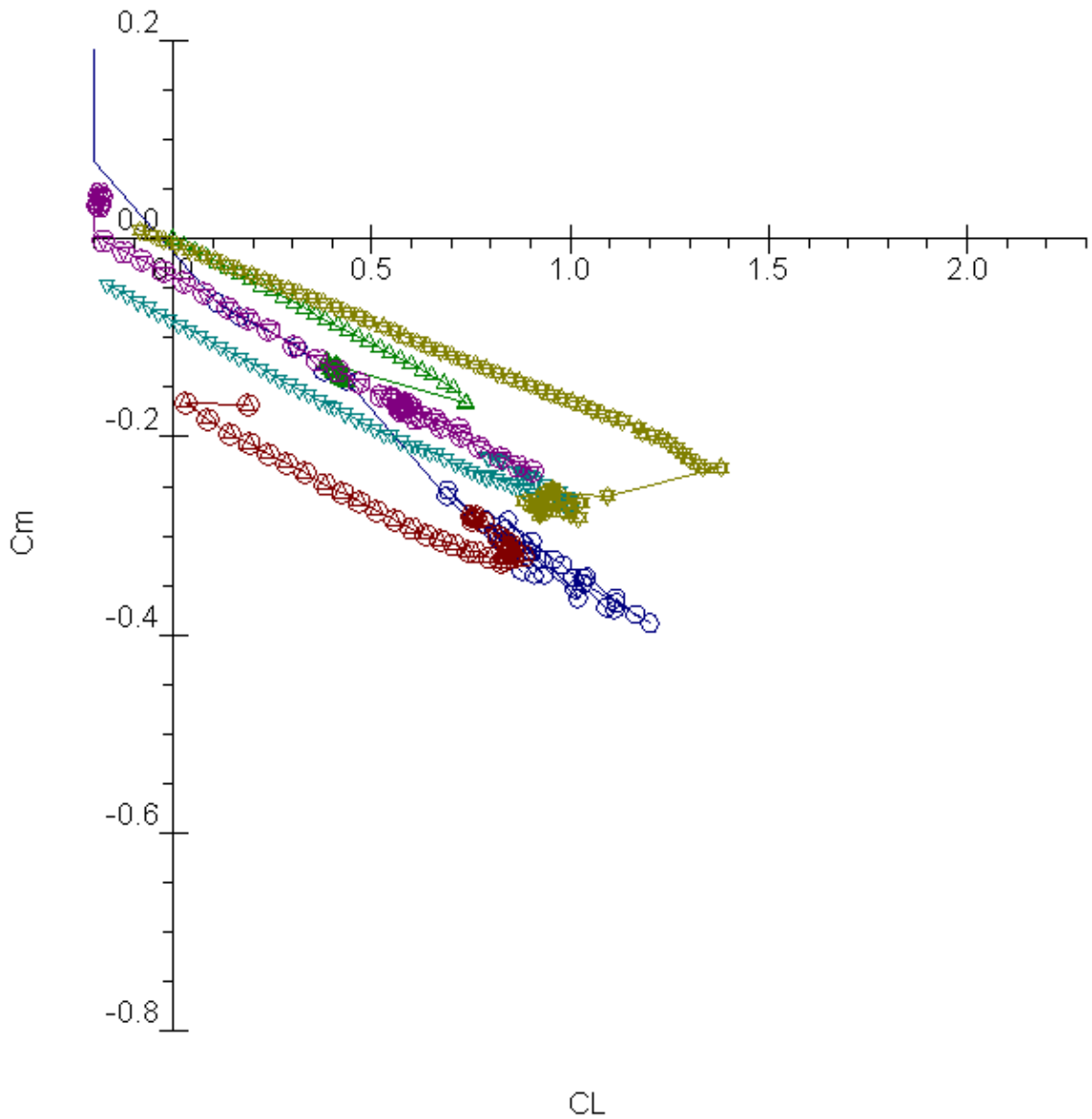


Figure 25 Instantaneous characteristics of aerodynamic profiles. $M = 0.15$. $Re = 100000$.

2.2.2. Development Of A Profile Of A Working Surface Of The Wind Turbine

The ideology of constructing the contour of the profile of the work surface is as follows:

The profile should be mechanized, with the most technological contours, acceptable efficiency of mechanization. In fig. 26 shows a comparison of two contours and bearing properties of mechanized profiles, with mechanized rear or front edge.

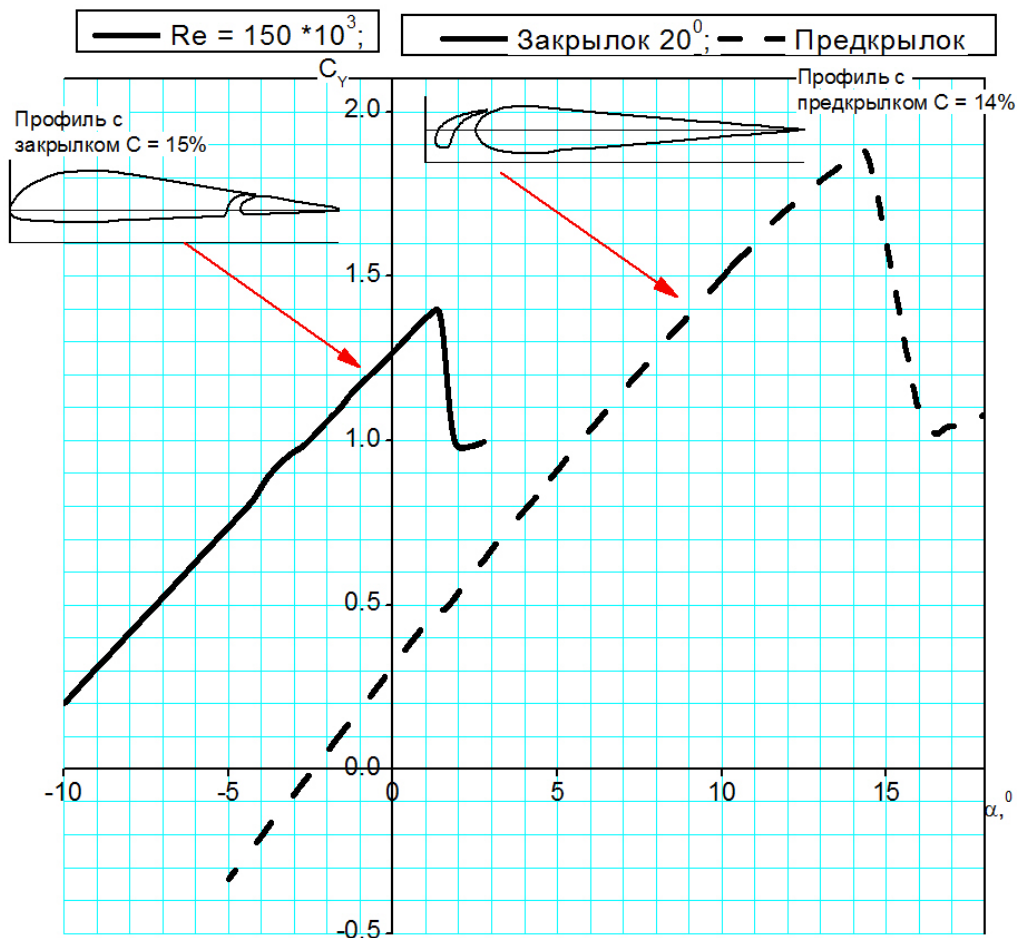


Figure 26 Comparison of bearing properties of aerodynamic profiles. $M = 0.15$.
 $Re = 150000$.

From the above dependences it follows that the profile with a flap is more attractive for further design. The ideology of construction of a profile contour and characteristic distribution of loading on a chord are given in fig. 27-28

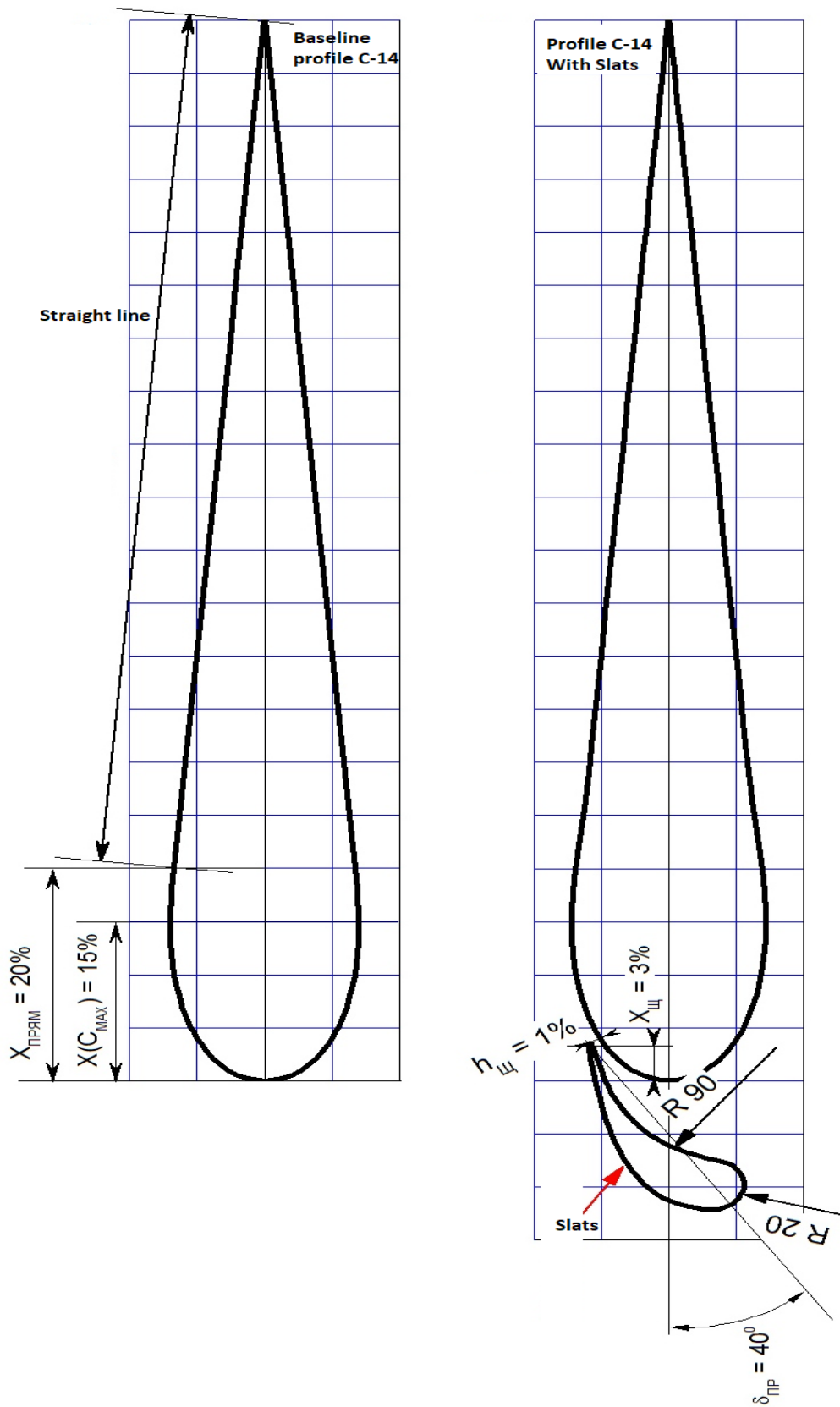


Figure 27 Ideology of wind generator profile construction.

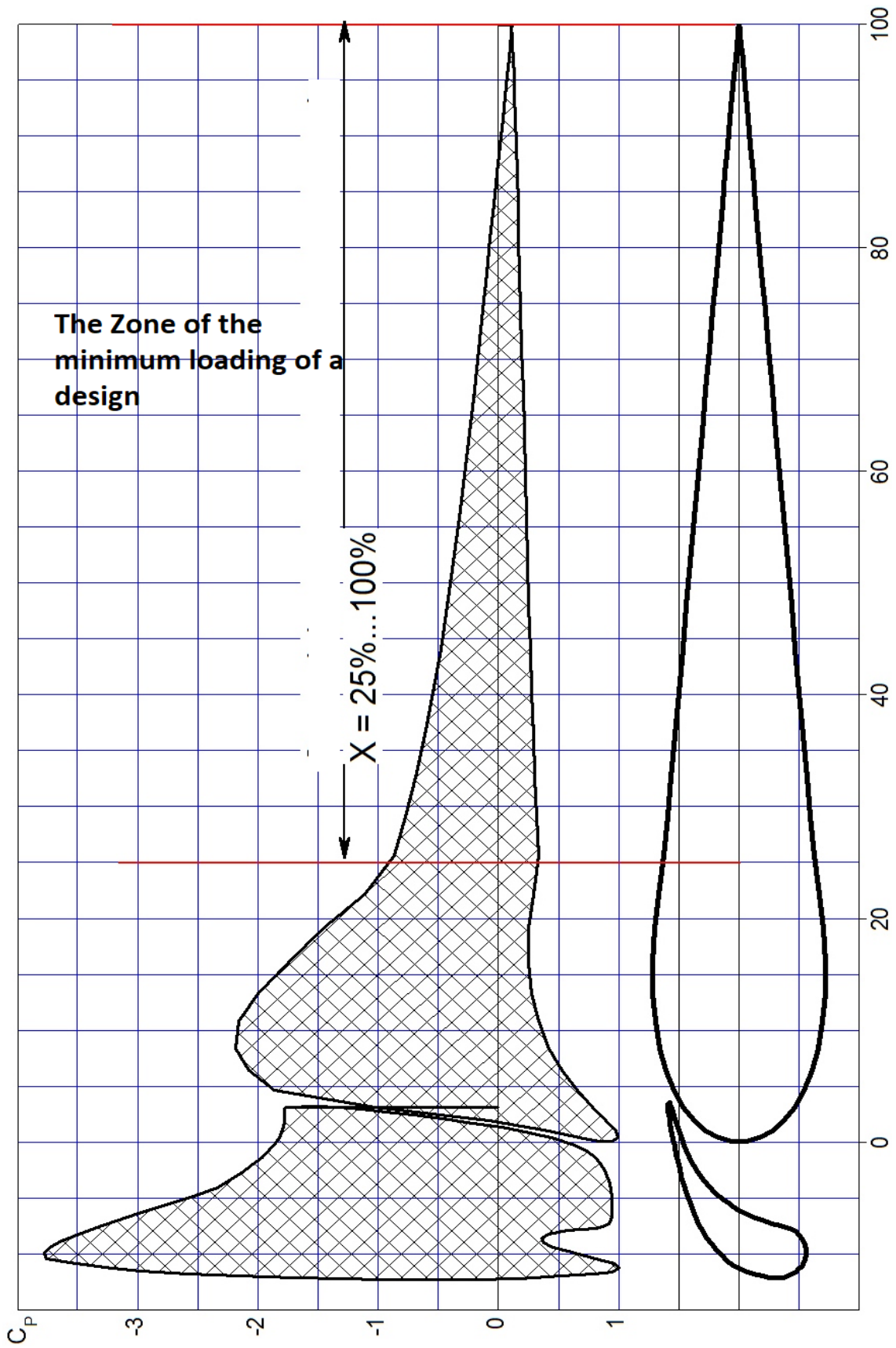


Figure 28 Characteristic load distribution on the wind turbine profile.

2.2.3. Calculation Of Aerodynamic Characteristics Of The Proposed Profile

The method of calculating the characteristics is to solve the equations of the boundary layer on the basis of certain boundary conditions:

The conditions of continuity of static pressure at the boundary of the jet flow and the velocity tangent to the cross-sectional surface are defined as:

$$(P^+ - P^-)_J = 0 \quad (V_{\tau_1} - V_{\tau_2})_a = 0$$

Intensities of sources and vortices on the surface of the active section of the jet:

$$\tilde{q} = 2\tilde{V}_n(1 - \sqrt{\rho_J}) / (1 + \sqrt{\rho_J}) \quad \tilde{\gamma} = 2\tilde{V}_\tau(1 - \sqrt{\rho_J}) / (1 + \sqrt{\rho_J})$$

The intensity of the layer of vortices on the surface of the jet is equal to:

$$\tilde{\gamma}^{(0)} = \tilde{V}_{J\infty} - V_\infty$$

The density of the source layer in the active section is determined by the formula:

$$\tilde{V}_{na}^{(0)} = (\tilde{V}_{J\infty} + V_\infty) / 2$$

The obtained intensity distribution of all hydrodynamic features on the aircraft surface, jet boundaries and active currents determines the velocities at the control points of the jet panels, active sections and vortex trail. New limits of jet flow, a new distribution of hydrodynamic features on the surface and a new shape of the vortex trail are determined by the obtained values and the direction of velocities. The intensities of hydrodynamic features on the surface panels of jets and active currents are determined by the above equations. This iterative process continues until convergence is reached.

The detachable flow around the surface of the aircraft is determined by a system of Navier-Stokes equations, averaged over time for compressing my turbulent flow:

$$\begin{cases} \frac{\partial}{\partial s}(\rho u) + \frac{\partial}{\partial n}[(1 - k_w n)(\rho v)] = 0 \\ \frac{\partial}{\partial s}(\rho u^2) + \frac{\partial}{\partial n}[(1 - k_w n)(\rho uv)] - k_w \rho uv = -\frac{\partial p}{\partial s} + \frac{\partial}{\partial n}[(1 - k_w n)\tau] - \frac{\partial}{\partial s}(\overline{\rho u'^2}) - k_w \overline{\rho u'v'} \\ \frac{\partial}{\partial s}(\rho uv) + \frac{\partial}{\partial n}[(1 - k_w n)(\rho v^2)] + k_w \rho u^2 = -(1 - k_w n) \frac{\partial p}{\partial n} - \frac{\partial}{\partial n}[(1 - k_w n)\rho v'^2] - \frac{\partial}{\partial s}(\overline{\rho u'v'}) - k_w \overline{\rho u'^2} \\ \tau = \mu \frac{\partial u}{\partial n} - \overline{\rho u'v'} \end{cases}$$

(2.6)

s -length of the forming arc; n-normal; k_w - surface curvature; ρ - density;

u, v - tangent and normal components of velocity; p - pressure; μ - viscosity coefficient; u' , v' - pulsation components of velocity.

In the dissertation it is proved that the solution of the problem of flow around the surface by a flow of viscous turbulent gas can be reduced to the solution of the equivalent nonviscous problem, which is determined by the system of Euler equations:

$$\begin{cases} \frac{\partial}{\partial s}(\rho_i u_i) + \frac{\partial}{\partial n}[(1 - k_w n)(\rho_i v_i)] = 0 \\ \frac{\partial}{\partial s}(\rho_i u_i^2) + \frac{\partial}{\partial n}[(1 - k_w n)(\rho_i u_i v_i)] - k_w \rho_i u_i v_i = -\frac{\partial p_i}{\partial s} \\ \frac{\partial}{\partial s}(\rho_i u_i v_i) + \frac{\partial}{\partial n}[(1 - k_w n)(\rho_i v_i^2)] + k_w \rho_i u_i^2 = -(1 - k_w n) \frac{\partial p_i}{\partial n} \end{cases}$$

With the following boundary conditions on the body surface of the flow:

$$\begin{cases} v_{iw} = \frac{1}{\rho_{iw}} \frac{d}{ds}(\rho_{iw} u_{iw} \delta^*) & (a) \\ \frac{d\theta}{ds} + (H + 2 - M^2) \frac{\theta}{u_{iw}} \frac{du_{iw}}{ds} - \frac{1}{2} C_f \approx 0 & (b) \\ u_{iw} - u_w \approx k^* u_{iw} (\theta + \delta^*) & (c) \end{cases}$$

(2.7)

$$\delta^* = \frac{1}{\rho_{iw} u_{iw}^2} \int_0^\delta (\rho_i u_i - \rho u) dn; \quad \theta = \frac{1}{\rho_{iw} u_{iw}^2} \int_0^\delta [\rho u (u_{iw} - u) - \rho_i u_i (u_{iw} - u)] dn; \quad \bar{H} = \frac{\delta^*}{\theta}$$

The solution of this system of equations allows to form the boundary conditions on the surface of the flow body and the vortex trace behind the body, necessary for the solution of the equivalent non-viscous problem and to obtain the solution of the real viscous problem.

Having obtained by the methods described above for solving the problem of flow around the surface of an aircraft, it is necessary to determine the correspondence of the reality of the pressure distribution over the surface obtained by calculation and, as a consequence, the aerodynamic characteristics of the aircraft. The methodology for the computational and experimental evaluation of the aerodynamic characteristics of an aircraft with a powered wing, described in the dissertation work, suggests the use of correction of the

calculation results of the accepted calculation method. The correction parameter suggests a relative function:

$$F_A(x, y, \dots, n) = \frac{Cp^X_{-E}(x)}{Cp^X_{-P}(x)} \quad (2.8)$$

$Cp^X_{-P}(x); Cp^X_{-\varnothing}(x)$ = respectively, the values of the partial derivatives of the diagram of the distributed

pressure obtained by calculation and physical experiment.

$F_A(x, y, \dots, n)$ = correction parameter, function of n parameters of influence - geometry, surface condition, external conditions, etc.

The value of the pressure coefficient using the correction parameter is defined as:

$$Cp_{-H}(x) = Cp^X_{-\varnothing}(x) * F_A(x, y, \dots, n) * x + Cp_{-H}(x = 0)$$

The physical meaning of the correction parameter corresponds to the physical meaning of the distributed pressure derivative. How can the pressure factor be defined as:

$$Cp_i = 1 - \left(\frac{V_i}{V_\infty} \right)^2 = 1 - \frac{a * x}{V_\infty^2} \quad (2.9)$$

V_i, V_∞ - respectively, the flow velocity at a point and at infinity and the square of the velocity is determined by the acceleration $V_i^2 = a * x$ then the value of the derivative of the distributed pressure is proportional to the average acceleration of the fluid fraction during the change in the amount of motion. And the correction parameter is the ratio of the averaged accelerations of the fluid fraction obtained by calculation $a_{cp-P}(x)$ and physical experiment $a_{cp-\varnothing}(x)$

$$Cp_i^x = -\frac{a}{V_\infty^2} \quad F_A(x, y, \dots, n) = \frac{Cp^X_{-\varnothing}(x)}{Cp^X_{-P}(x)} = \frac{a_{cp-\varnothing}(x)}{a_{cp-P}(x)}$$

Considering the balance of energy and work of the gas particle in the adiabatic flow process, we can determine that the sum of the work of friction and pressure forces should be equal to the kinetic energy of the particle:

$$L_{\infty-x} + \left(\frac{Vx^2 - V_\infty^2}{2} \right) + L_{TP\infty-x} = 0 \quad L_{\infty-x} + L_{TP\infty-x} = \int_0^x F_\Sigma(x) ds = \int_0^x F_{\Sigma CP} ds$$

Simultaneously with Newton's first law:

$$F_{\Sigma}(t) = m * a(t) \qquad F_{\Sigma_{cp}}(x) = m * a_{cp}(x)$$

or in the projection in some direction n:

$$F_{\Sigma_{cp_n}}(x) = m * a_{cp_n}(x)$$

Then we can determine that the value of the derivative of the distributed pressure is the result of the consumption of the initial kinetic energy of the gas particle E_{∞} to carry out the work of friction forces and pressure on the trajectory of the particle:

$$-a_{cp}(x) = V_{\infty}^2 * Cp_i^x \quad L_{\infty-x} + L_{TP_{\infty-x}} = -V_{\infty}^2 * Cp_i^x * x$$

$$Cp_i^x = -\frac{L_{\infty-x} + L_{TP_{\infty-x}}}{V_{\infty}^2 * x} = A_{V_{\infty}} * (L_{\infty-x} + L_{TP_{\infty-x}}) = A_{V_{\infty}} * (E_{\infty} - E_x)$$

The pressure coefficient can be defined as the ratio of kinetic energies:

$$Cp_i = 1 - \left(\frac{V_i}{V_{\infty}}\right)^2 = 1 - \frac{E_x}{E_{\infty}} \qquad (2.10)$$

The value of the work of friction forces, obtained in a physical experiment and by calculation, according to scientific sources, satisfactorily coincides with the value obtained by calculation. However, the work of pressure forces in kind depends on a large number of parameters, as shown in Figure 29

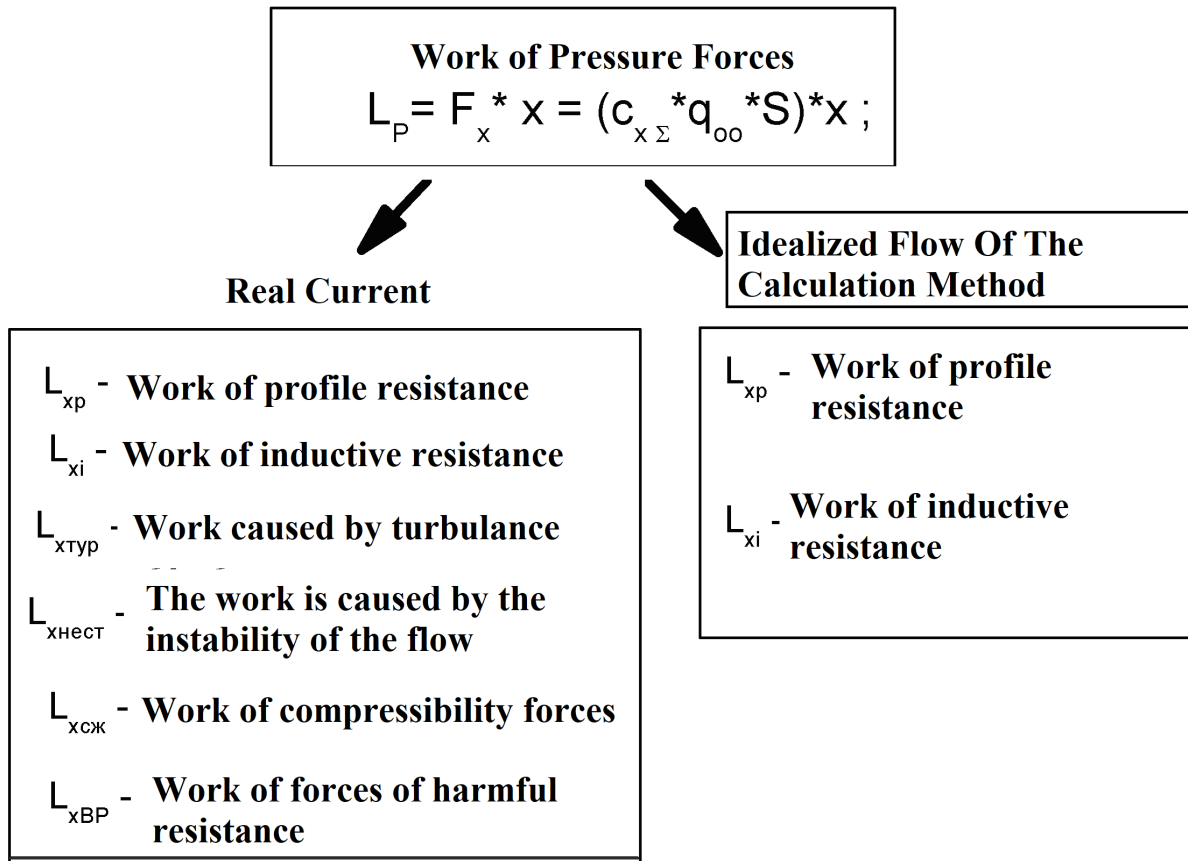


Figure 29 Components of the work of pressure forces.

Qualitative consideration of the influence of many of the factors shown in Fig. 29, the methods of calculated aerodynamics is not possible today. The paper evaluates the coincidence of the values of the total work of the pressure forces acting on the surface of the mechanized wing compartment. The difference between the integrated aerodynamic characteristics obtained by calculation and experiment is obvious.

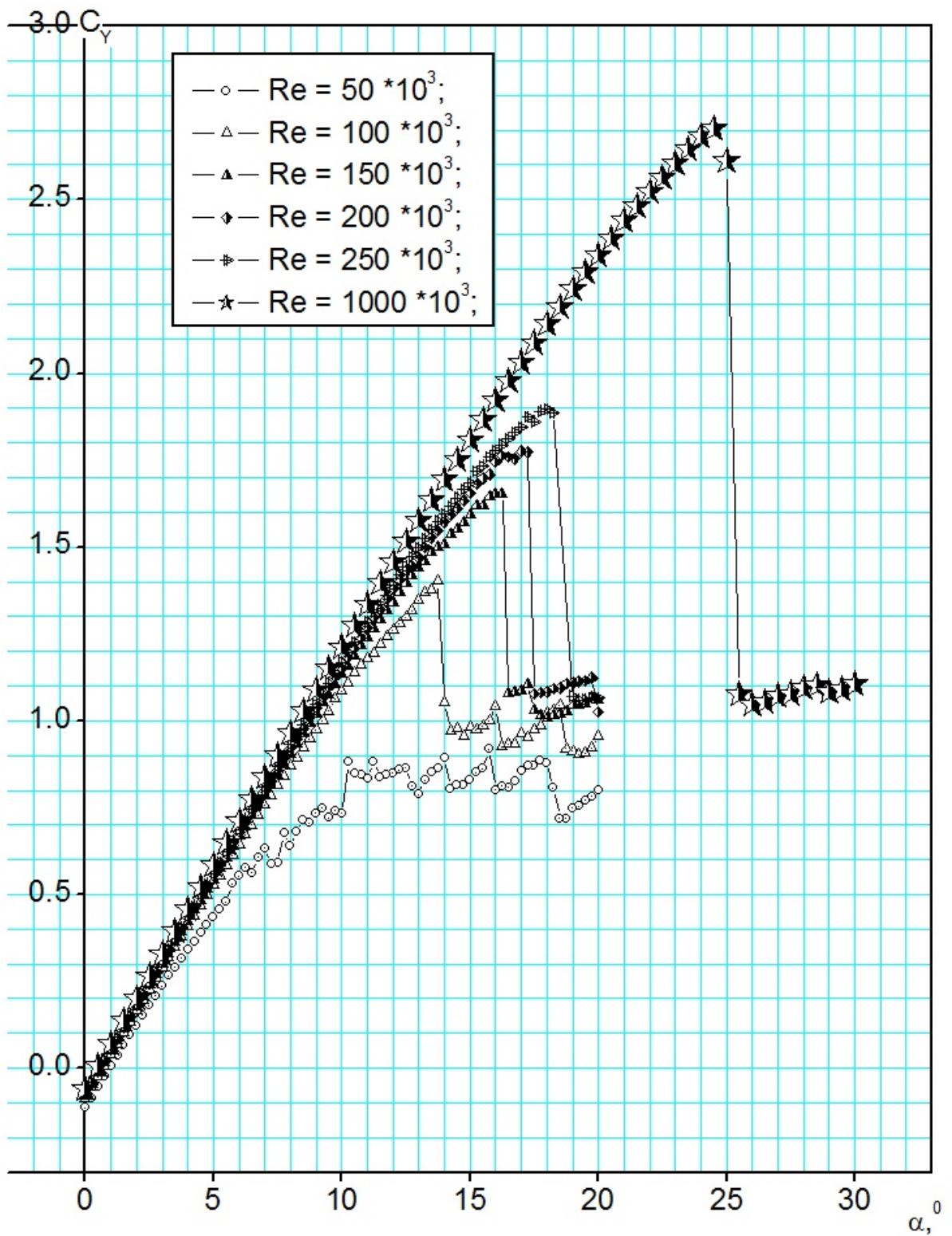
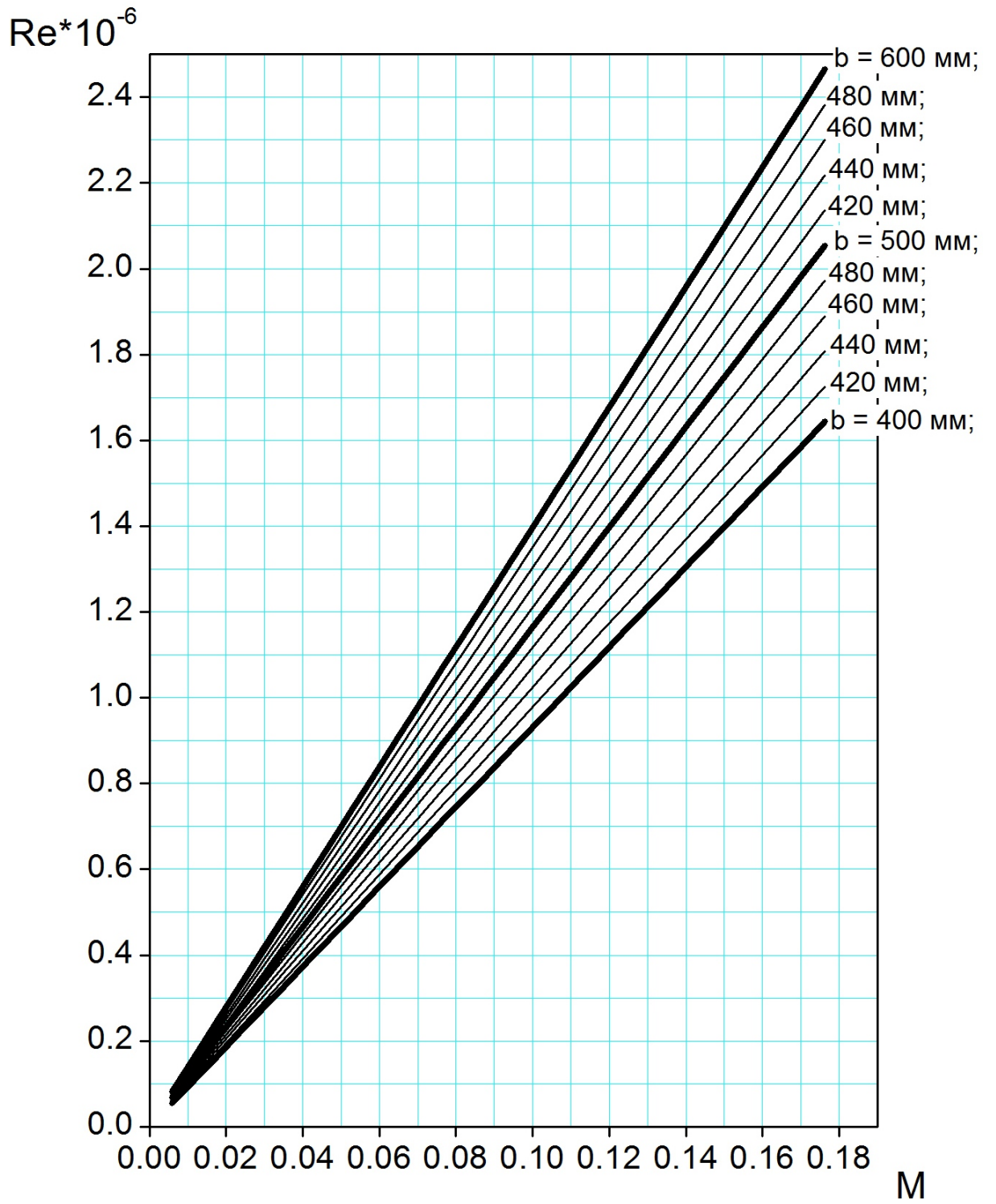


Figure 30 Aerodynamic characteristics of the designed profile



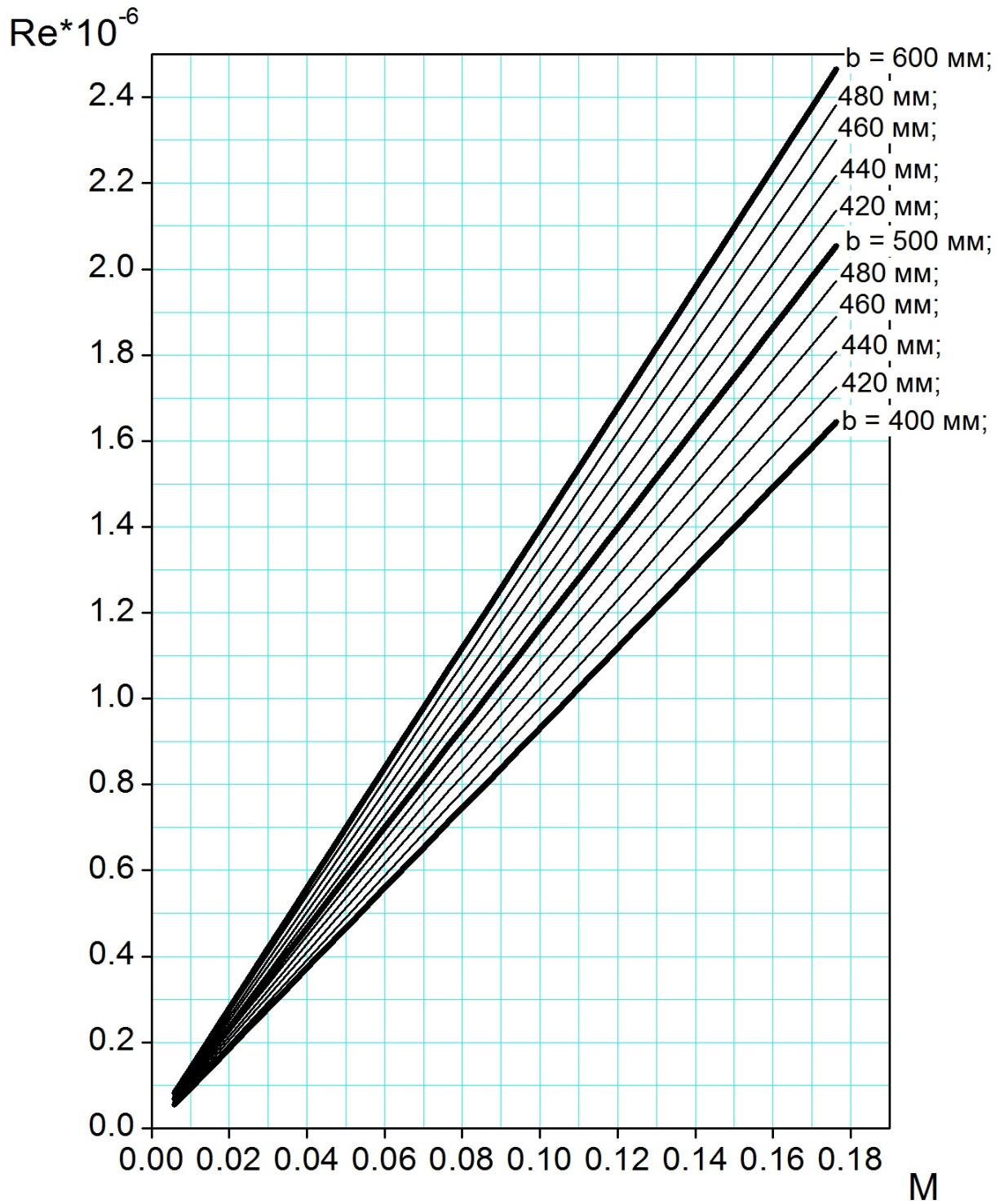


Figure 31 Range of settlement cases.

2.3. Aerodynamic Design Of The Working Surface Of The Wind Turbine

The working surface of the wind turbine is a normal wing mounted vertically. It is subjected to aerodynamic load, which is perceived by the design of the working surface in the form of bending M_x and torque M_z moments and cutting force Q_N .

One of the main features of a projected wind generator should be the use of inexpensive and affordable building materials, in particular, ordinary moisture-resistant plywood, wood, foam, etc. The assembly technology should exclude the use of expensive equipment and scarce imported materials. Because of this, the shape of the work surface is chosen rectangular, without twisting, the value of elongation is taken $\lambda \approx 7$ units, as for a typical wing of a general purpose aircraft. The design solutions that will be used in the construction are well known in the practice of wooden aircraft construction. The method of installation of work surfaces will be defined in Section 3 of the diploma project, but for solving the problems of aerodynamic design it is not essential.

2.3.1. Method Of Calculating The Aerodynamic Characteristics Of The Working Surface Of The Wind Turbine With The Proposed Profile

To determine the aerodynamic characteristics of the work surface, I use the panel-vortex method of symmetrical features, which allows you to perform with acceptable accuracy.

The boundary and initial conditions for the continuity equation, the equation of momentum for a small element of a liquid, and the equation of the law of conservation of energy for a control volume define the motion of a viscous incompressible fluid as the base.

$$\frac{\partial \rho}{\partial t} + \nabla^*(\rho v) = 0 \quad \frac{d}{dt} \int \rho v dV_{cs} = \sum F$$

$$\int_v \rho \frac{D}{Dt} \left[e + \frac{q^2}{2} \right] dV = \int_v \rho f^* v dV + \int_s n^* (v \sigma - \dot{Q}) dS \quad (2.11)$$

In the absence of detachable flow around the surface of the aircraft and small values of takeoff and landing speeds, the flow is determined by the Laplace equation for the velocity potential:

$$\Delta \Phi = 0.$$

The velocity of the flow at a point in space distant to infinity coincides with the undisturbed value:

$$\text{grad}(\Phi)|_{\infty} = V_{\infty}$$

On the surface S of the calculation model, the condition of non-flow is fulfilled - the absence of a normal velocity component:

The velocity of the flow at a point in space distant to infinity coincides with the undisturbed value:

$$Vn|_S = 0$$

On the trailing edge of the wings and other load-bearing elements of the layout. There is no static pressure drop on the surface of the vortex veil. The resulting vortex circulation and the intensity of the sources on the panel are constant. The velocity component caused by a continuous vortex layer is approximated as:

$$\vec{V}^{\gamma} = \sum_{i=1}^N \vec{V}_i^{\gamma} \bar{\gamma}_i$$

$\bar{\gamma}_i = \frac{2i-1}{N^2}$, \vec{V}_i^{γ} -The velocity component created by the i-th U-shaped vortex;

N is the number of discrete features on the panel.

In the center of the calculation panel shown in Fig.32, the speed is defined as:

$$\begin{aligned} \vec{V}_i^{\gamma} = & \frac{1}{4\pi} \left(\frac{CA \times CM}{|CA \times CM|^2} \left[\frac{CA \times CM}{|CM|} - \frac{CA \times \vec{q}_i}{|\vec{q}_i|} \right] \right) + \frac{1}{4\pi} \left(\frac{\vec{a}_i \times \vec{q}_i}{|\vec{a}_i \times \vec{q}_i|^2} \left[\frac{\vec{a}_i \times \vec{q}_i}{|\vec{q}_i|} - \frac{\vec{a}_i \times \vec{p}_i}{|\vec{p}_i|} \right] \right) + \\ & + \frac{1}{4\pi} \left(\frac{BD \times DM}{|BD \times DM|^2} \left[\frac{BD \times \vec{p}_i}{|\vec{p}_i|} - \frac{BD \times DM}{|DM|} \right] \right) \end{aligned}$$

(2.12)

$$\vec{q}_i = CM - \left(\frac{2i-1}{2N} \right) CA \quad \vec{p}_i = DM - \left(\frac{2i-1}{2N} \right) BD \quad \vec{a}_i = CD - \left(\frac{2i-1}{2N} \right) (CA + BD)$$

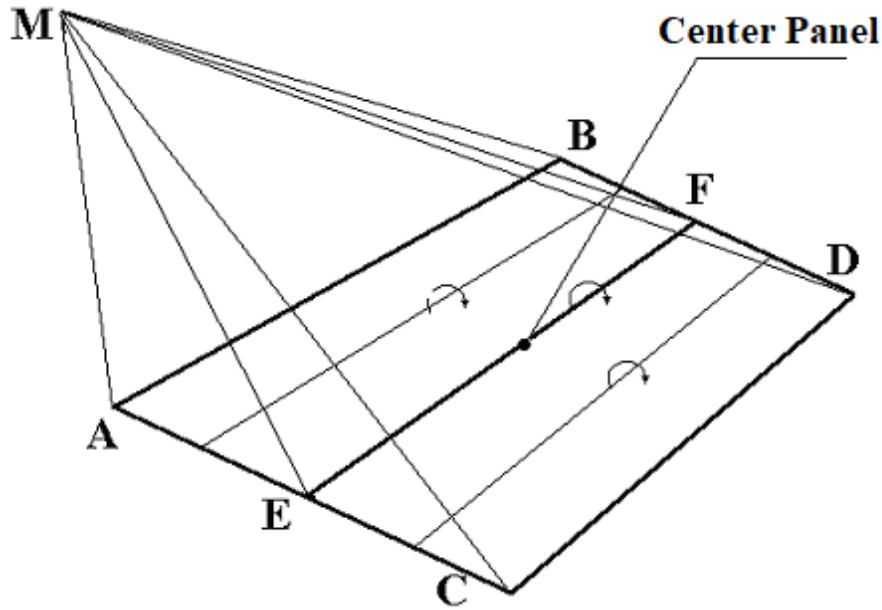


Figure 32 Calculation scheme of the basic method.

The component of the speed caused by the distribution of sources on the surface of the panel:

$$\vec{V}^\sigma = \sum_{i=1}^N \vec{V}_i^\sigma \bar{\sigma}_i$$

$$\bar{\sigma}_i = \frac{1}{N} \quad \vec{V}_i^\sigma = \frac{1}{4\pi} \frac{[\vec{a}_i \times \vec{q}_i] \times \vec{a}_i}{|\vec{a}_i \times \vec{q}_i|^2 |\vec{a}_i|} \left[\frac{\vec{a}_i \times \vec{q}_i}{|\vec{q}_i|} - \frac{\vec{a}_i \times \vec{p}_i}{|\vec{p}_i|} \right] + \frac{1}{4\pi} \frac{\vec{a}_i}{|\vec{a}_i|} \left[\frac{1}{|\vec{p}_i|} - \frac{1}{|\vec{q}_i|} \right] \quad (2.13)$$

Simple equations that determine the perturbation of velocity from sources and vortices, can significantly reduce the required computer resources compared to the algorithm for solving the exact values of the integrals in continuous layers of sources and vortices on the panel.

2.3.2. Estimated Model Of The Working Surface Of The Wind Turbine

The calculated model of the working surface of the wind generator for the panel-vortex method is shown in Fig.32

The calculation was performed for 2 cases - wind speed 7 m / s and wind speed 17 m / s (respectively $Re = 200000$ and 500000)

The main geometric parameters of the working surface of the blade are shown below in Fig.33

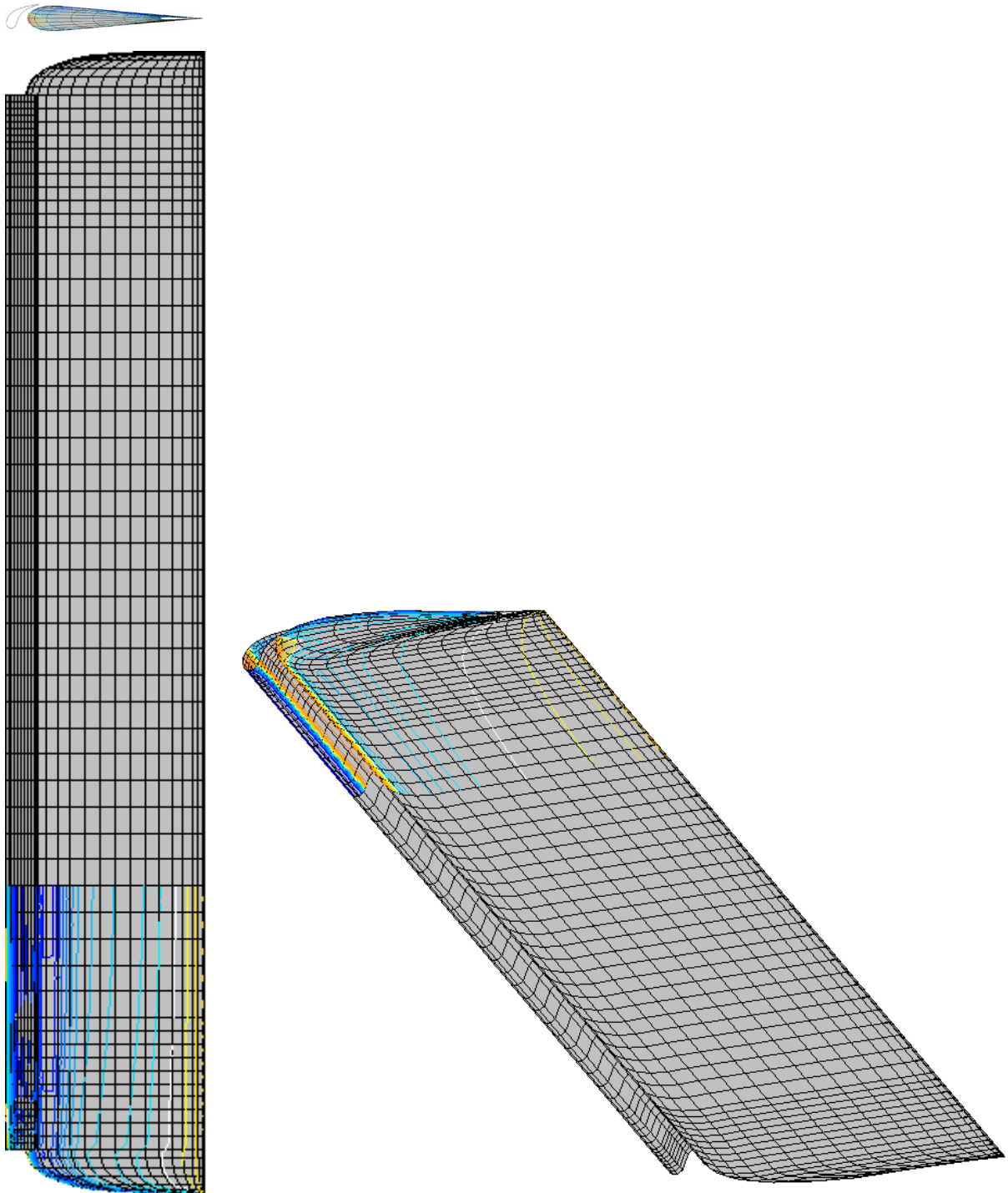


Figure 33 Calculated model of the work surface

Geometric characteristics of the work surface

Parameter				
Blade area	S	=		1.18 m ²
Blade chord	b	=		0.428 m

The height of the blade is total	1	=	2.78 m
----------------------------------	---	---	--------

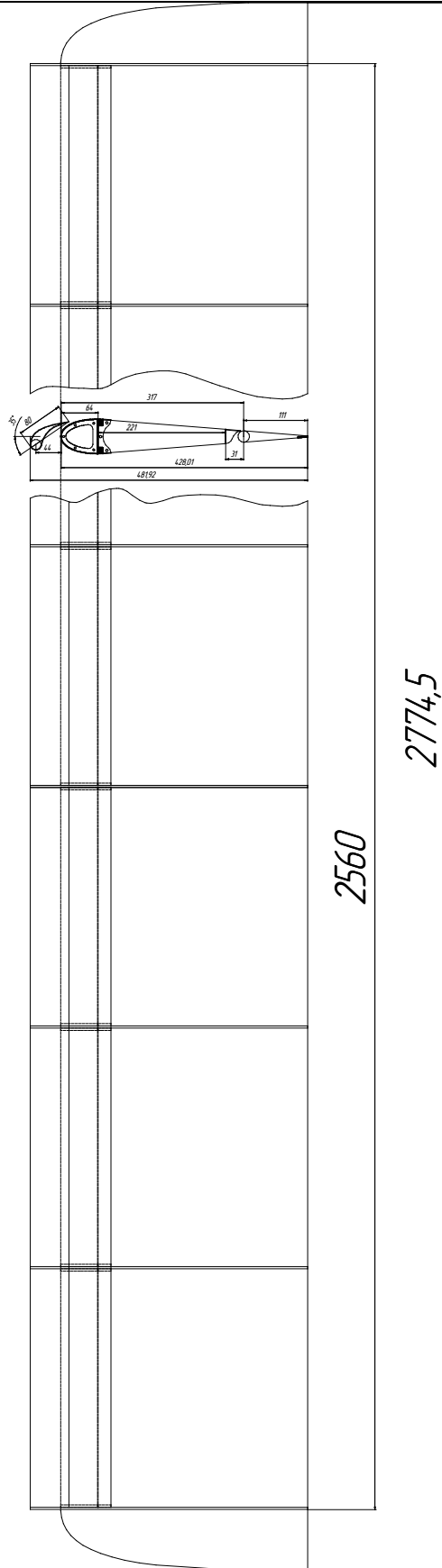


Figure 34 General view of the work surface.

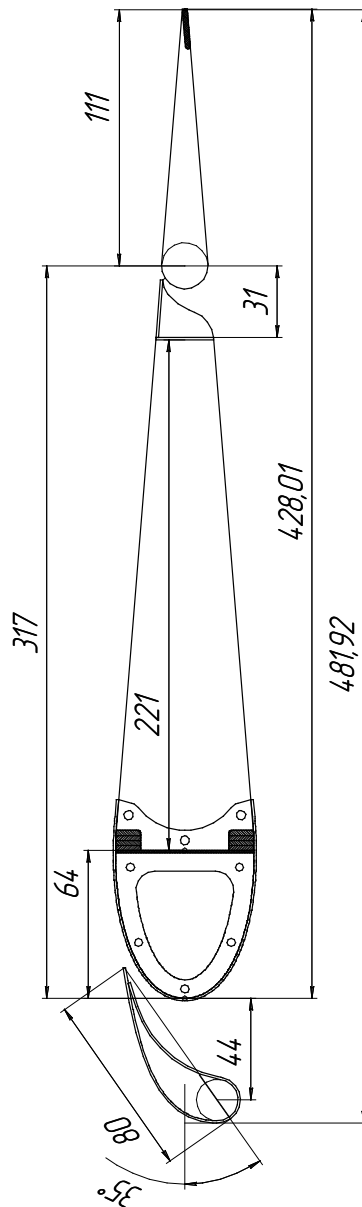


Figure 35 Typical cross section of the work surface

2.3.3. The Results Of The Calculation

The results of the calculation in the form of the dependence of the coefficient of lifting force on the angle of attack and the relative position of the center of application of aerodynamic force on the value of the coefficient of aerodynamic force.

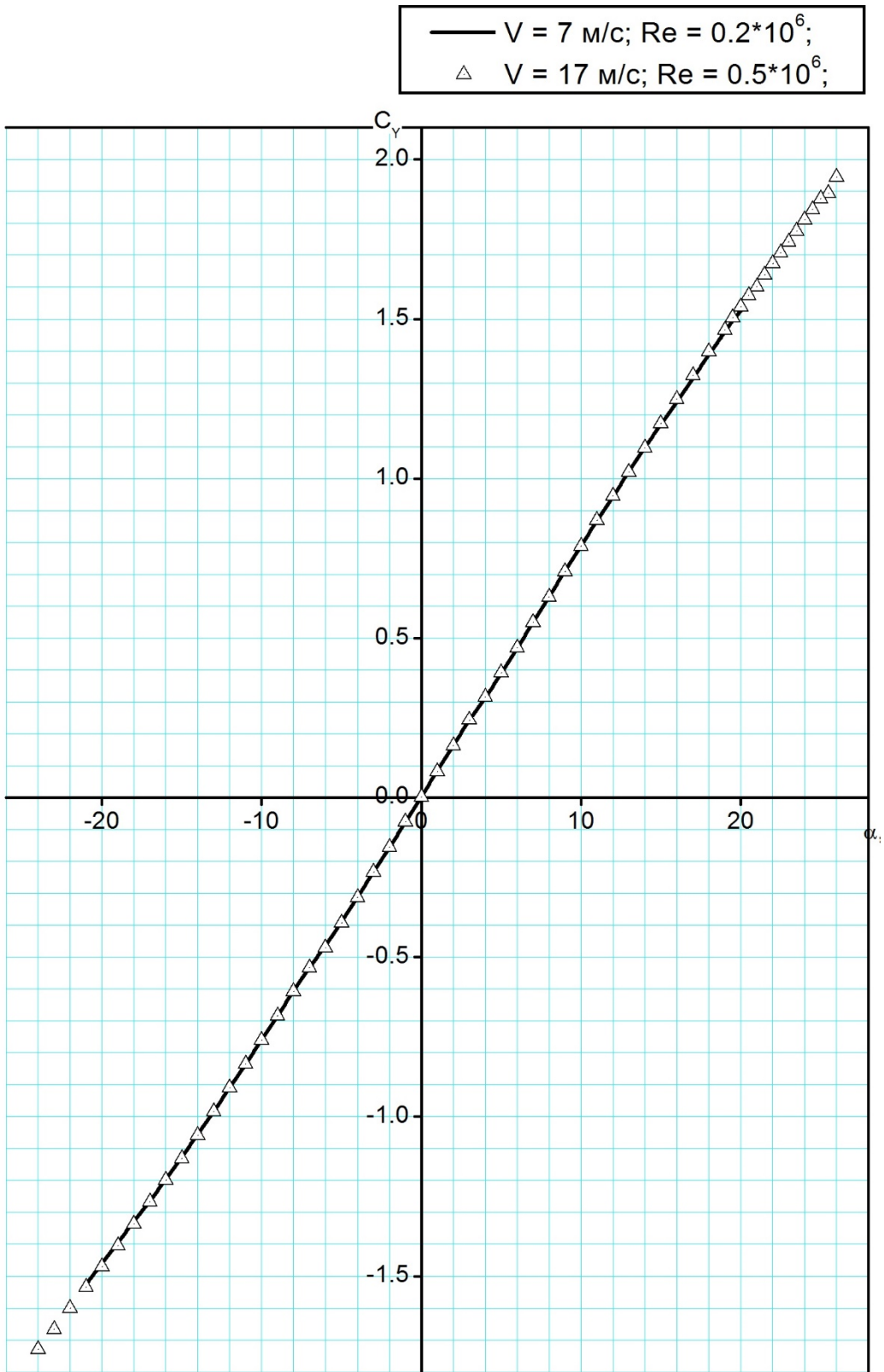


Figure 36 Dependence of the coefficient of aerodynamic force on the angle of attack

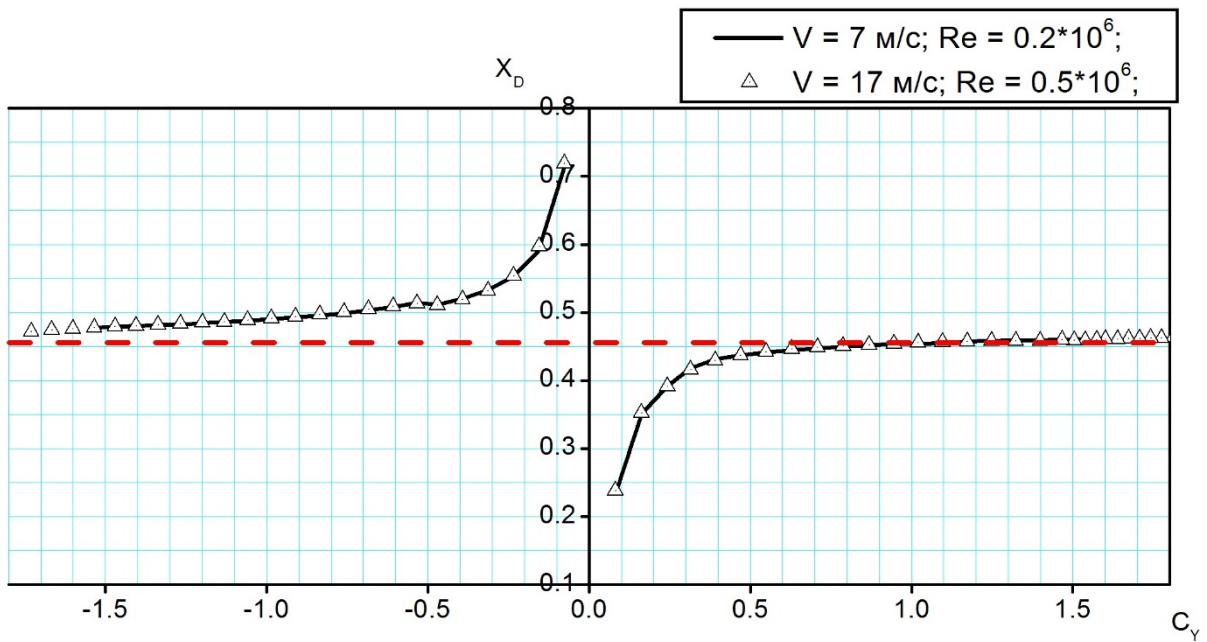


Figure 37 Dependence of the relative position of the center of application of aerodynamic force on the value of the coefficient of aerodynamic force.

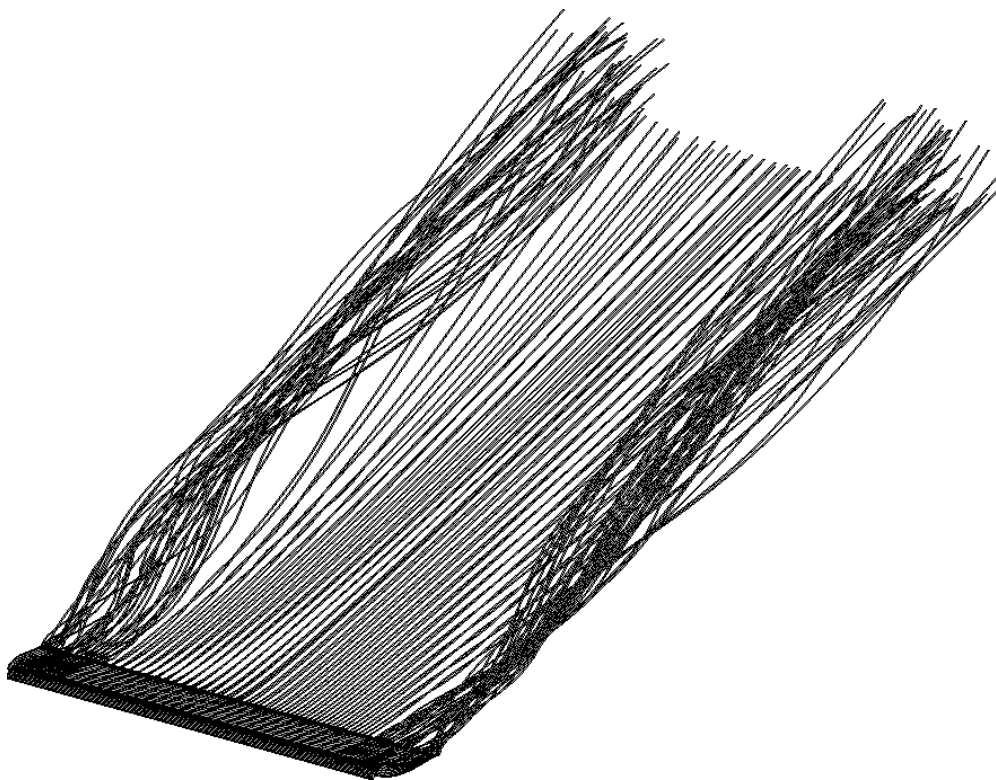


Figure 38 Vortex veil blade wind turbine. Critical angle of attack

AERODYNAMIC CHARACTERISTICS OF THE BLADE DURING CIRCULAR BLOWING.

Combining the results of the calculation of the flow of the working blade of the wind turbine with the experimental data of the circular blowing of the wing compartment, we obtain the initial data for the calculation of the torque of the wind turbine.

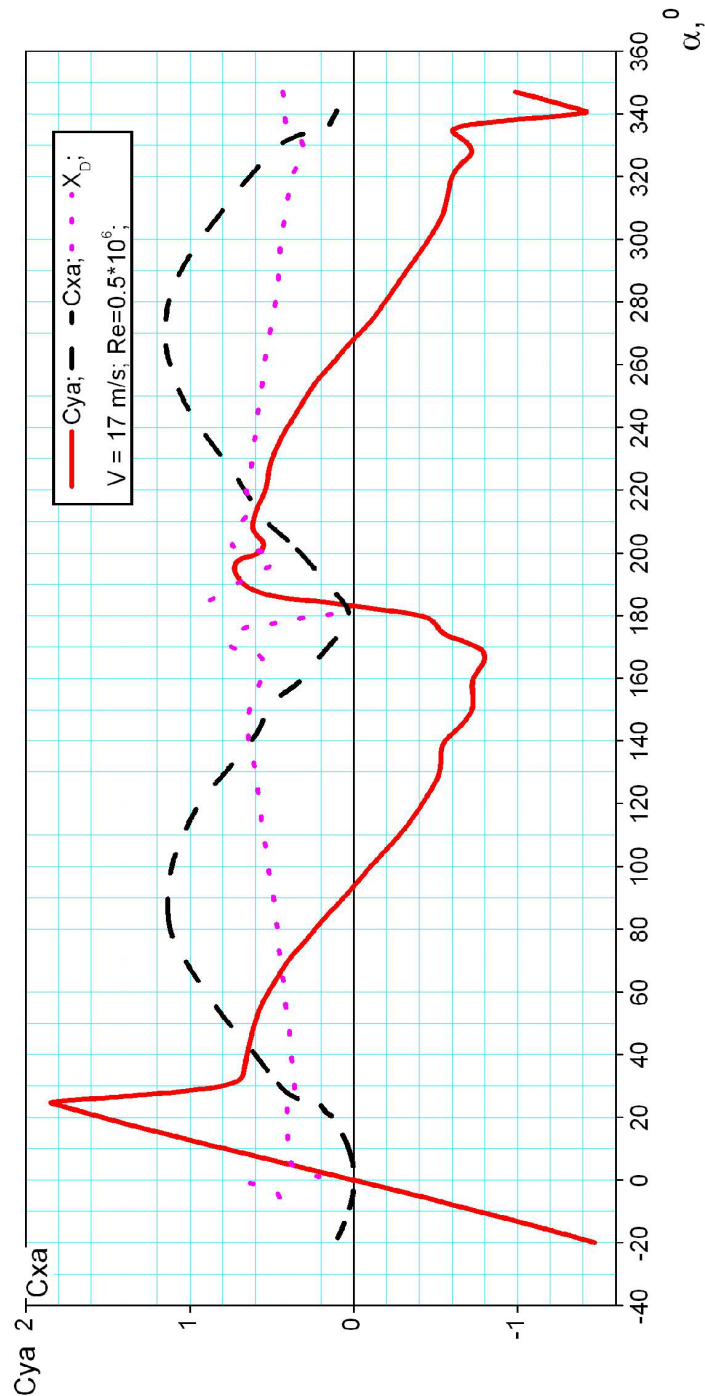


Figure 39 Aerodynamic characteristics of the blade with circular blast.

Conclusions On The Section.

1. To form the surface of the working blade of the wind turbine, it is advisable to use a mechanized profile with a fixed flap. This will allow you to get 1.5 times more torque on the axis of the wind turbine in the mode of continuous flow around the blade or increase the efficiency of the wind turbine at low air speeds. The use of mechanization of the rear edge is impractical due to the low efficiency of the flaps at low air speeds;
2. In the range of angles of attack and rotation, in which the flow around the blade surface without separation of the flow is impossible, the aerodynamic characteristics of the blade, according to experimental studies, practically do not depend on the type of airfoil.

3. DESIGN PART. DEVELOPMENT OF WINDOW GENERATOR WORKING STRUCTURE

3.1. Wind Turbine Torque

To determine the torque of the unit at different angles of rotation, it is necessary to determine the angle of the blade relative to the axis of rotation in the case of the possibility of realizing the maximum possible torque.

That is, between the direction of action of the total aerodynamic force R_a and the axis of rotation must be equal to the radius:

$$M_{ZiMAX} = R_{aMAX} * r$$

According to the results of the calculation of the aerodynamic characteristics of the working blade of the wind turbine, the maximum value of the total aerodynamic force can be realized at an angle of attack $\alpha = 25^0$.

The arm of the wind turbine blade relative to the axis of rotation in the first approximation is taken equal to 1 m. Actually, this parameter requires further study, and the selected value is approximate. The number of blades of the wind turbine is taken equal to 3 pcs.

Below, in Fig.40-41 and in table. 3.1-3.2 shows the results of calculating the torque of the wind turbine blade relative to the axis of rotation and the actual total value of the torque of the entire wind turbine depending on the angle of rotation.

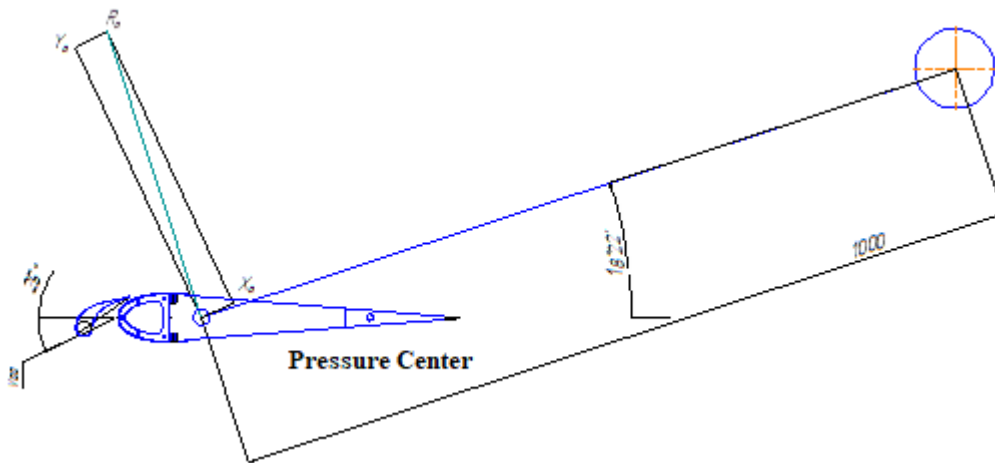


Figure 40 Determining the angle of installation of the working blade of the wind turbine.

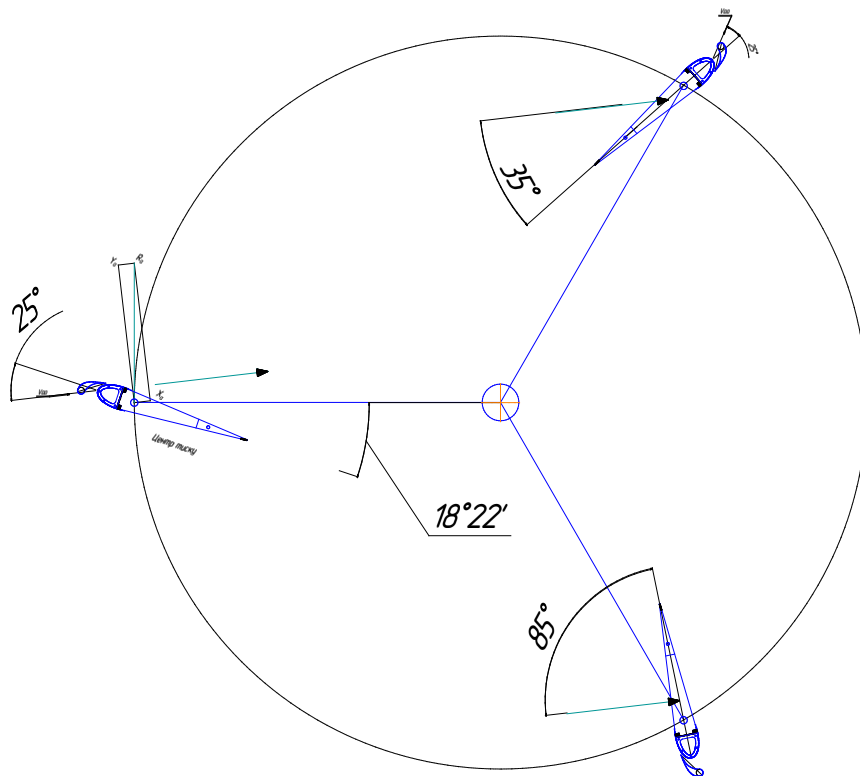


Figure 41 Calculation scheme for determining the angle of installation of the working blade of the wind turbine.

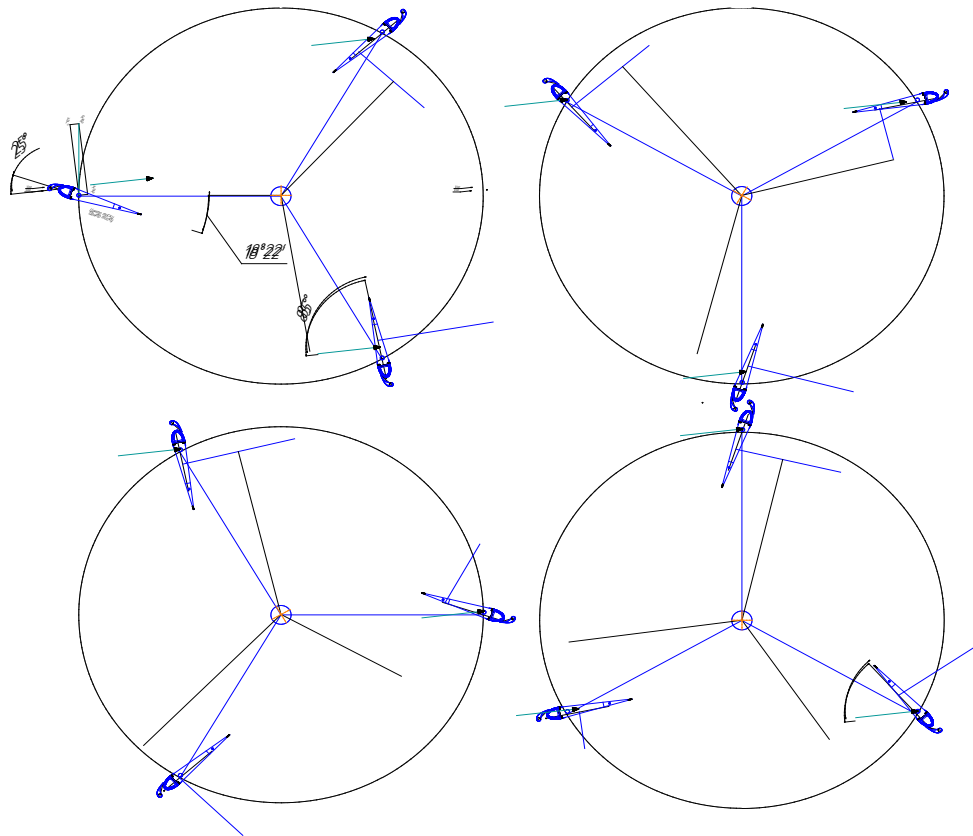


Figure 42 Calculation scheme for determining the total torque of the wind turbine blades.

Table 3.1. The results of calculating the aerodynamic force and torque of the wind turbine blade.

φ_{vg}	α_l	S_{Yal}	S_{Xal}	X_{DI}	S_{Rl}	h_l	M_{krutl}
						m	kg*m
0	25	1.8761	0.2172		1.8886	1	37.5248
30	55	0.562	0.8333	0.408	1.0051	0.907	18.1129
60	85	0.14	1.13	0.467	1.1386	0.891	20.1574
90	115	-0.362	1	0.526	1.0635	0.878	18.5526
120	145	-0.662	0.572	0.65	0.8749	0.821	14.2714
150	175	-0.545	0.072	0.72	0.5497	0.773	8.4431
180	205	0.578	0.413	0.742	0.7104	-0.679	-9.5838
210	235	0.452	0.862	0.61	0.9733	-0.766	-14.8134
240	275	0.062	1.15	0.53	1.1517	-0.841	-19.244
270	295	-0.391	1	0.452	1.0737	-0.87	-18.5602
300	325	-0.68	0.552	0.32	0.8758	-0.973	-16.9321
330	355	-0.3927	0.0075	0.46	0.3928	-0.862	-6.7266
360	25	1.8761	0.2172	--	1.8886	1	37.5248

φ_{vg} - angle of rotation of the wind turbine;

α_l - angle of attack of the wind turbine blade;

S_{Yal} - coefficient of lifting force of the wind turbine blade;

S_{Xal} - coefficient of drag of the wind turbine blade;

S_{Rl} - coefficient of total aerodynamic force of the wind turbine blade;

X_{Dl} - relative coordinate of application of equivalent total aerodynamic force;

h_l - the actual arm of the full aerodynamic force of the wind turbine blade;

M_{krutl} - torque of the wind turbine blade;

Figure 42 shows the construction of the values of total aerodynamic force and torque for the wind turbine blade with a step $\Delta\varphi_{vg} = +300$ for complete rotation of the structure. The direction and scale of the vectors of action of the total aerodynamic force of the blade corresponds to 1 unit = radius of rotation (equal to 1000 mm).

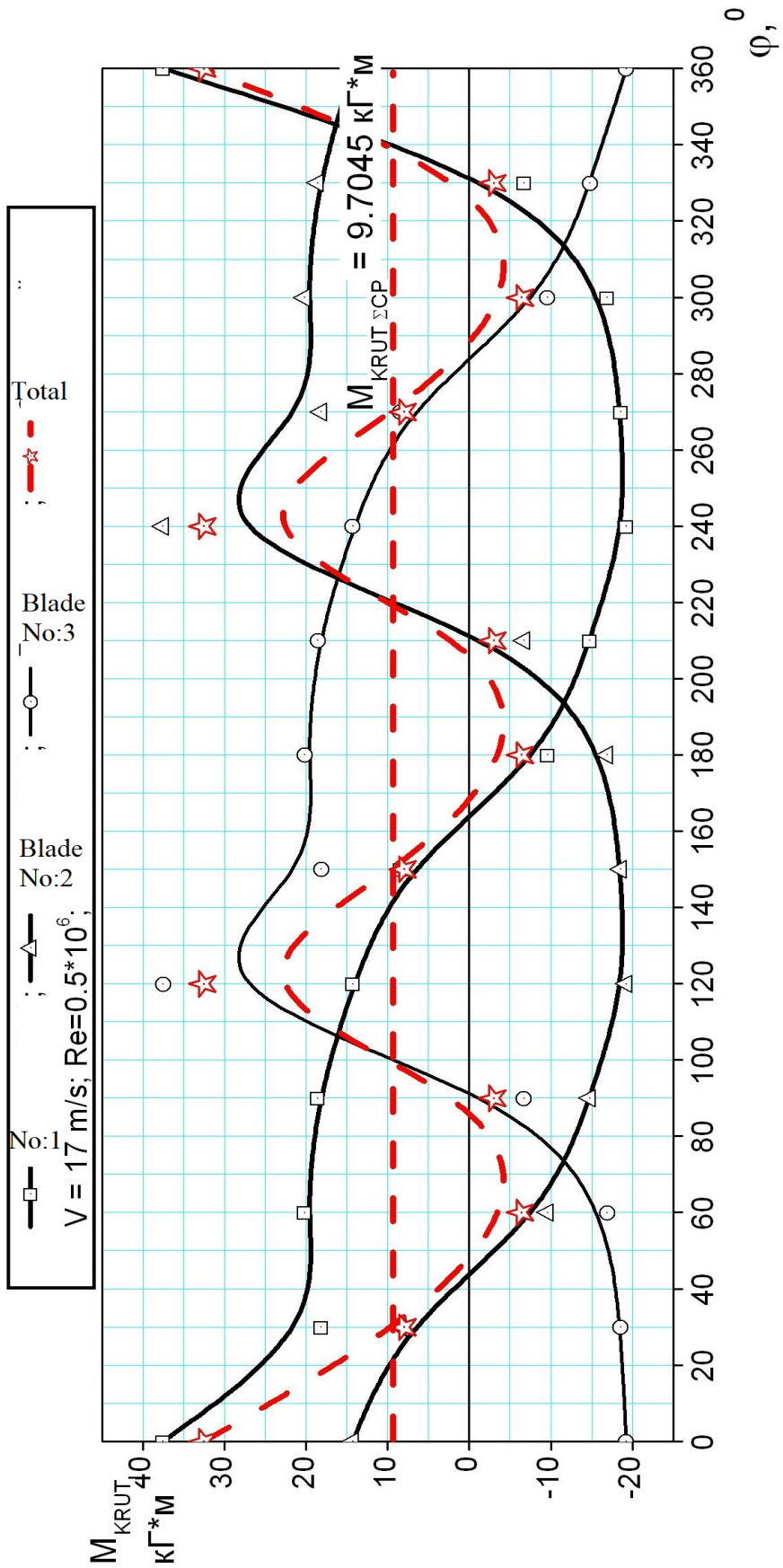


Figure 43 Dependence of the torque of the wind turbine blade on the angle of rotation.

Table 3.2. The results of the calculation of the total torque of 3 blades of the wind turbine.

φ_{vg}	$M_{krut\ 1\ 1}$	$M_{krut\ 1\ 2}$	$M_{krut\ 1\ 3}$	$M_{krut\ 1\ \Sigma}$
	kg*m	kg*m	kg*m	kg*m
0	37.5248	14.2714	-19.244	32.5522
30	18.1129	8.4431	-18.5602	7.9959
60	20.1574	-9.5838	-16.9321	-6.3585
90	18.5526	-14.8134	-6.7266	-2.9874
120	14.2714	-19.244	37.5248	32.5522
150	8.4431	-18.5602	18.1129	7.9959
180	-9.5838	-16.9321	20.1574	-6.3585
210	-14.8134	-6.7266	18.5526	-2.9874
240	-19.244	37.5248	14.2714	32.5522
270	-18.5602	18.1129	8.4431	7.9959
300	-16.9321	20.1574	-9.5838	-6.3585
330	-6.7266	18.5526	-14.8134	-2.9874
360	37.5248	14.2714	-19.244	32.5522

3.2. Aerodynamic Loads

To calculate the strength of the wind turbine blade structure and determine the available strength reserves using the calculated model of the blade shown in Fig. 44 in my work, the surface flow was modeled on the mode of maximum bearing properties of the wing: $\alpha = 25^\circ$ by the panel-vortex method of symmetrical features.

The results of the calculation in the form of the distribution of the coefficients of the normal and tangential components of the aerodynamic load in the connected coordinate system by the span of the wing and fender console are presented in Fig.45, respectively. -3.6. and Table. 3.3.

The plane of symmetry of the wind turbine blade is taken as the origin, the calculation results are given for one half of the blade. It is understood that the installation of the blade on the axis of the wind turbine will take place in one mounting assembly in the plane of symmetry.

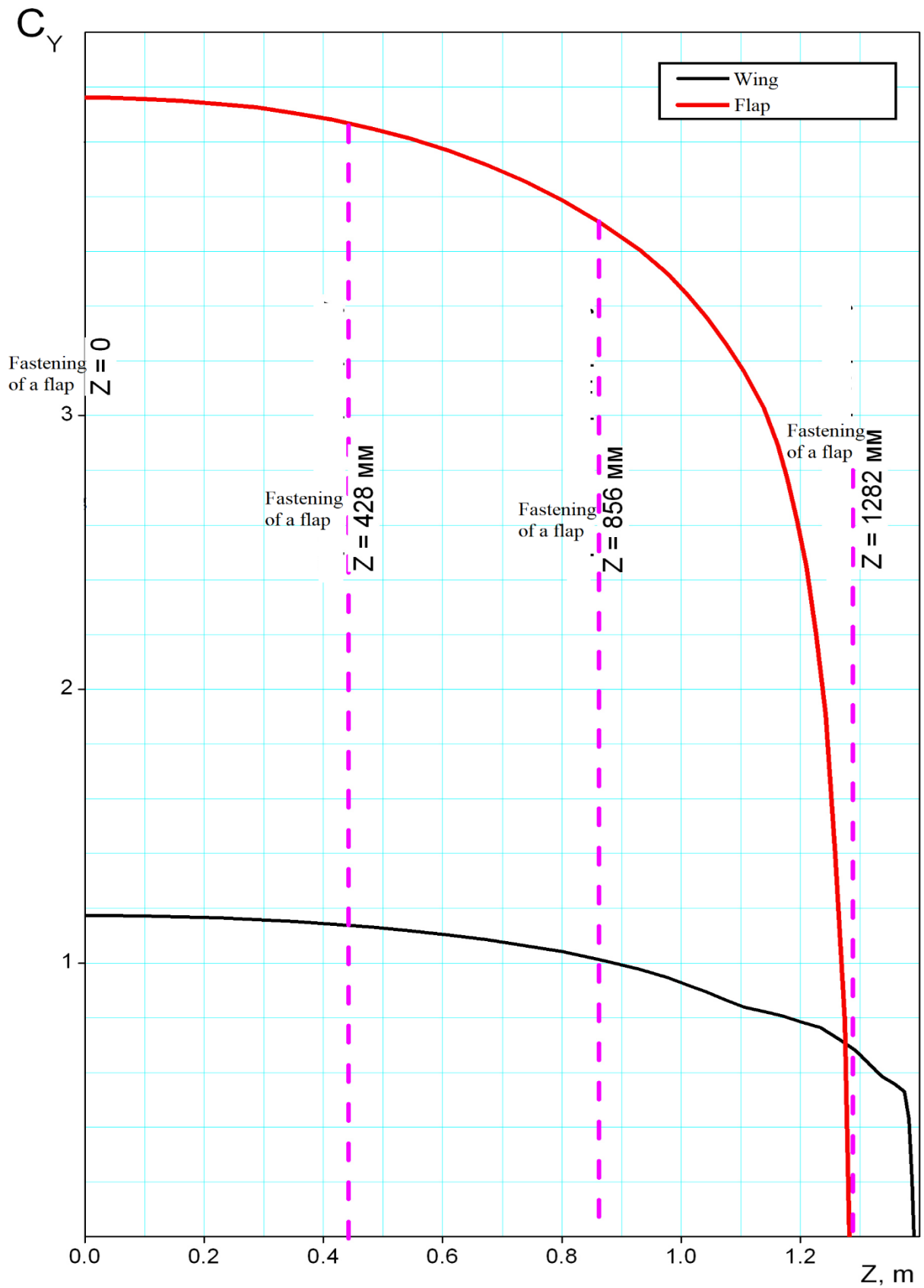


Figure 44 Dependence of the coefficient S_u of the normal component of the aerodynamic load of the blade elements of the wind generator in terms of span. $\alpha = 25$, $V = 17\text{ m/s}$

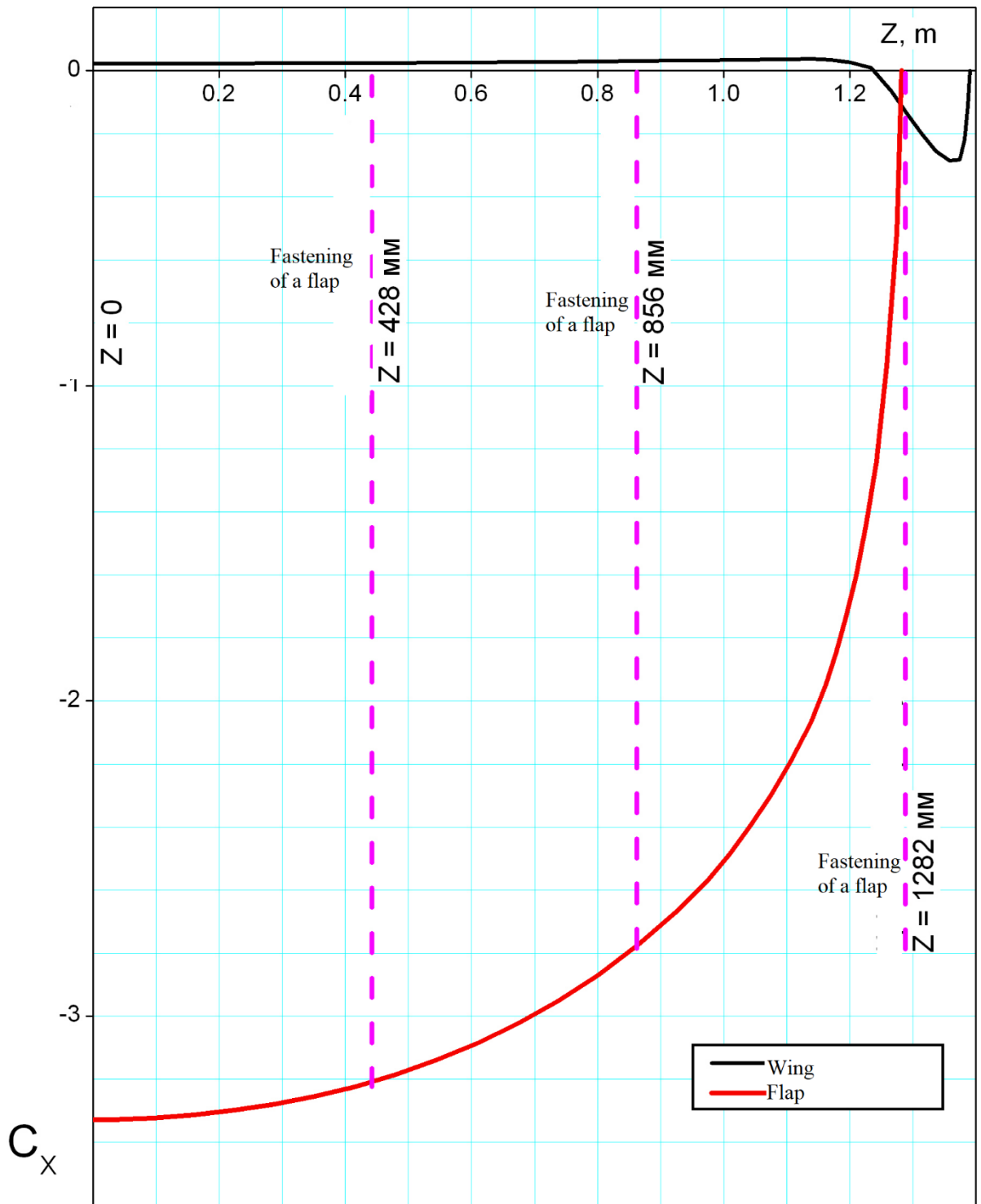


Figure 45 Dependence of the coefficient C_x of the tangential component of the aerodynamic load of the elements of the wind turbine blades on the scope.

The values of normal N_i and tangential T_i components of the aerodynamic load acting on the design of the wind turbine blades are defined as:

$$N_i = C_y * q_\infty * S_i; \quad (3.1)$$

$$T_i = C_x * q_\infty * S_i ;$$

C_y, C_x – coefficients of normal and tangential components;

q_∞ - velocity head, kg / m²;

S_i – estimated area of the unit, m²;

The values of the longitudinal normal q_{Ni} and tangential q_{Ti} components of the aerodynamic load acting on the structure of the wind turbine blade are determined for the intersection with the z coordinate as:

$$q_{Ni}(z) = C_y * q_\infty * b_i(z); \quad (3.2)$$

$$q_{Ti}(z) = C_x * q_\infty * b_i(z); ;$$

$b_i(z)$ – own chord of the unit, m;

The values of N_i and T_i can also be determined by integrating:

$$N_i = \int q_{Ni}(z) dz ; \quad (3.3)$$

$$T_i = \int q_{Ti}(z) dz;$$

The values of the coefficients of normal C_n and tangential C_τ components of the aerodynamic load are determined by integrating the plot of the distribution of the pressure coefficient C_p on the surface of the unit:

$$C_n = \int_0^1 (C_p) dx; \quad (3.4)$$

$$C_\tau = \int_0^{\bar{y}} (C_p) dy$$

$C_p = \frac{\Delta p}{q_\infty}$ - pressure coefficient, defined as the ratio of excess pressure Δp_i to the velocity pressure of the incident flow q_∞ .

The coordinate of the resulting application is defined as:

$$\bar{X}_d = \frac{\sum C_{ni} \times \bar{X}_{di}}{C_{n_\Sigma}} \quad (3.5)$$

The calculation is performed for the conditions: $H = 0$, CA, wind speed 17 m / s
 Speed pressure and Mach number M are defined as:

$$q_{\infty i} = 0,5 * \rho * V_{\infty i}^2 = 0,0625 * V_{\infty i}^2; \quad M = V_{\infty} / a \quad ;$$

The obtained values of the aerodynamic loads of the wind turbine blade for the design conditions $\alpha = 25^\circ$, $V = 17$ m / s, namely: the dependences of the bending M_x and M_y the custom moments of the wind turbine blade, the dependence of the normal Q_y and tangentially Q_x components of the aerodynamic load of the wind turbine blade along the span and the distribution of the pressure coefficient with the chord the blades are shown in Fig. 46-49.

Tab. 3.3. Summarized aerodynamic options for bursting into the generator over a swing

Z	$Q_{y\Sigma}$	$M_{x\Sigma}$	$Q_{x\Sigma}$	$M_{y\Sigma}$
m	κkg	kg*m	kg	kg*m
1.39	0	0	0	0
1.358	0.0762	9.75E-04	-0.0397	-5.08E-04
1.266	0.5412	0.0288	-0.1854	-0.015
1.106	2.0869	0.2389	-0.5406	-0.0565
0.9294	4.201	0.8176	-1.111	-0.2045
0.8654	5.0212	1.1229	-1.3436	-0.2631
0.6731	7.6347	2.4286	-2.0984	-0.6032
0.4808	10.3824	4.3274	-2.913	-1.0968
0.3526	12.2624	5.7899	-3.4778	-1.5171
0.2243	14.1687	7.6464	-4.0542	-2.0546
0	17.5322	11.3471	-5.0765	-3.1167

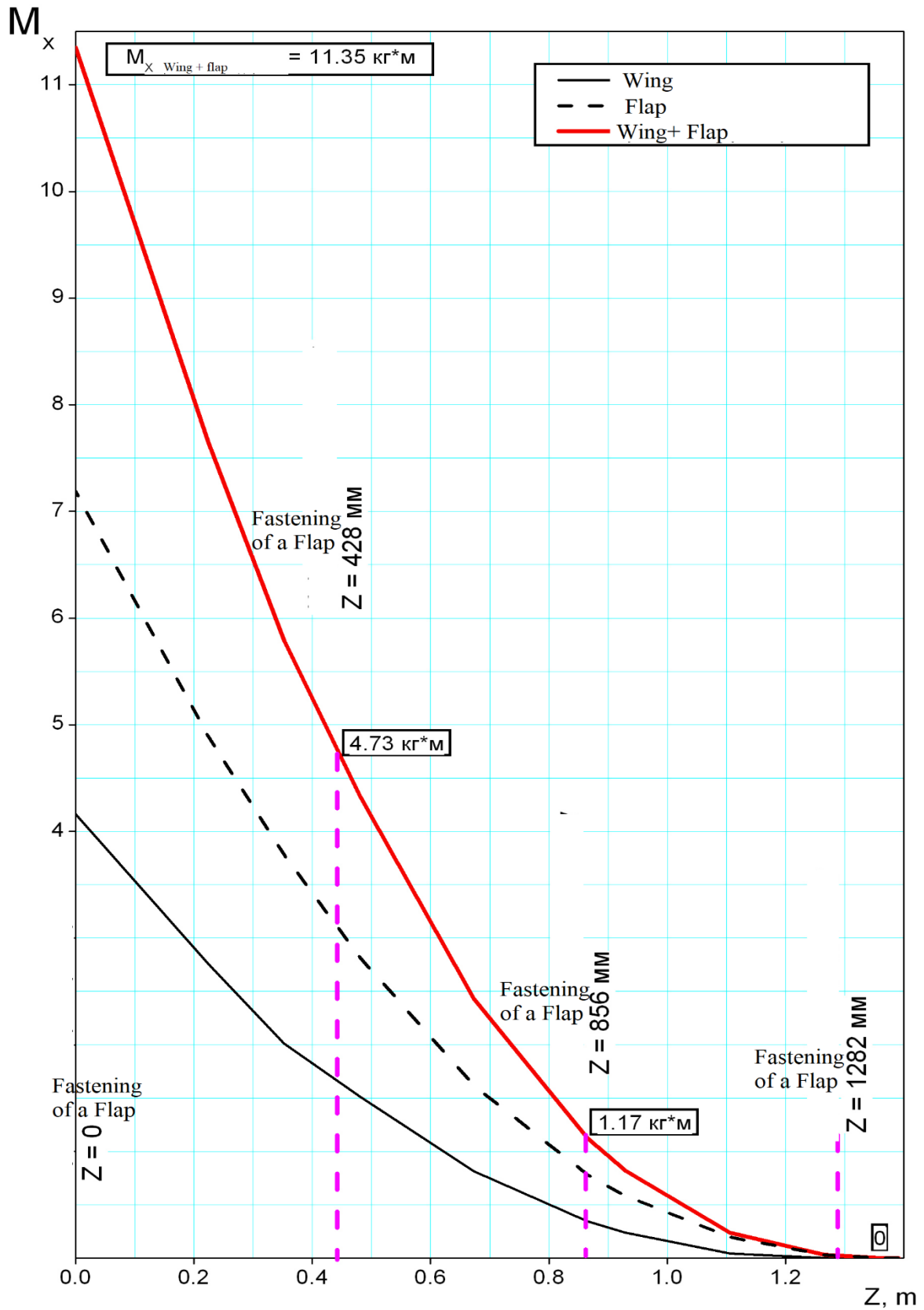


Figure 46 Dependence of the bending moment of the aerodynamic load M_x of the wind turbine blade on the scope. $\alpha = 25$, $V=17\text{m/s}$

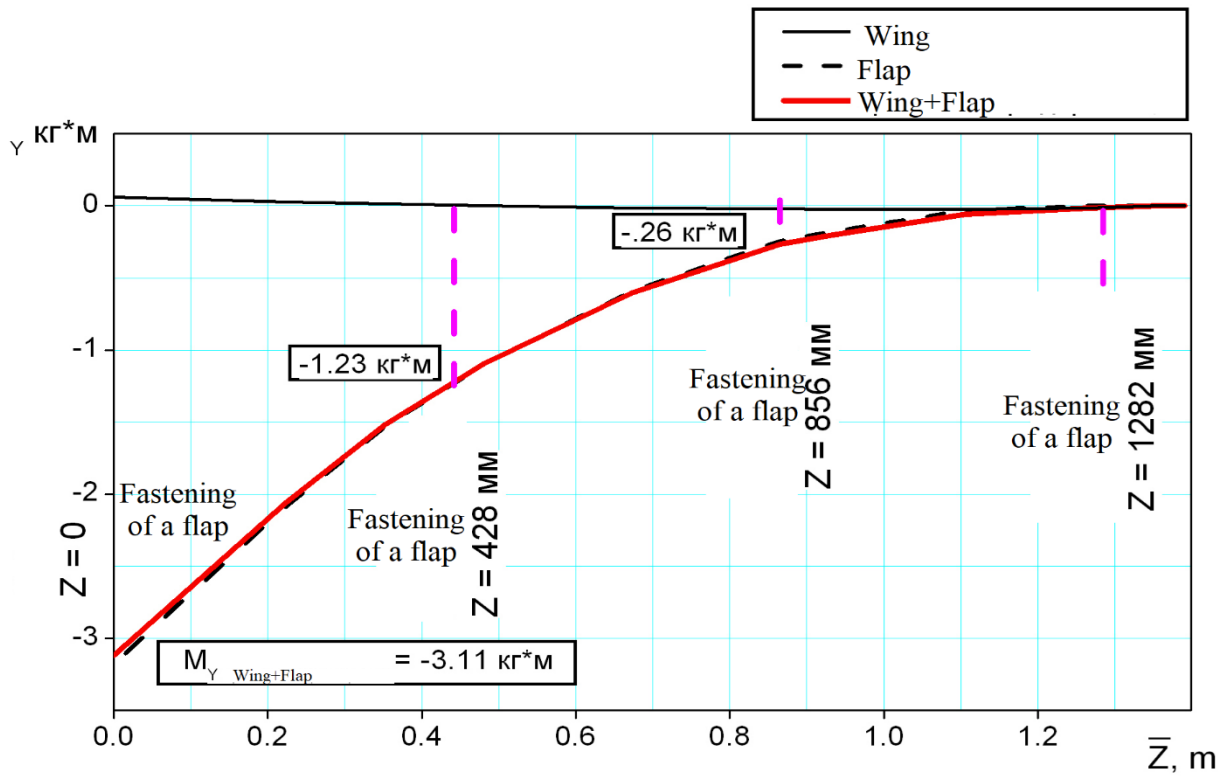


Figure 47 The dependence of the bending moment of the aerodynamic load M_Y of the wind turbine blade on the scope. $\alpha = 25$, $V=17\text{m/s}$

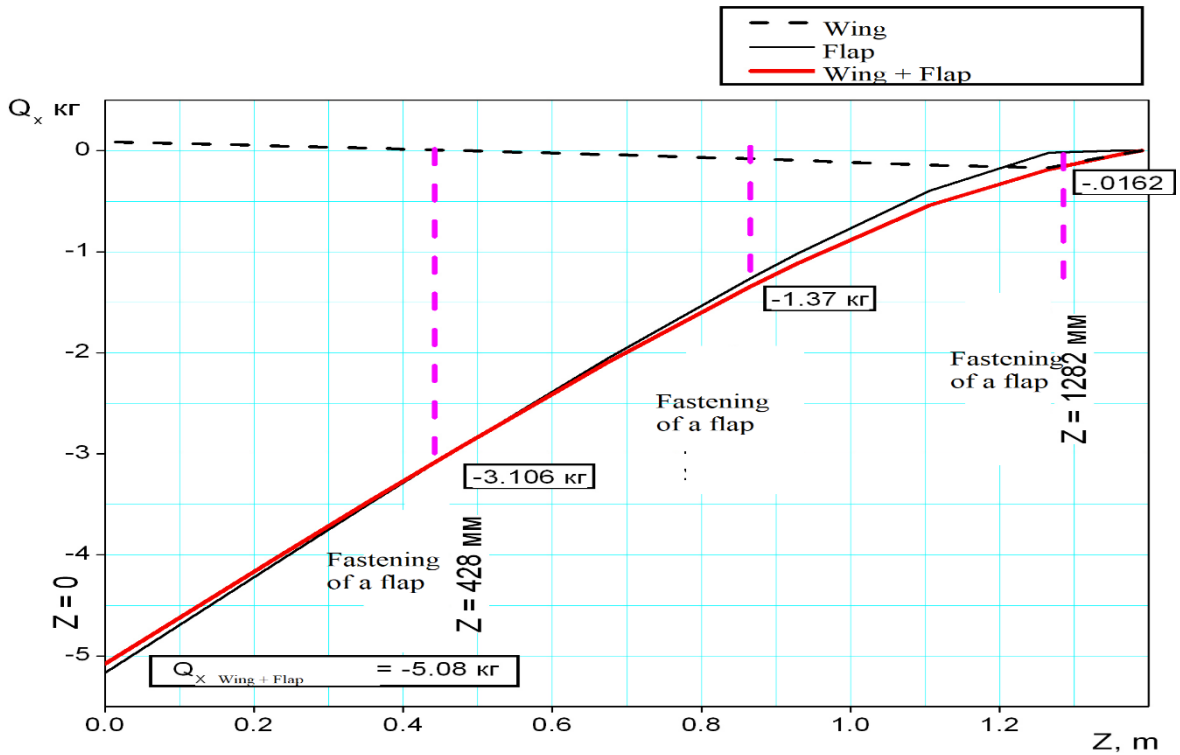


Figure 48 Dependence of the tangential component of the aerodynamic load Q_X of the wind turbine blade on the scope. $\alpha = 25$, $V=17\text{m/s}$

Initial data for calculating the design of the blade for strength:

Components of the bending moment:

$$M_{X \text{ MAX}} = 11.35 \text{ kg} \cdot \text{m}; M_{Y \text{ MAX}} = -3.1167 \text{ kg} \cdot \text{m};$$

Components of normal strength:

$$Q_{Y \text{ MAX}} = 17.53 \text{ kg}; Q_{X \text{ MAX}} = -5.08 \text{ kg};$$

Blade torque:

$$M_{Z \text{ MAX}} = Q_{Y \text{ MAX}} * (X_D - X_{IIK}) 17.53 * 0.0343 = 0.601279 \text{ kg} \cdot \text{m};$$

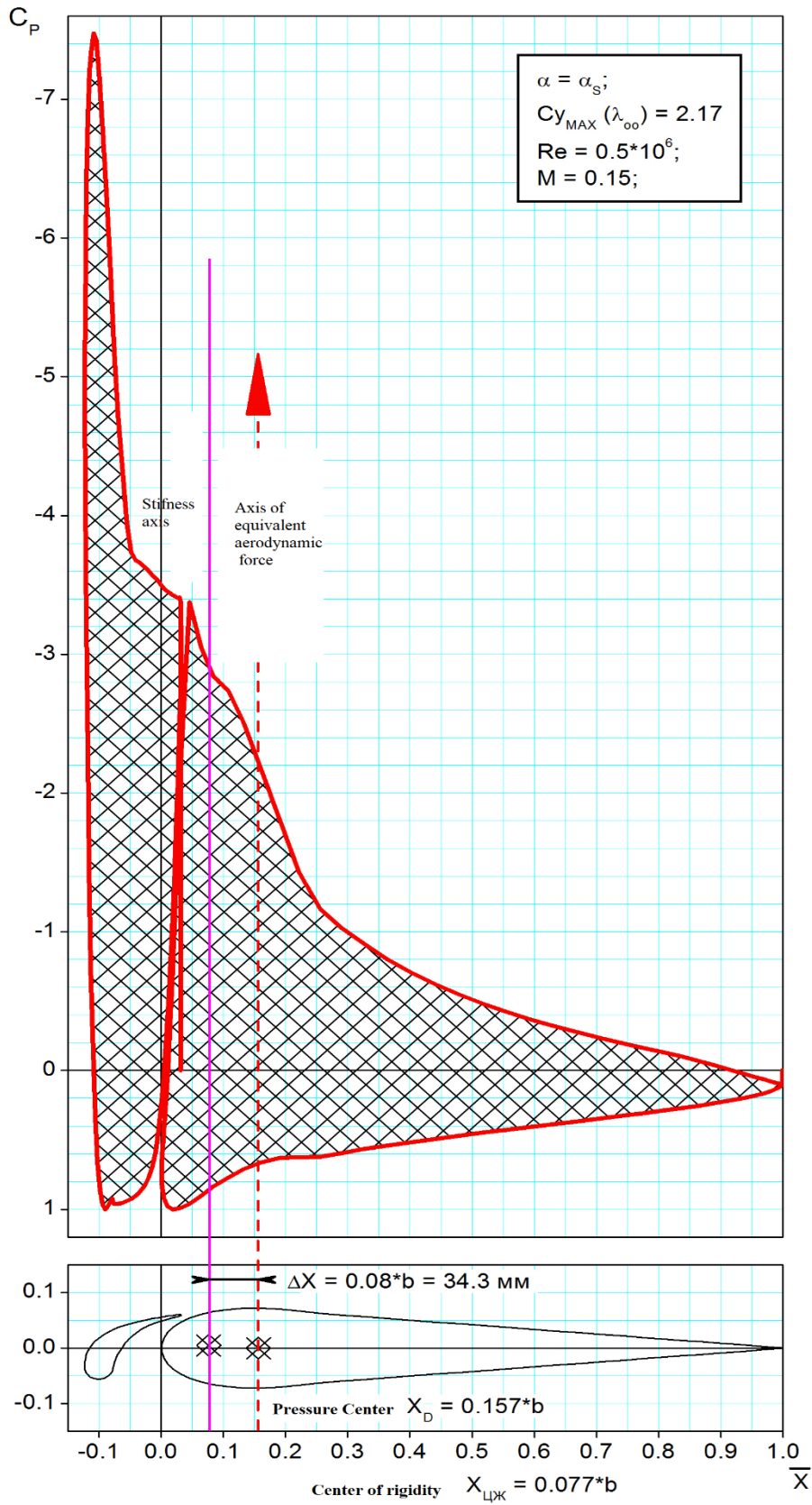


Figure 49 Distribution of the coefficient of pressure Wed on the chord of the blade. $\alpha = 25$, $V=17\text{m/s}$

According to the results of the analysis of the MCC of flat figures in the program Compass V13 the following characteristics of the section were obtained:

Date 21.09.2020

Document

Calculation of the ICC of flat figures

Number of bodies $N = 2$

Number of holes $N1 = 2$

Area $S = 619.648431 \text{ mm}^2$

Mass center $X_c = 32.867755 \text{ mm}$

$Y_c = 1.933387 \text{ mm}$

In a given coordinate system:

Axial moments of inertia $J_x = 308894.660826 \text{ mm}^4$

$J_y = 1752969.452801 \text{ mm}^4$

Centrifugal moment of inertia $J_{xy} = 13317.912655 \text{ mm}^4$

In the central coordinate system: $J_x = 306578.424462 \text{ mm}^4$

$J_y = 1083569.880265 \text{ mm}^4$

$J_{xy} = -26058.319159 \text{ mm}^4$

In the main central coordinate system:

Axial moments of inertia $J_x = 305705.475406 \text{ mm}^4$

$$J_y = 1084442.829320 \text{ mm}^4$$

Inclination angle of the main axes

$$A = 358^\circ 4' 52.748778'' (358.081319^\circ)$$

Bend relative to the axis 0x:

Strength condition:

$$[\sigma]_W \geq \sigma = f^* M_{X \text{ MAX}} / W_X ;$$

$[\sigma]_W = [\sigma]_B = 750 \text{ kg/cm}^2$ - strength of aviation plywood according to
 $f = 1.5$ – safety factor;

$M_{X \text{ MAX}} = 11.35 \text{ kg} \cdot \text{m} = 1135.0 \text{ kg} \cdot \text{cm}$ - calculated bending moment;

$$W_X = 2 * J_X / h_{\text{MAX}} = 2 * 308894.661 / 62 = 9964.344 \text{ mm}^3 = 9.964344 \text{ cm}^3$$

$$\sigma = 1,5 * 1135.0 / 9.964344 = 170.86 \text{ kg/ cm}^2;$$

Actual flexural strength relative to the x-axis:

$$f_{\Phi \text{ AKT}} = [\sigma]_W / \sigma = 750 / 170.86 = 4.39$$

The condition of bending strength relative to the x-axis is fulfilled.

Bend relative to the axis 0y:

Strength condition:

$$[\sigma]_W \geq \sigma = f^* M_{Y \text{ MAX}} / W_Y ;$$

$[\sigma]_W = [\sigma]_B = 750 \text{ kg/cm}^2$ - strength of aviation plywood according to
 $f = 1.5$ – safety factor;

$M_{Y \text{ MAX}} = 3.12 \text{ kg} \cdot \text{m} = 312 \text{ kg} \cdot \text{cm}$ – torque;

$$W_Y = 2 * J_y / x_{\text{MAX}} = 2 * 1752969.453 / 140 = 25042.421 \text{ mm}^3 = 25,04 \text{ cm}^3$$

$$\sigma = 1,5 * 312 / 25,04 = 18,7 \text{ kg/ cm}^2;$$

Actual flexural strength relative to the x-axis:

$$f_{\Phi \text{ AKT}} = [\sigma]_W / \sigma = 750 / 18,7 = 40,1$$

The condition of bending strength relative to the x-axis is fulfilled.

Vertical Section (offset + torsion):

Total cutting force:

$$Q_{MAX} = (Q_{Y MAX}^2 + Q_{Y MAX}^2)^{0,5} = (17.53^2 + 5.08^2)^{0,5} = 18.25 \text{ kg}$$

Strength condition:

$$[\tau]_B \geq \tau = f * (M_{Z MAX} / (2 * S_{МИД} * \delta) + K * Q_{MAX} / S) ;$$

$S_{МИД} = 41.0 \text{ cm}^2$ – intersection area

$[\tau]_B = 200 \text{ kg/cm}^2$ - strength of aviation plywood on section according to

$f = 1.5$ – safety factor;

$Q_{MAX} = 18.25 \text{ кг}$ – total cutting force;

$M_{Z MAX} = 0.601279 \text{ kg*m}$ – torque;

$S = 6.2 \text{ cm}^2$ – intersection area

$$\tau = 1.5 * (0.6013 / (2 * 41 * 0.1) + 18.25 / 6.2) = 4.52 \text{ kg/cm}^2$$

The actual margin of safety of the cross section

$$f_{ФАКТ} = [\tau]_B / \tau = 200 / 4.52 = 44.2$$

The condition of cross-sectional strength is fulfilled.

3.4. Assembly Of The Blade

Structurally, the blade of the wind turbine is made of affordable and cheap materials that provide the minimum cost of production and the maximum possible service life.

The use of composites based on epoxy resins and fiberglass is planned to be limited, due to the property of such a composite to accumulate moisture in the capillaries of the power element and the impossibility of its removal. The effect of ambient temperature below 0 degrees leads to the destruction of the structure of the element at the level of brittle and inelastic fiberglass fibers of the composite due to the expansion of H₂O droplets during the transition to solid ice and fatigue cracks, which significantly reduce the strength of the product. To

avoid the influence of capillary moisture in the material of the power elements of composite structures, excessive strength reserves, dense multilayer coating of external and internal surfaces with wet repellent varnishes and paints and other time-consuming and expensive measures are usually used in the design.

Given the fact that the wind turbine by definition must work around the clock in any weather conditions, for the manufacture of power structures it is advisable to use this type of composite, which does not accumulate moisture in its structure, and exchanges it with the environment depending on humidity and temperature. . The fiber structure of the selected material should be elastic and highly reserved.

These requirements are fully met by aviation multilayer plywood, with appropriate antiseptic protection and moisture-repellent coating. The practice of world aircraft construction knows numerous examples of power aircraft wooden structures that have been in operation for several decades. Below in fig. 51 shows a photo of a 1927 De Havilland DH-82 Tiger Moth aircraft that has been in flight operation for 77 years. The design of the glider is completely wooden, treated with antibacterial protection and covered with a protective layer of varnish and paint. The claimed life of any composite structure does not exceed ten years due to objective factors that significantly reduce the strength parameters of the structure.

Below in fig. the general view of components of a design of a blade of the wind generator is resulted. Working drawings of structural parts and 3-dimensional model of assembly of the unit in the environment Compass 3D V13 are shown on the posters.

The design of the wind turbine blade is an integral one-piece beam with a working casing and a foam filler of the tail unloaded part. The connection of all components is carried out by gluing with polyurethane glue ISOL 3100 MONO, which is used in the practice of building yachts and is a certified adhesive joint.

The power frame of the blade consists of longitudinal and transverse power elements. The upper and lower shelves of the spar are the main elements that absorb the load on the bend. The rigid casing of the blade together with the wall form a closed power circuit that perceives torque. The flap is a closed power beam formed from a working casing and a transverse power set. Fastening of a flap occurs through assembly apertures in power ribs that forms a single whole with a covering of the main part of a shovel.



Figure 51 Power wooden construction

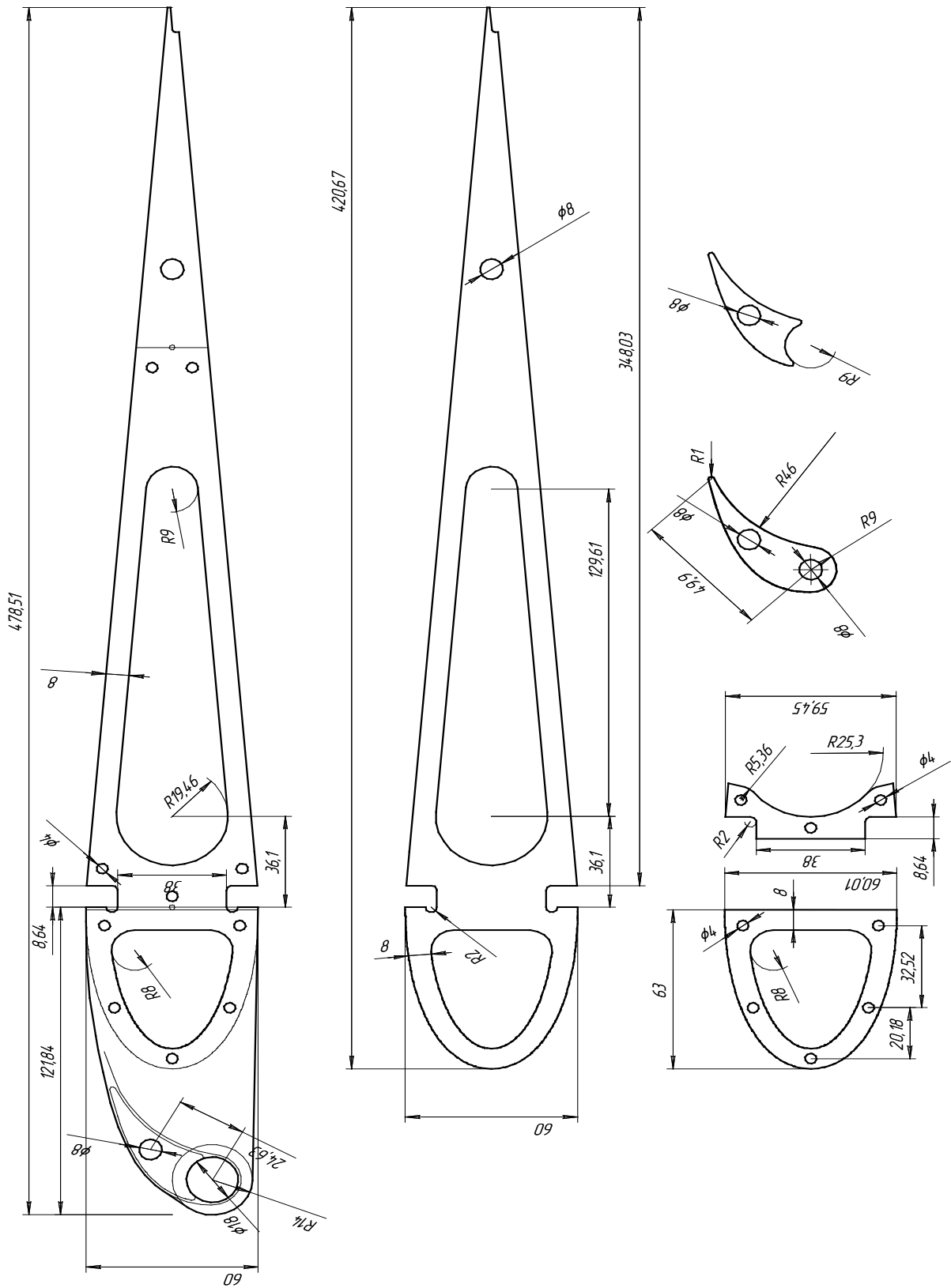


Figure 52 Components of a blade design.

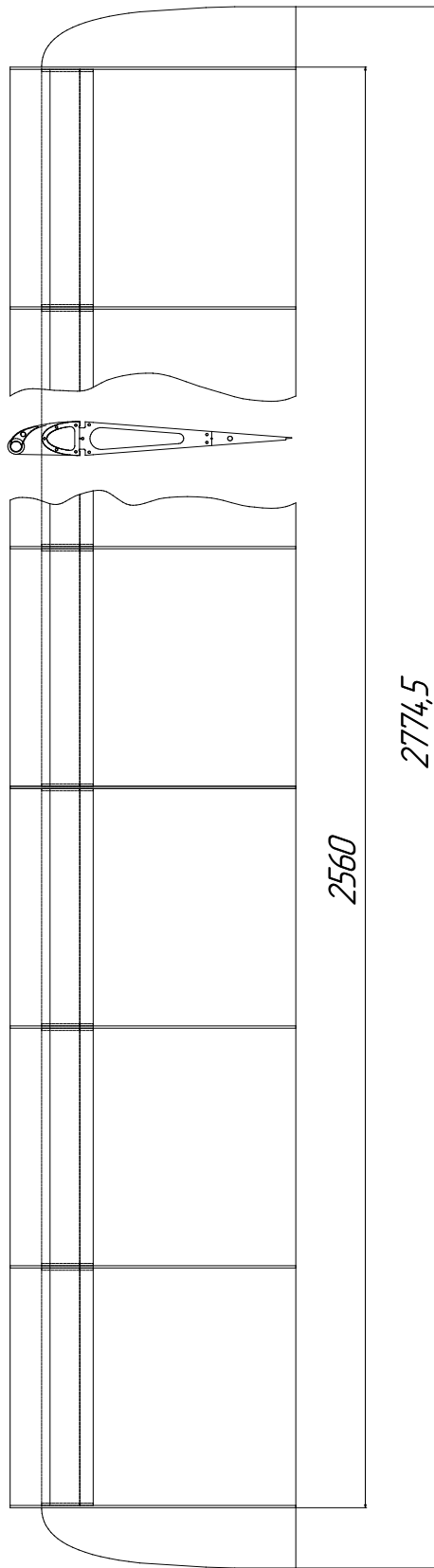


Figure 53 General view of the blade.

Conclusions On The Section.

1. Based on the results of calculation of external loads and analysis of the strength of the power section, the strength reserves of the blade structure are determined;
2. According to the results of design elaboration of structural elements, the characteristic dimensions of parts are obtained, which is sufficient for the formation of a 3D model of product assembly and working drawings in the environment of automatic design Compass.

4. TECHNOLOGICAL PART

4.1. Laser Cutting

The design of the wind turbine blade is as simple and technological as possible. The main technological processes are laser cutting and gluing.

The most widely used in industry is laser cutting of sheet materials, both metallic and non-metallic [1]. Laser cutting provides a cutting speed: 10 m / min, which cuts steel sheets up to 15... 20 mm thick, cutting thin sheets (up to 5 mm) provides excellent cleanliness of the cut, for sheets of large thickness - satisfactory. The use of laser cutting (hereinafter LR) is recommended for urgent orders. Modern laser cutting machines are equipped with a computer control system that allows you to quickly change the program of the technological process of cutting individual parts.

The basis of laser cutting is the thermal effect on the material of the absorbed laser radiation. When the laser radiation falls on the material, the energy efficiency of the laser beam depends on the surface properties of the material, in particular on the reflection coefficient. The reflection coefficient is the ratio of the intensity of the reflected light wave to the intensity of the incident laser beam and is determined by the optical characteristics of the material and the condition of the surface.

Areas of application of laser cutting are various. Examples include POS materials such as price tags, product stands, booklet and postcard stands, shelf packers and racks, as well as three-dimensional faceplates, logos and any decorative elements.

Similarly, the technology of laser cutting of plastic is used in the manufacture of various pockets, plastic folders, stands for shop windows for mobile phones, jewelry and so on.

In recent years, developers of turbojet engines have shown great interest in this technology. These parts work in extreme conditions, so require additional strengthening treatment. Laser strengthening technology is a multifactorial process that depends on more than thirty different factors, almost all of which together cannot be controlled at the same time.

Laser cutting machine has been used frequently in many fields recently. Many jobs such as wood laser cutting and engraving, plexi cutting, cardboard cutting, sponge cutting, leather and fabric cutting are done with laser cutting machines.

European-made laser cutting machines in the first year, then Far East made using laser cutting machines in the domestic market yayılmıştır.so time laser cutting machine models manufactured in Turkey has been released.



Figure 54 Laser Machine

The basis of laser cutting is the thermal effect on the material of the absorbed laser radiation. When the laser radiation falls on the material, the energy efficiency of the laser beam depends on the surface properties of the material, in particular on the reflection coefficient. The reflection coefficient is the ratio of the intensity of the reflected light wave to the intensity of the incident laser beam and is determined by the optical characteristics of the material and the condition of the surface.

In practice, the term absorption coefficient is often used, which characterizes the absorption of radiation by a material with a certain wavelength.

The absorption coefficient of polymers for infrared (IR) radiation ($5 \dots 15 \mu\text{m}$) is in the range of $0.86 \dots 0.98 \mu\text{m}$, and for the visible and near-infrared range ($\sim 1 \mu\text{m}$) these values are lower. In contrast to metals, in which the absorption of radiation occurs in the surface in the skin layer with a thickness of about $9 \dots 10 \text{ nm}$, the thickness of the absorbing layer in polymeric materials is much larger, ie in many cases laser heating can be considered volumetric. The mechanism of radiation absorption in polymers is quite complex and can differ significantly in different spectral ranges. This fact makes it difficult to determine the parameters of laser cutting of the polymer by calculation. Only the

accumulated experimental data allow to choose the parameters of laser cutting with some accuracy (Fig. 55).



Figure 55 Laser cutting of plastic

Laser cutting of plastic is one of the modern ways of cutting this material. The main advantage of this type of plastic processing is the ability to make complex molds. Laser cutting of plastic allows you to implement the boldest design ideas, including options for exclusive design. Gas lasers based on a mixture of CO₂-He-N₂ gases are used for laser cutting of plastic

This type of laser allows you to cut both metals and non-metals, including plastic, hardboard, wood and more. The use of quality equipment determines the price of laser cutting of plastic. In comparison with traditional methods of cutting materials, laser cutting of plastic has a number of undeniable advantages:

- at laser cutting mechanical influence on material is absent;
- focused laser flux allows to achieve a very smooth "mirror" surface;
- the installation of the laser cut is less than 0.1 millimeters, which allows you to perform parts with a high degree of accuracy of mutual fit;
- application of laser cutting is possible on easily deformed and not rigid details;
- the use of laser cutting technology allows you to create holes with a diameter of half a millimeter;
- due to the high power of laser radiation, high productivity of the laser cutting process is ensured.

Laser cutting allows you to make products of varying complexity, including options that are not available when using other cutting technologies.

Laser cutting services for plastic are performed with greater accuracy and with less waste. Laser cutting requires less cut tolerance, and all orders are executed in the shortest possible time and in large batches.

Areas of application of laser cutting are various. For example, these are POS-materials (Fig. 56), such as: price tags, stands for products, stands for booklets and postcards, shelf packers and racks, as well as front panels of three-dimensional letters, logos and any decorative elements. Similarly, the technology of laser cutting of plastic is used in the manufacture of various pockets, plastic folders, stands for shop windows for mobile phones, jewelry and so on.

The prices of laser cutting of plastic are relatively not high, even taking into account the high quality of products and in the absence of the need for additional processing. In addition, the number of manufactured parts has almost no effect on the final cost of laser cutting of plastic.



Figure 56 Pos-materials

Plastic cutting is most common in advertising for the production of pos-materials, souvenirs, plates, signs, etc.

The cutting speed of 3 mm plastic on a laser machine with a CO2 laser with a power of 60 W is usually 1... 1.3 meters per minute. The width of the cut is 0.1... 0.2 mm, the edge is close to polished, and does not require further processing. On such a laser machine you can cut acrylic, plexiglass up to 30

mm. Naturally, with increasing thickness, the cutting speed decreases. The dependence of the cutting speed on power is close to linear. Compared to milling plotters, the laser machine is characterized by approximately 10 times higher cutting speeds.

For the production of pos - materials requires high - precision cutting of product parts. For cutting elements, as a rule, laser equipment with a large cutting table up to 1600x2000 mm is used. Acrylics, polystyrenes, petg, etc. are used as raw materials.

To bend the plastic, a "string" is used, which is a table with a stretched string, which is supplied with electric current and due to which it is heated.

The product is placed on a table above the string, and as soon as the plastic is heated and it becomes plastic, it is deformed and fixed. Once the plastic cools, it will "remember" its condition.

Economic advantage: Laser cutting is a profitable choice of technology. Careful analysis of the features of the most affordable cutting systems guarantees the optimal result in the following aspects:

- reduction of overall work;
- increasing product quality;
- technological advantage;
- laser cutting is, first of all, an accurate, clean and quiet method of material processing.

In addition, laser cutting has the ability to perform work on complex profiles and with very small beams of curvature. Unlike traditional cutting systems, light has no mechanical pressure on the parts. Laser contactless tool that guarantees:

- complete absence of mechanical pressure on parts;
- no tool wear.

The ability to cut depends on the hardness of the material, the coating, or the treated surface of the materials. Laser cutting also has a high degree of automation and flexibility, and is able to offer: ease of integration with other automated systems, very high cutting ability, quick ability to adapt to changing production needs. In many cases, laser cutting can produce ready-made pieces that do not require further processing (grinding, burr removal, processing, etc.).

Machines For Processing Materials



Figure 57 Installation of laser cutting of TRUMATIC LC-3030

Characteristics of the laser installation of the world-famous company TRUMPF (Switzerland), which is a recognized leader in the market of equipment for high-quality laser cutting of various materials. (Fig 57.):

- thickness of the processed sheet: 0.6 mm ... 20 mm;
- dimensions of the processed sheet: 1500mmx3000 mm;
- accuracy of program execution: ± 0.1 mm;
- cutting edge from Ra 3.2 at a thickness of 1 mm to Rz 320 at a thickness of 20 mm.

The main area of application of the RV6L and RLP16 machines is cutting the lining of the car interior. The advantage of laser cutting is the simultaneous compaction of the cut and the reduction of processing steps.

4.1.2 Principle Of Operation, Structure And Characteristics Of Co2 Laser

Molecular gas-discharge lasers (molecular GRL) are widely used in various fields, including medicine. There are more than 100 types of molecular GRL, produced by both domestic and foreign firms

As the active medium is mainly used CO₂ gas with various impurities (N₂, He), which increase the radiation power and efficiency of these devices.

In fig. 58 shows diagrams of the energy levels of the main electronic states of CO₂ and N₂ molecules. Since N₂ is a diatomic molecule, it has only one oscillating mode, the two lower energy levels of which ($v = 0$, $v = 1$) are shown in the figure.

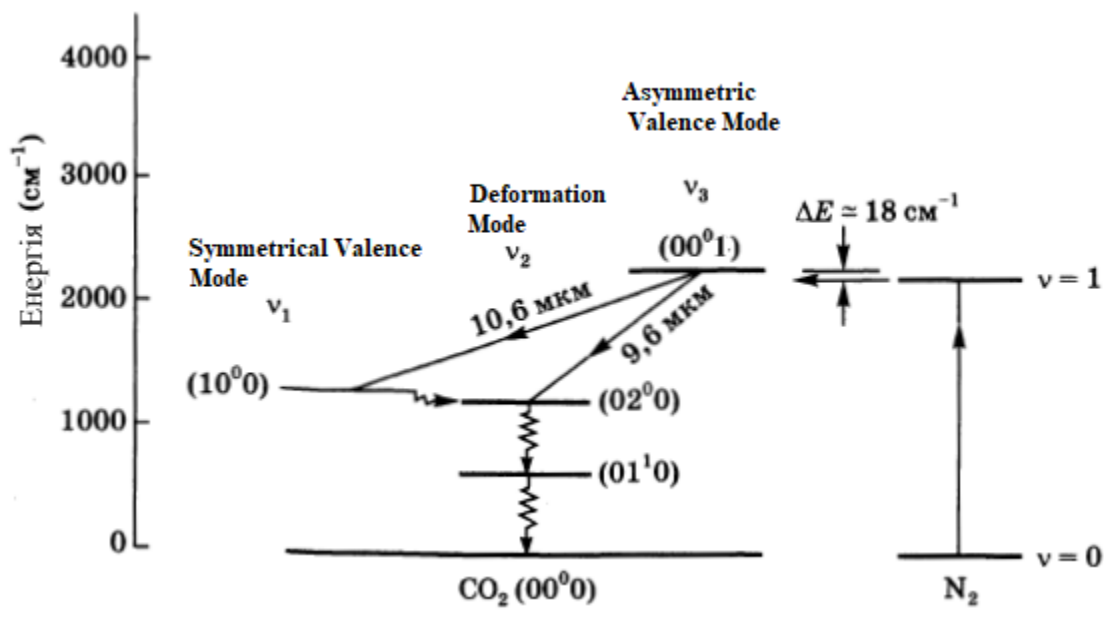


Figure 58 Lower vibrational levels of the ground electronic state of CO2 and N2 molecules (for simplicity of drawing, rotational levels are not shown here)

The structure of the energy levels of the CO2 molecule is more complex because this molecule is linear triatomic. There are three degenerate oscillating modes namely:

- 1) symmetric valence mode;
- 2) deformation mode;
- 3) asymmetric valence mode.

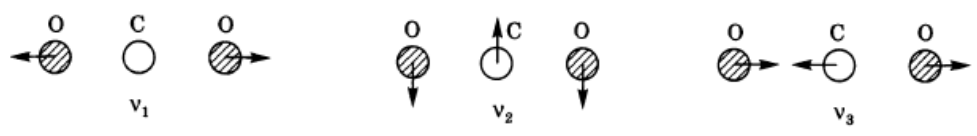


Fig. 58. Three fundamental vibrational modes of the CO2 molecule: (v1) symmetric valence mode, (v2) deformed mode, (v3) asymmetric valence mode

Therefore, the oscillations of the molecule are described by three quantum numbers n_1, n_2, n_3 , which determine the number of quanta in each oscillatory mode. This means that the energy calculated from the zero level is given by expression (2.1)

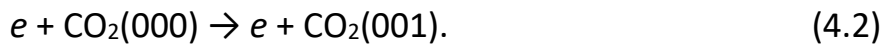
$$E = hv_1 + hv_2 + hv_3, \quad (4.1)$$

v_1, v_2 and v_3 - resonant frequencies of three modes.

Generation occurs at the transition between CO2 and 1000 levels ($\lambda = 10.6 \mu\text{m}$), although it is also possible to obtain generation at the transition between levels

$00^0 1$ and $02^0 0$ ($\lambda = 9.6 \mu\text{m}$). Pumping to the upper laser level $10^0 0$ is effective due to the following two processes:

1) direct collisions with electrons. Obviously, the main type of collisions to be considered is (2.2):



2) resonant energy transfer from the N_2 molecule. This process is also very efficient due to the fact that the energy difference between the excited levels of the two molecules is small ($\Delta E = 18 \text{ cm}^{-1}$). In addition, the process of excitation of the N_2 molecule from the ground state to the level of $v = 1$ is very effective in collisions with electrons.

From the point of view of a design of this CO_2 laser it is possible to divide into eight types:

- 1) lasers with slow longitudinal pumping;
- 2) unsoldered lasers;
- 3) waveguide lasers,
- 4) lasers with fast longitudinal pumping;
- 5) lasers with diffusion cooling;
- 6) lasers with transverse pumping;
- 7) lasers with transverse excitation at atmospheric pressure (TEA lasers);
- 8) gas-dynamic lasers.

The studies were performed using a desoldered type CO_2 laser. Therefore, the design of this type of laser will be considered in more detail.

The desoldered laser is a further development of a laser with slow longitudinal pumping. In a laser with slow longitudinal pumping, the gas mixture is slowly pumped along the laser tube only to remove dissociation products, in particular CO , which contaminate the laser medium (Fig. 59).

If the device shown in Fig. 59, stop pumping the gas mixture, then after a few minutes the generation will stop, because the products of the chemical reaction (in particular, CO molecules) formed in the discharge will not be removed but absorbed by the walls of the tube or begin to interact with electrodes, thus disturbing the mixture $\text{CO}_2\text{-CO} - \text{CO}_2$.

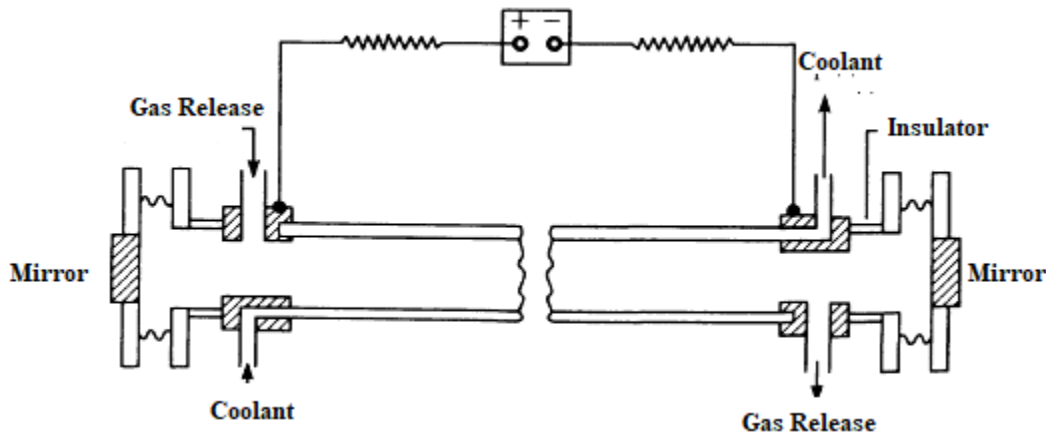


Figure 59 Schematic representation of a CO₂ laser with late gas flow

Eventually, this will lead to the dissociation of a large number of CO₂ molecules in the gas mixture. To ensure the regeneration of CO₂ molecules from CO, a certain catalyst must be present in the gas discharge tube of the desoldered laser. To do this, you can simply add a small amount of water vapor (about 1%) to the gas mixture. In this case, the regeneration of CO₂ molecules is carried out by the following reaction (2.3):



In which oscillatingly excited molecules of CO and CO₂ take part. The required relatively small amount of water vapor can be obtained by adding gaseous hydrogen and oxygen to the discharge. In fact, only hydrogen needs to be added to the mixture, as oxygen is formed during the dissociation of CO₂ molecules.

Another possibility of initiating a relaxation reaction is based on the use of a hot (300 °C) nickel cathode, which acts as a catalyst. The application of these methods has led to the creation of desoldered tubes with a durability of more than 10,000 hours.

The output power of desoldered lasers per unit length is about 60 W / m. Low-power (about 1 W) desoldered lasers with a short resonator (allows you to work in single-mode) are often used as local oscillators in experiments on optical heterodyne.

Soldered CO₂ lasers with a higher power (about 10 W) are widely used in laser microsurgery, as well as in micromachining.

The main parameters of CO₂ lasers are shown in table 1.

Laser type	Wavelength λ , мкм	Energy in momentum, E, J	Pulse duration, τ , с	Pulse frequency, f, Гц	Power (non- trans.), P, Вт	Angular discrepancy, α ,	KKD η , %
Pulse mode							
CO ₂ with radio frequency pumping	10,6	$5 \cdot 10^{-2}$	10^{-4}	100–2500	–	4	≤ 10
CO ₂ -TEA	10,6	10^{-1} 20	10^{-5} 10^{-6}	10^2 200	–	2,5 10	≤ 10 ≤ 10
Continuous mode							
CO ₂ , with slow longitudinal pumping	10,6	–	–	–	100– 1000	1	10
CO ₂ , high power	10,6	–	–	–	200	1,5	12
With slow longitudinal pumping, diffuse cooling, multibeam	10,6	–	–	–	To 3 КВт/м	1	9
With fast longitudinal pumping, convective cooling	10,6	–	–	–	To 5 КВт/м	1,3	8
With transverse pumping, convective cooling	10,6	–	–	–	To 100 КВт/м	1,5	≤ 10
Gas-dynamic, convective cooling	10,6	–	–	–	More 100 КВт/м	1,5	1

4.1.3 Interaction Of Laser Radiation With Polymers

Laser cutting of polymeric and composite materials is widely used in technological processes of manufacturing products. The use of laser radiation (LV) allows to solve complex technical problems, automate technological processes, significantly improve the productivity and quality of products

The process of laser cutting of polymers and composites is based on thermochemical and thermophysical mechanisms of material destruction. The energy of laser radiation is absorbed by materials, converted into heat, which causes rapid heating and destruction of the material.

The efficiency of laser destruction of polymeric materials depends on the amount of energy absorbed at a certain power density. Under the action of infrared (IR) laser radiation (CO₂, CO - lasers) on polymers and composites, there is a surface energy absorption, the depth of the layer is from particles to tens of micrometers and depends on the composition of the polymer and

composite. The relaxation time of laser energy into heat in polymeric materials is 10^{-12} - $3 \cdot 10^{-10}$ s, which is a high-intensity heat source.

The thermophysical properties of the material have a great influence on the process of destruction of polymeric materials. For most polymers, the thermal conductivity is in the range $(0.15, 0.50) \cdot 10^{-2}$ W / cm * K. Polymers are poor conductors of heat and all the effects associated with the destruction will be superficial.

The processes of destruction of polymers under laser radiation have distinctive features, in comparison with metals. The kinetics and mechanism of laser destruction of polymeric materials depend on their structure and vary greatly, which creates certain difficulties in generalizing the facts of the process of destruction of polymers.

Polymers are divided into three categories depending on their behavior under laser exposure:

- polymers that melt and spray;
- polymers that form a layer of coal on the surface;
- polymers that evaporate without residue.

The first group includes mainly thermoplastic polymers: polyethylene, polypropylene, polyethylene succinate, nylon, nylon, polystyrene, polymethyl methacrylate (PMMA).

The second group includes, first of all, aromatic thermoactive polymers (polybenzimidazole, polycyanurates, polyphenylenes), as well as some thermoplastics (polyphenylene oxide, polyphenylquinoxaline, polyarylate, etc.), polycarbonate (PC), polyfluorochloroethylene (PTFE).

The third group includes polymers: polytetrafluoroethylene (PTFE), polymethylstyrene, polyethyl methacrylate, as well as PMMA and PS. The difficulty of choosing technological modes of laser cutting of non-metallic composite materials is that the reinforcing fibers and binders have different characteristics, such as thermal conductivity, evaporation and melting temperatures, optical properties for a given wavelength and others. The thermal conductivity of a fiber is an anisotropic property, while for a binder it is a bulk property.

The results of experimental studies on laser cutting of polymeric materials have shown that the difference in thermophysical properties of the constituent material components requires optimization of energy and spatial parameters of

laser radiation used for cutting, as well as cutting speed. To ensure high quality of the cut, it is necessary to use single-mode radiation with Gaussian distribution, which provides the locality of heating and destruction of the composite. Studying the effect of laser radiation with different wavelengths, it was found that composites based on fiberglass (T10 + EBSM, etc.), organotissue (SVM + ELUR - 008PA), carbon fiber (UT - 900-30A) can be cut by laser radiation CO₂ - laser laser and C - laser, respectively, 10.6 μm; 1.06 μm and 0.578 μm. It should be noted that the quality of the cut increases when using the pulse-periodic nature of the radiation.

Laser cutting of non-reinforced polymers has its own features, which depend on the thermophysical properties of the processed materials:

Cutting acrylic glass (Fig. 60). The usual mode of laser cutting is the process of exposure to laser radiation on the material, the movement of the impact zone and the supply of compressed air to the impact area. The surface of the cut has a characteristic roughness in the form of "teeth", this is due to the physics of the laser cutting process in this mode.

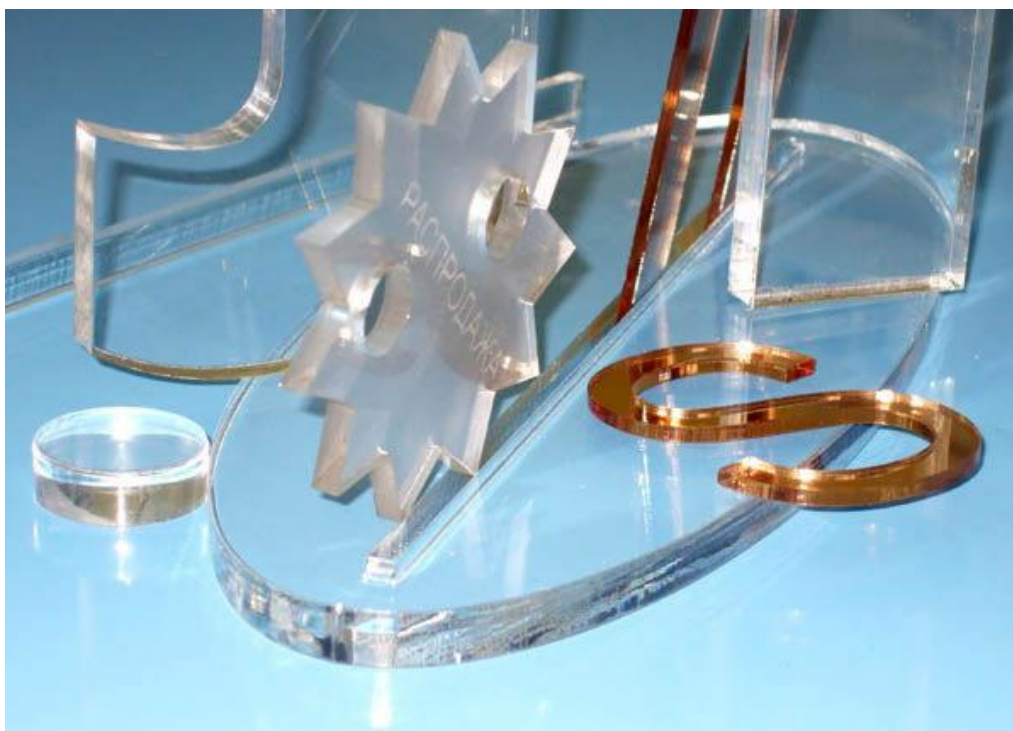


Figure 60 Cutting acrylic glass

Polishing cut mode. In this mode, compressed air is not supplied to the cutting area, the cutting speed is reduced. In this case, under the influence of laser radiation, the surface of the cut melts and under the action of surface tension forces, a polished surface is formed. On colored acrylic glass, the effect

of a polished cut is less pronounced. It should be noted that acrylic is prone to the formation of microcracks from the end of the cut.

Cutting of foamed PVC plastics. The end surface of the cut is brown. Formed in the process of cutting PVC vapors are absorbed into the porous surface of the cut, giving it a dark color to some depth. Increasing the air supply to the cut area slightly reduces the blackness of the cut, which turns light brown.



Figure 61 Foamed PVC sheets

Cutting of polystyrene. When cutting polystyrene, melting processes predominate. If compressed air is supplied to the cutting zone at low pressure, a cut is formed on the lower surface of the cut. With increasing pressure, the burr decreases, but filamentous products of destruction are formed, blows out of the cutting zone. The cutting speed of polystyrene is slightly less than that of acrylic glass.

Cutting of polyester glass PTEF. This material is well cut by laser radiation. The end surface of the cut is transparent, the roughness is slightly less than that of acrylic glass.

Powerful laser radiation, when interacting with polymers there are irreversible changes in their structure. The method used refers to calorimetric, in which thermal effects are recorded in a sample to record the absorbed radiation power in a sample. As a result of nonradiative relaxation transitions, the sample is periodically heated with a frequency equal to the modulation frequency.

In the process of heat transfer, part of the heat flow is transferred to the surrounding gas, the periodic heating of which leads to a change in pressure in the KLA. According to the one-dimensional model of the "acoustic piston", the illumination of the optical-acoustic signal (OAS) is mainly due to heating from the sample of a thin near-surface layer.

This layer with periodic thermal expansion acts like a piston, causing a change in gas pressure in the KLA. The joint solution of the equations of thermal conductivity and gas dynamics in the framework of a one-dimensional model of an acoustic piston leads to the expression for the intensity of SCA

$$J_{OAC} = \left| \frac{\gamma P q_0 A S (l_T^r)^2}{2\sqrt{2TV} \lambda_r} e^{i(\omega t - \frac{\pi}{4})} \right| \quad - (4.4)$$

P, T, V - pressure, gas temperature and volume of KLA, respectively; h is the thickness of the sample; l is the length of thermal diffusion in the sample; A is the thermal conductivity of the sample; thermal conductivity of gas, respectively; J is the ratio of the heat capacity of the gas at constant pressure and volume; q₀ is the power density of the laser radiation on the sample; S is the area of the irradiation zone.

Equation (2.4) does not take into account the release or absorption of energy due to thermal effects in physicochemical processes occurring in the material, and can be used to analyze and evaluate SLA in an "inert" substance in which these processes do not occur during laser heating. In this case, the generation of sound is due to thermal expansion, heated areas of the material and the surrounding gas layer, and the optical-acoustic curve (UAC) - depending on q₀ - is linear.

The energy spectrum obtained by the optical-acoustic method allows to quantify the threshold value q₀, to qualitatively assess the intensity of thermal effects during physicochemical processes. To study the main stages and threshold characteristics of the action of laser radiation on materials, an optical-acoustic method was used, which is based on the established fact of changes in the intensity of the acoustic signal due to physicochemical transformations in the sample. These transformations, accompanied by an exothermic or endothermic effect, lead to a deviation from the linear law of the optical-acoustic curve, which characterizes the dependence on q₀.

The studies were performed using a continuous CO₂ laser. As the main characteristics of the radiation were measured and calculated energy characteristics: laser power P₀ and power density q₀ on the surface of the material (measured after passing the laser beam of the optical system); threshold values of radiation power density. To register the energy spectrum and determine the threshold characteristics of the interaction of laser radiation with

materials, an installation was created, the scheme of which is shown in Figure 62

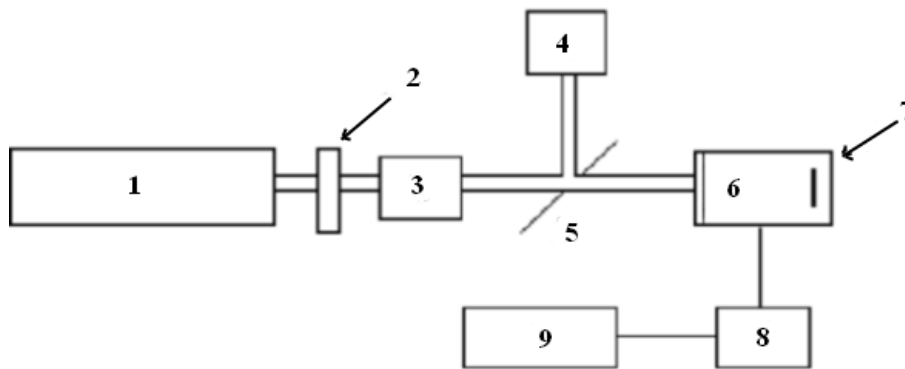


Figure 62 Scheme of experimental optical-acoustic installation:

1 - CO₂ laser; 2 - attenuator; 3 - power density control unit; 4 - power meter IMO-2; 5 - rotary mirror; 6 - optical-acoustic cell; 7 - sample; 8 - amplifier; 9 - oscilloscope.

The radiation of the continuous CO₂ laser (1) by the modulated attenuator (2), after the optical system consisting of the fine power density control unit (3), enters the optical-acoustic cell (6), in which the sample (7) is located. Gas pressure fluctuations in the optical-acoustic cell are recorded by a microphone, the signal from which after passing the amplifier (8) is output to a digital memory oscilloscope (9) type C9-8 [24]. The optical system is designed to specify the required power density of laser radiation. The unit (3) of precise power density control is a set of plane-parallel CsJ - plates.

The research was carried out in the mode of discrete scanning q_0 , which allows to trace the time course of the SLA as a transient function to the external influence, and to determine the threshold characteristics of the destructive processes from the form of the SLA.

These diagrams can be interpreted as follows: the first stage corresponds to the linear section of the OA curve, which characterizes the elastic oscillations of both individual fragments and the entire polymer system. The linear dependence on q_0 shows that due to the decrease in q_0 the sample does not accumulate the amount of heat required to start the destructive processes.

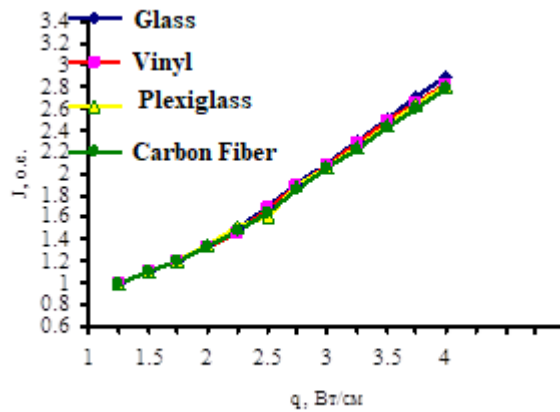


Figure 63 Optical-acoustic diagram

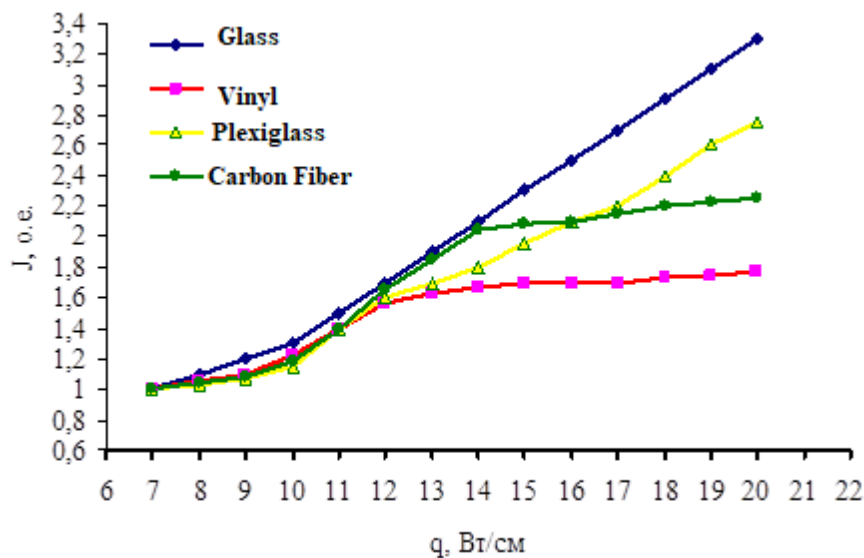


Figure 64 Optical-acoustic diagram

The effect of laser radiation does not change the physical state of the polymer system, and the generation of sound is due to the thermal expansion of the areas of the material heated by the radiation and heat transfer in the gas layer. As the power density q_0 increases (the second stage of the process (Fig. 64)), the total amount of heat released in the irradiated area of the material increases.

The OA curve at this stage is complex. The second stage is characterized by the presence of exothermic and endothermic effects. A further increase in q_0 leads to the rapid formation of a condensed structure (such as pyrocarbon). The

OA curve extends to a linear segment. The further linear character of the curve is due to thermal expansion and, as a result, thermoelastic oscillations form a condensed structure.

In the course of experimental studies it was found that at a laser power density in the range of $0 \dots 7.3 \text{ W / cm}^2$ the optical-acoustic signal for all studied materials has a linear dependence, which indicates the absence of destruction processes in these materials. When the energy threshold is exceeded, destructive processes begin, different for the studied materials. The dynamics of destructive processes was studied and the dependences obtained allow to determine the threshold characteristics of the effect of high-power laser radiation on polymers.

Experiments on laser cutting of the investigated polymers presented above were also carried out. To do this, developed and manufactured the installation shown in Figure 65.

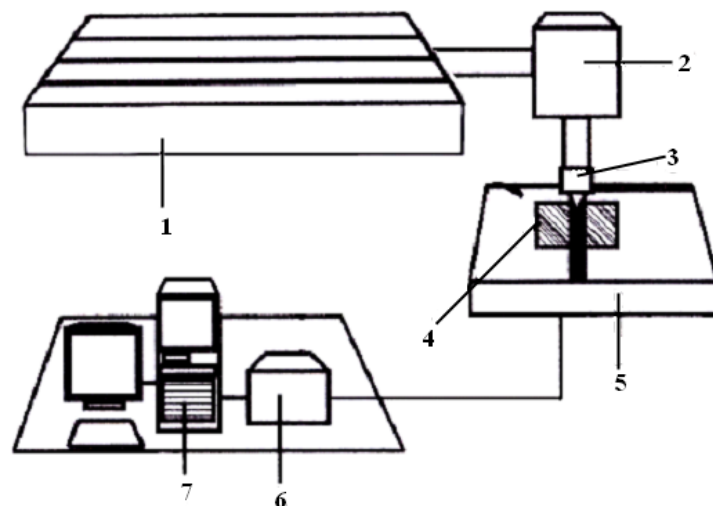


Figure 65 Scheme of the experimental setup:

1 - CO₂ laser, 2 - optical-mechanical unit, 3 - condenser lens, 4 - test sample; 5 - two-coordinate recorder, 6 - device for communication with a computer; 7 - IBM PC

To achieve the best laser cutting parameters, the optimal distance from the lens to the sample was selected.

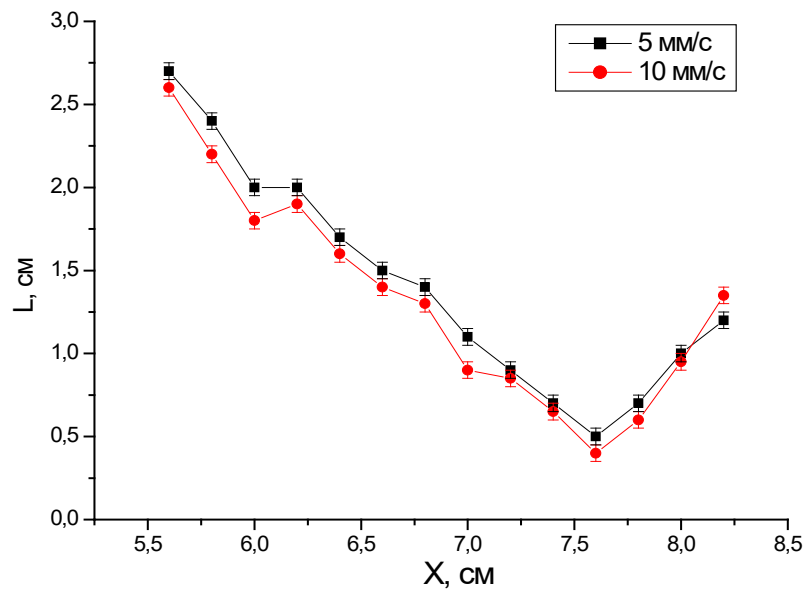


Figure 66 Determination of the optimal distance from the lens to the sample

From the graph in Fig. 67 shows that the best parameters of the cut are achieved at a distance between the lens and the material $L = 7,6$ cm

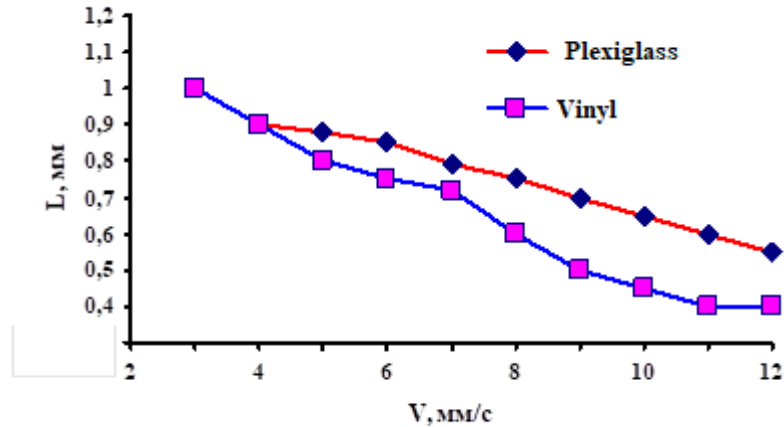


Figure 67 Dependence of the width of the cut on the speed of the laser for plexiglass and vinyl

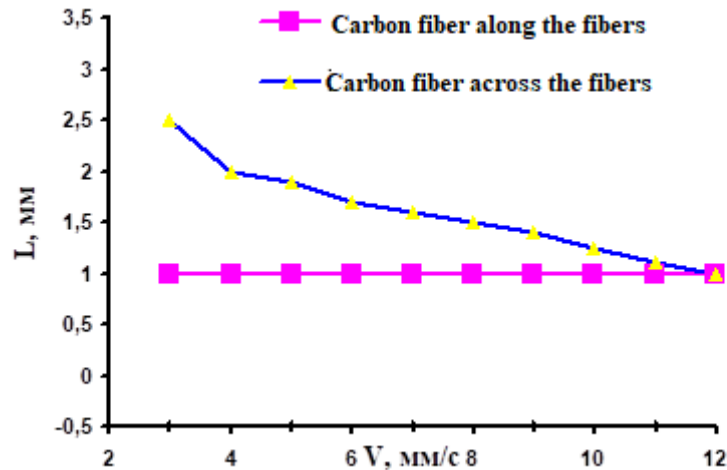


Figure 68 Dependence of the width of the cut on the speed of movement of the laser for carbon fiber

The invariance of the width of the cut along the fibers can be explained by the fact that the structure of carbon fiber (Fig. 68) along the reinforcing fibers of the isotropic has the same absorption coefficient, so that the impact of powerful laser radiation in this direction proceeds equally, regardless of.

4.2. Bonding Wood

Bonding is the main type of connection of details in joiner's and furniture production as a result of which it is possible to make details of any sizes and forms.

The main types of gluing are:

Gluing of bars or boards by planes in blocks for production of details of big section (fig. 68., a); gluing boards by edges in boards for increase in width (fig. 68., b); gluing of thin plates of wood (veneer) with simultaneous bending for production of bent (bent glued) details (fig. 68. in); facing, ie pasting of wood parts of low-value breeds with thin veneer of more valuable wood species (Fig. 68., d) \ gluing of bars, glued plywood or veneer in hollow boards with different filling (Fig. 68., e); connection of details in knots and products at their assembly (fig. 68., is); pressing of small wood (shavings, sawdust, etc.) mixed in glue, in various details and knots.

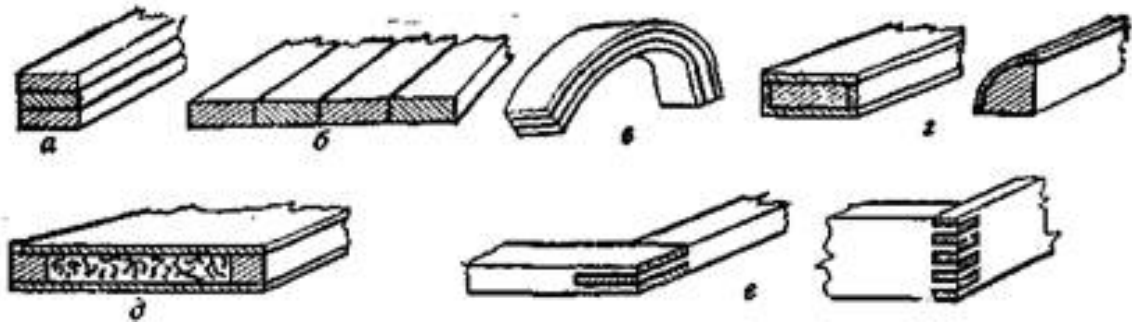


Figure 69 The main types of gluing wood

The technological process of gluing consists of the following operations: preparation for gluing parts and veneer; preparation of adhesive solution; applying an adhesive solution to the wood; pressing of glued parts and keeping them in a compressed state until the glue sets; keeping the glued parts after pressing.

The glue applied on a surface of details gets into intercellular and intracellular spaces of wood, hardens there and as a result as if sews up glued surfaces by thin threads (villi). At the same time, a very thin layer of glue (0.08-0.15 mm) is formed between the glued surfaces. When the thickness of the adhesive seam is less than 0.08 mm, its strength decreases, and this bonding is called "hungry". At a thickness of more than 0.15 mm, the strength also decreases, because the villi lubricated with glue do not touch, and a thick adhesive layer cracks over time.

The strength of adhesive joints depends on the uniformity of the adhesive layer, the tightness of the bonded planes, as well as the quality of the adhesive. In the laboratory, the bonding strength is determined by breaking the glued samples on special breaking machines. In production conditions, the strengthening of bonding is determined by splitting the glued wood samples with a chisel along the seam.

There are four characteristic splits: on wood, on wood - glue, on glue - wood and on glue.

Splitting on wood means that the adhesive seam is stronger than wood. The split on the wood - glue also indicates the high strength of the adhesive seam, because more than half of the gluing area split on the wood, and less - on the glue. Split on glue - wood indicates low strength of the adhesive seam, because more than half of the bonding area split on the glue and less - on the wood. Splitting on the glue indicates low bond strength. This glue can not be used in any case.

For high-quality gluing it is necessary to choose correctly type of glue, to prepare an adhesive solution; apply it evenly on the wood and strictly adhere to the gluing modes.

Choice of glue and preparation of glue solutions

Preparation of working solutions of gluten glues. Gluten glues come into production in the form of tiles, shavings and galleys. When preparing an adhesive solution from tile adhesive, the tiles are placed in a vessel with water for 6-12 hours to swell. The ratio of water and glue in the solution is taken depending on the type and type of glue, as well as the type of bonding.

Its concentration, viscosity and density are of great importance for the quality of the adhesive solution.

The concentration of the adhesive solution is called the percentage in the solution of commercial dry glue. The concentration of commodity-dry glue in the solution of core glue for gluing bars should be 30-35%, for cladding - 35-40%, bone for bars 35-40%, for cladding 45-50%. For facing take thicker glue that there was no "punching" it on the front side of an interline interval.

The amount of tile or chip glue GK to prepare the required amount of adhesive solution of a given concentration is determined by the formula, kg,

$$G_x = \frac{kN(100 - W_1)}{100(100 - W_2)}, \quad (4.5)$$

k is the specified concentration of the solution,%; N - the required amount of adhesive solution, kg; W1 - humidity of commodity-dry glue, which is 15-17%; W2 - humidity of the available glue,%,

Hence the amount of water GB to be added to the glue, determine kg:

$$GB = N - GK$$

After swelling of tile glue (chip and gallet without swelling) it is cooked at a temperature of 70 .80 ° C in an oilcloth or a boiler with double walls. It is not recommended to cook glue for a long time at a temperature above 80 ° C, because under such conditions its stickiness decreases. If the glue foams, it should be boiled for 5-10 minutes and remove the foam. The solution is suitable for use if there are no clots when stirring. During operation, the temperature of the working solution should be 60 .80 ° C, so all utensils should have double walls ", between which hot water is poured to maintain the appropriate temperature of the adhesive solution. Gluten adhesives should be prepared in the amount required by no more than one two days, because they harden, and if the

adhesive solution hardens, it is heated again, and the bonding strength of gluten glues is 6-8 MPa.

To prepare the solution, pour the required amount of water into the vessel and, stirring constantly, add the glue powder. Stirring is continued until complete dissolution of the powder (30-60 minutes) and the formation of a homogeneous creamy mass. Depending on the required viscosity, 1.7-2.3 parts by weight of water at room temperature (18-20 °C) are taken for 1 part by weight of glue. The glue cannot be dissolved in hot water, because casein twists and loses its stickiness. The glue solution of casein glue can be used for no more than 6 hours. Bonding strength - 8-10 MPa. Mechanical adhesive mixers are used to prepare the solution.

Preparation of working solutions of synthetic (resin) glues. A hardener that causes a chemical reaction is added to the dissolved resin of the appropriate grade. For hot bonding the hardener is ammonium chloride (NH_4Cl), which is taken 0.2-1.5% by weight of the resin, and for cold - 10% oxalic acid in the range of 1.5-2.8% or 40% lactic acid in the range of 4-6% (the latter for M-60 glue).

The viscosity of resin adhesives should be in the range of 30-300 s according to VZ-4. To reduce the viscosity of the glue add a certain amount of water, and to increase it add wood flour or other filler.

The optimal amount of hardener for different resins, depending on their properties, is specified in the instructions for bonding or is established experimentally. The viability of synthetic adhesives is small (2-6 hours) and depends on the temperature of the adhesive solution. Even with a slight increase in temperature (25 °C) the service life of the adhesive solution is significantly reduced. Therefore it is more expedient to keep ready solutions of glues in a vessel with double walls, the space between which is filled with cold water that prolongs service life of glue.

To prevent the release ("puncture") of the adhesive solution through the veneer, as well as to reduce its costs urea-formaldehyde adhesives are foamed before use. To do this, when mixing the resin with the hardener, a substance is added to the resin that promotes the formation of foam (usually 0.5-1% of powdered albumin by weight of the resin). Mixing of these components takes place in special mixers with lattice blades, making about 300 rpm for 30 minutes. Most resins are foamed at atmospheric pressure, and the resin MF-17 requires an excess pressure of about 0.2 MPa, which is achieved by supplying compressed air to a hermetically sealed boiler.

After foaming, the adhesive foam becomes 3-4 times more than the adhesive solution. The foamed glue has small spillage that gives the chance to spend it economically.

Preparation of the surface of parts for gluing and application of adhesive solutions on them

For high-quality bonding, the adhesive solution is applied to a well-prepared flat and smooth surface so that the bonded sides fit well together. The surface roughness should be within the 7th-8th class (GOST 7016-82). This surface can be achieved by milling parts on machines with diameters of knife shafts of 120-150 mm, rotating with a frequency of 5000-6000 rpm at a feed rate of 8-10 m / min. Sanding, which was previously widely used before bonding and cladding, is not recommended because it thickens the adhesive layer, which greatly reduces the bonding strength.

The adhesive solution is usually applied only to one of the glued parts. And only at gluing of thorn connections, and also end faces and chipboards glue put on both glued details in a uniform layer with a small margin on extrusion.

There are three ways to heat the adhesive joints: heating through wood, preheating the wood and direct heating of the adhesive seam.

When heated through wood, the heat from the heater passes through a layer of wood into the adhesive seam. The thicker the layer of wood, the more time it takes to heat it up. This method can only be effective for gluing thin parts or sheet materials. In particular, it is widely used in cladding, as the thickness of the veneer is 0.6-1.0 mm.

Preheating the wood, or heat accumulation in the wood, is that one or both glued parts are heated before applying the glue, and then compress them. Heated wood transfers heat to the adhesive seam, which hardens due to rising temperatures. For fast heating of wood the temperature of heaters should be about 200 ° C. At higher temperatures, the destruction of the wood surface begins (thermal destruction), at lower temperatures, the amount of accumulated heat decreases or the preheating time increases. This method can be used for parts not less than 10 mm thick.

Direct heating of the adhesive seam is the most effective way. It is carried out using high frequency currents (microwave). To do this, the glued parts are placed between the metal plates-electrodes, to which high-frequency current is applied. A high-frequency field is formed between the electrodes, which penetrates the bonded material. This field interacts with molecules and atoms of the material, causing the displacement of their positively and negatively charged

parts. Since the field is variable, the displacement of the parts occurs in one or the other direction. High-frequency oscillations of the parts inside the material occur with the overcoming of internal forces that balance the system. The energy expended on this is released in the form of heat.

High-frequency generators are used to convert industrial frequency current into high frequency current.

Gluing modes

The gluing process consists of operations that must be performed sequentially under certain conditions. The set of rules that indicate how and under what conditions gluing is performed is called the gluing mode.

The main factors of the mode are the amount of glue applied per unit area of the glued surfaces, room temperature, wood temperature, glue solution temperature, holding time in pressing (open and closed), pressure, temperature at pressing; press exposure time.

Depending on the type of glue, its costs can be different. It is established that good quality of gluing can be reached at the expense of glue solutions, g / m²:

Collagen (gluten) 200-350

Casein 160-280

Urea (K-17, MF, M-60, M-70) 140-200

Phenol-formaldehyde 160-250

When gluing stud joints of half-end surfaces, as well as when gluing with simultaneous bending, the consumption of the adhesive solution should be increased by 50%. At this rate of consumption, the thickness of the adhesive layer is 0.08-0.15 mm, and this provides high bonding strength.

Humidity and temperature of wood. The moisture content of wood has a great influence on the bonding strength. We have the highest strength of glued parts at humidity within 8-10%, and veneer - 6%. It is not necessary to glue details of various humidity as at drying they groove, on the more damp party the concavity is formed, and in a glue seam - internal stresses.

The normal temperature of wood is considered to be 18 .25 ° C. And at low temperatures, collagen adhesives quickly dredge, and synthetic cold-curing adhesives slowly harden. When the wood is very hot, collagen adhesives will remain liquid for a very long time and can be easily squeezed out under

pressure, and even seep through the veneer when facing. Synthetic adhesives can cure prematurely even before pressing, which greatly reduces the bond strength.

Table 4.2. Wood Gluing Modes

Element Mode	Mode indicator for		
	Gluten Glue	Casein Glue	Synthetic Glue
Room temperature, ° C	18 .25	12 .22	16 .22
The temperature of the adhesive solution, ° C	60 .80	12 .22	18 .22
Relative humidity, %	65	65	65
Spreading the adhesive solution: at the same direction of fibers			
wood	—	One-sided	—
at different directions of fibers			
wood	—	Bilateral	—
Duration of open and closed impregnation, min	To 1	4—6	До 20
Duration of exposure under pressure, h			
details from coniferous breeds	4—5	3—4	2—3 хВ
details from firm deciduous breeds	5—6	4—5	3—4 хВ
Pressure during pressing, MPa	0,3—0,8	0,3—0,5	0,5—1,2
The optimal thickness of the adhesive layer is mm		0,08— 0,15	0,08—0,15 0,08—0,15

Exposure time of parts after pressing before further processing, h	24—48	20—24	2—4
The cost of the adhesive solution in the product	60—300	60—300	60—300
but-dry calculation, g / m ²		Catch —	
		Hit	3—4 3-6
The viscosity of the adhesive solution at a temperature of 18 .20 ° C on the viscometer VZ-4, with	8±2	8±2	8±2
Viability of the working solution at a temperature of 18 .20 ° C, h		Not lower than the 8th	

Note: When the temperature of the press plates increases to 90 .120 C, the duration of exposure is significantly reduced (up to 5-10 minutes)

Temperature and humidity. For normal working conditions and for high-quality bonding with collagen adhesives, the room temperature should be 18 .25 ° C, and synthetic - 16 .22 C. For casein adhesives, it can be within 16 .25 ° C.

Air humidity in the gluing room should be 50-60%. Exposure before pressing is divided into periods of open and closed impregnation. The open period is understood as the time interval from spreading to the connection of the glued surfaces, and the closed period is the time interval from the connection of the glued surfaces to the creation of pressure. The duration of open and closed leakage depends on the type of adhesive and its concentration, the temperature of the wood, adhesive solution, ambient air and gaskets.

Pressing time and pressure. Pressing is done so that the glued surfaces are tightly adjacent to each other and evenly moistened with an adhesive solution over the entire surface. In addition, under pressure, the adhesive solution penetrates better into the open pores of the wood. Pressing should be carried out before the glue hardens. The duration of exposure in the press depends on the type of glue, the temperature of the plates of the press and the heating rate of the adhesive seam. In some cases, it is 5-10 minutes for synthetic adhesives (when

the adhesive seam is heated to 90-120 ° C), and without heating for all adhesives - 2-6 hours.

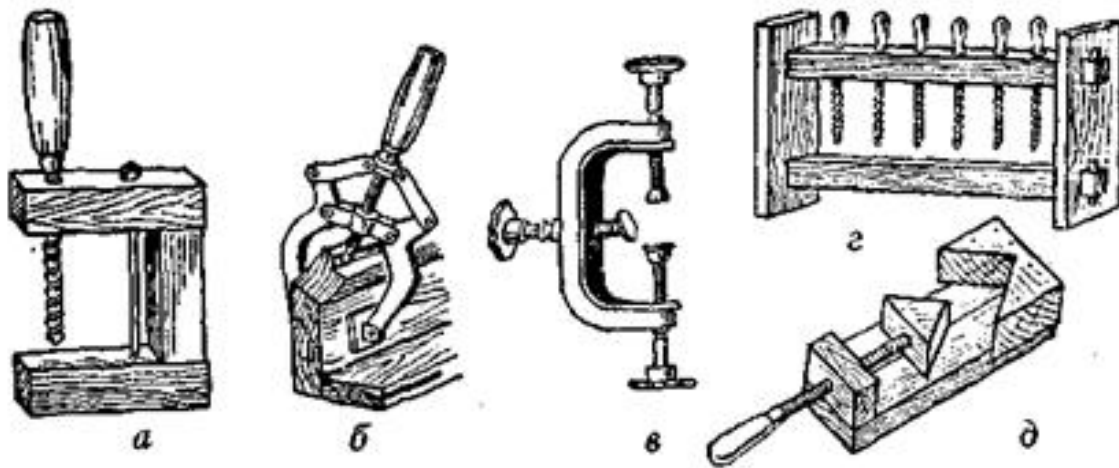


Figure 70 Clamps:

a - ordinary screw, b - lever, c - for edges, d - clamps, d - angular {wooden and metal)

The gluing pressure should be 0.3-1.2 MPa. The holding time after the reprocessing should be at least 24 hours, and for large parts - even 48 hours.

So, since the bonding mode depends on a number of factors, then for each specific batch of glue in the laboratory of the enterprise, the corresponding modes are drawn up (Table 1). The developed modes are hung out at the workplaces of gluing machines or lining workers.

Bonding equipment

For a snug fit of the glued surfaces in the presence of certain equipment or devices, an appropriate pressure is created (0.3-1.2 MPa). Different equipment is used depending on the size and shape of the parts to be glued.

The simplest devices are ordinary wooden and metal clamps of different shapes and designs. The simplest of them are U-shaped, consisting of three bars and a screw. To strengthen them parallel to the middle bar (next to it) put a metal bolt. For compression of the details connecting on "mustache", apply angular clamps wooden or metal. However, when using conventional clamps, a lot of time is spent on screwing and unscrewing, so a number of high-speed clamps have been created.

Simple metal clamps or staples are used for gluing sections of boards to boards. In the weims, the sides of the rails on which the sections of the boards

are placed must be equal and the stops perpendicular to them. At simultaneous pasting of several sites apply the devices which press all planes of sites to rails.

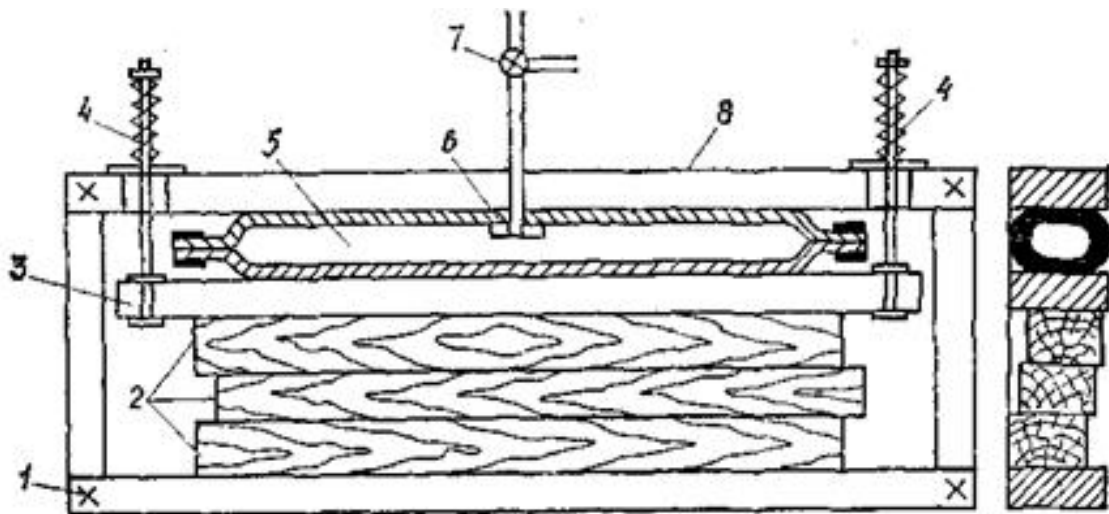


Figure 71 Pneumatic hose press (vaima)

For gluing areas into panels or blocks, it is advantageous to use pneumatic hose presses or clamps, the designs of which can be different and depend on their purpose.

In fig. ... 71. shows a diagram of a hose press for gluing sections of boards into blocks. Between the fixed beam 8 and the movable beam 3, there is a hose 5 made from a segment of a conventional fire hose with tightly wound ends, the hose is connected through a nipple 6 and a tap 7 with a compressed air mesh. In the idle state, the crane is flattened by beams under the pressure of springs 4. Block 2, which is to be glued, is installed between the movable beam 3t of a persistent 1. When filled with compressed air, the hose takes a cylindrical shape and, pushing the beam 3, compresses the adhesive block.

For facing and assembly of units, groups and products, special equipment is used.

Organizational workmanship and technology of safety when gluing

Only for the minds of the correct organization of the workmanship is possible for the mother of high-quality adhesive data. The gluing is necessary for a verstat or on a table of a kind with a flat ditch. Verstat chi stiles are required to change bile vaim or other attachments in the country, as I can put glued dylyans without additional transitions.

On a working misci mae buti:

a sufficient supply of preparation before gluing the parts (if the gluing of the universities is ready, the parts are supplied in full);

a sufficient number of properly prepared glue lines;

necessary attachments for sealing glued universities and applying glue rosters;

necessary cutting and measuring and checking tools for preparing parts for gluing, checking the dimensions and angles of the products to be glued.

The work area must be clean and well lit, the clothes and hands of the gluer worker must be clean. Cleaning materials should be available in the workplace to remove squeezed glue.

For an hour, robots trim the glue in glue sticks with sub-strings and bottom. When glutinous glue is implanted, glue is poured into hot water, synthetic - cold. Glutin and synthetic adhesives are prepared in a galvanized or omeled dish, and casein - in porcelain. Utensils for glue and penzli were fired by the robots in hot water, ale without cute. To see the surplus of resin glue, the dishes are heated to 80 ° C, when I tap on the walls, and the hard glue comes out of it.

The fragmentation temperature in the glue shops is adjusted (20-30 ° C), synthetic glues cause toxic substances, that is, in the cikh shops there is a ventilation pressure. The door to other workshops is required to be closed without opening or extending.

5. OCCUPATIONAL HEALTH AND SAFETY IN EMERGENCIES

5.1 Introduction

Graduation project topic: vertical axis wind turbine. The purpose of the diploma project is to design a wind generator with a capacity of 2 kW, with a vertical turbine, which starts up at a wind speed of 0.5 A and reaches its rated power at a wind speed of 3-4.

Types of work that are carried out to achieve the goal of the diploma project:

analysis of existing analogues as well as some of the proposed technical solutions, selection and analysis of statistical information for the formation of technical specifications;

aerodynamic design and aerodynamic calculation of a system of rotating blades

strength calculation of the blade system;

development of design documentation;

technology and equipment for manufacturing blades.

It is mainly work in CAD / CAM / CAE computer-aided design systems, ie it is mainly computer work. The scope of the projected facility is own production of electricity for household needs, for private houses, cottages, small farms and more. Operating conditions: the presence of constant winds with the required speed (3 - 10), turbulent design wind speed 55, air temperature range from -20 to +50 Co. Dangerous and harmful factors according to GOST 12.0.003 - 74:

Danger when installing a wind turbine;

harmful vibration level;

electrical equipment with voltage and current dangerous to human life is operated;

possible ignition of the mains as a result of a malfunction or emergency operation;

harmful factors for the wind turbine operator when working with a computer;

5.2 Safety Of Wind Turbine Operation.

5.2.1 Safety During Installation Of The Wind Turbine

The height at which the wind turbine is installed is 8 - 10 meters (this height of the wind turbine prevents injuries to people and animals during the operation of the wind turbine), so safety issues during installation work should include labor protection during high-altitude work.

According to clause 1.9 of SNiP. III-4-80 steeplejack work is considered to be work performed at a height of more than 5 m from the surface of the earth on which work is performed directly from structures during their installation or repair, while the main means of protecting workers from falling from a height is a safety belt. The following will be the general provisions on insurance.

To protect against falling from a height when performing climbing work, the following types of insurance are used:

upper loaded insurance;

the top is NOT loaded, rigidly fixed insurance;

lower dynamic insurance (live-performed by the second employee.);

lower insurance with a shock-absorbing device on a safety belt;

self-insurance to construction elements;

insurance to a horizontal, specially stretched safety cable (cable diameter not less than 15 mm).

All these insurances can be used separately or in any combination at the same time. The upper loaded insurance, if used separately, must be double.

upper loaded insurance;

the top is NOT loaded, rigidly fixed insurance;

lower dynamic insurance (live-performed by the second employee.);

lower insurance with a shock-absorbing device on a safety belt;

self-insurance to construction elements;

insurance to a horizontal, specially stretched safety cable (cable diameter not less than 15 mm).

All these insurances can be used separately or in any combination at the same time. The upper loaded insurance, if used separately, must be double.

It is forbidden to work on a single loaded insurance.

In all cases, when moving a worker on the structure, there should be no moments when he remains without insurance. This is ensured by duplication of insurance and self-insurance.

When performing climbing work by rope, the work is carried out directly from the ropes, to which is attached a safety belt with shoulder and leg straps.



Figure 72 Wind Turbine Work Safety

In NPAOP 0.00-5.40-89 the rules of admission to installation works, detailed instructions on labor protection at carrying out climbing works are considered.

Equipment for climbing works must comply with GOST 12.4.087-80 and GOST 12.4.089-86.

5.2.2 Measures To Reduce The Level Of Vibration During Operation Of The Wind Turbine

Various methods are used to combat vibration of machines and equipment and to protect workers from vibration. Vibration control at the source is associated with establishing the causes of mechanical oscillations and their elimination, such as replacement of crank mechanisms evenly rotating, careful selection of gears, balancing rotating masses, etc. (these factors will be taken into account during design). To reduce vibration, the effect of vibration damping is widely used - the conversion of energy of mechanical vibrations into other types of energy, most often into thermal energy. To this end, in the design of parts through which vibration is transmitted, materials with high internal friction are used: special alloys, plastics, rubber, vibration-damping coating. To prevent general vibration, use the installation of vibrating machines and equipment on independent vibration damping foundations. To reduce the transmission of vibration from its sources to the floor, workplace, seat, handle, etc. widely used methods of vibration isolation. To do this, in the path of vibration propagation, an additional elastic bond is introduced in the form of vibration isolators made of rubber, cork, felt, asbestos, and steel springs.

Rubber vibration isolators are sufficient to protect against vibration during the operation of the wind turbine, which occurs in the gearbox. In addition, the wind turbine operator is not constantly in its area of operation. This means that it is protected from the negative effects of vibration by time (time) and distance.

5.2.3 Measures To Ensure Electrical Safety During Operation Of The Wind Turbine

The wind generator generates electricity, and then with the help of an inverter generates an electric industrial electric current (220V, 50 Hz), then one of the factors of operational safety will be electrical safety.

According to GOST 12.038 - 82 the allowable value of the contact voltage and current flowing through the human body in the normal mode of operation of the electrical installation:

Table 5.1. Maximum Allowable Values Of Contact Voltages And Currents

Type of current	U, B	I, mA
Variable, 50 Hz	not more:	
	2,0	0,3

Constant	8,0	1,0
----------	-----	-----

In this electrical installation, the contact voltage is 220V, so we conclude that in the event of an electric shock, a person may receive an electric shock. Therefore, it is necessary to consider the electrical safety equipment that will be used.

The main means and measures against electric shock are: organizational, technical and electrical protection.

Technical means and measures that are implemented in the design of the wind turbine in the process of its development, manufacture and installation. These include: protective grounding, insulation of live parts, unavailability of live parts.

Protective earthing is a deliberate electrical connection to earth or its equivalent of non-conductive metal parts of electrical installations that may be live (GOST 12.1.009 - 76). The equivalent of land can be river water or sea, coal and more.

Protective grounding is used in electrical networks up to 1000V with isolated neutral:

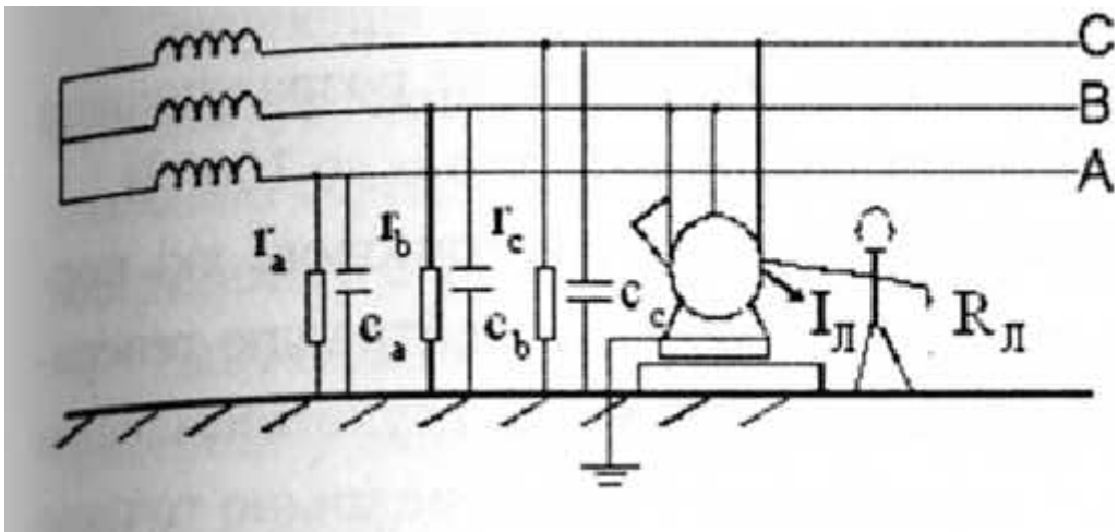


Figure 73 Grounding scheme of three-phase network with voltage up to 1000V.

Grounding is used to eliminate the risk of electric shock to the hull or other metal normally non-conductive parts of wind turbines, which are energized relative to the ground in case of short circuit to the hull or for other reasons (emergency operation, in this case, operation of wind turbine during

strong wind from 20 to 55). Principle of operation - is to reduce to safe values of step and contact voltage during short circuit to the body of the electrical installation.

Insulation of conductive parts is one of the main means of protection. It is working, additional, reinforced, double. During the development of electrical installations, the insulation resistance is taken as 1 kO / V. The insulation resistance for contactor coils, magnetic starters, switchgear, switchboards-conductors and lighting installations must be at least 0.5 MO, for switches and disconnectors - 1 Mm.

Inaccessibility of uninsulated conductive parts of electrical installations is achieved by placing them at an unattainable height, the use of shields, housings, casings, shells, cabinets, special chambers, hidden networks, stationary and portable solid or mesh fences.

All of the above protection will be taken into account when designing a wind turbine with a vertical axis, because the main causes of electric shock during operation of such installations are short circuits to the generator or inverter housing, these safety measures are sufficient for safe operation.

The turbine of the wind generator is at a height of 8 -10 meters, which increases the likelihood of lightning and ignition of the installation, so lightning protection will be considered.

5.2.4 Protection Of The Wind Generator From Lightning Strikes

Lightning is an electric discharge in the atmosphere, which is characterized by currents of hundreds of thousands of amperes, voltages of hundreds of thousands of kilovolts, temperatures of tens of thousands of degrees Celsius. There are primary and secondary manifestations of lightning. The primary include: electrical, thermal, electromagnetic, mechanical action. The secondary ones are electrostatic and electromagnetic induction and application of high potentials to the equipment located in buildings and structures, due to the external metal structures connected to them. Lightning strips are protected by lightning rods, which include a lightning rod, support, current collector and grounding device. They can be rod, cable, mesh or combined. To protect the wind turbine, a rod lightning rod must be used, which will be located at the top of the axis of rotation of the wind turbine, where the current collector will be the turbine shaft, which is grounded.

If multiple wind turbines are used, electrostatic and electromagnetic induction protection should be considered in the event of a lightning strike.

Protection against electrostatic induction must be performed by connecting all metal equipment and apparatus of the protected structure to a special grounding conductor for protection against electrostatic induction. Sequential inclusion of grounded elements in one circuit is not allowed.

It is recommended to place the earthing switch of protection against electrostatic induction on a contour of the protected construction. It is also allowed to place the grounding conductor in the trench at a depth of at least 0.8 m and at a distance of 0.8-1 m from the foundation. The magnitude of the current resistance of the grounding conductor laid along the contour of the building or structure, 10 Ohms. When installing such grounding conductors in separate cells, their total resistance to the spread of current of industrial frequency should not exceed 10 Ohms.

Underground protection of underground metal communications (water supply, sewerage, etc.) is allowed to the grounding of protection against electrostatic induction.

To protect against electromagnetic induction, it is necessary to weld or solder metal jumpers between pipelines and other long metal objects (frame of the structure, cable sheaths, etc.) at their distance of 10 cm or less every 20 m of length to prevent the formation open circuits.

5.2.5 Ensuring Fire Safety During Operation Of The Wind Turbine

The main causes of fire during the operation of electric wind turbines: short circuit, current overload, unsatisfactory condition of electrical equipment and appliances, violation of the rules of their installation and operation, atmospheric electricity discharges.

The wind turbine will be made of materials that operate at a temperature of 800 Co and above. The wind turbine is operated at temperatures below the ignition temperature, but the following combustible materials are used in the design of the wind turbine: insulation of live parts and paint, so its fire is likely.

If the installation is used in the home, you can use fire alarms to create fire extinguishing conditions, and fire extinguishers used to extinguish live networks.

As a fire alarm, you can use an automatic smoke detector, which responds to a certain concentration of aerosol products formed during combustion.

As a means of extinguishing a fire, it is advisable to use powder fire extinguishers, because powders differ from other fire extinguishers by high fire

extinguishing ability and versatility. They are used to stop the combustion of various solids, flammable liquids, gases, metals, live electrical installations.

If the wind turbine is used in small businesses, such as livestock farms, automatic fire extinguishers should be added to the above, and personnel should be instructed in the event of a fire.

5.2.6 Hazards That May Occur Under The Influence Of Meteorological Environmental Conditions

strong wind with a speed of 20 - 55 m / s;

thunderstorm (threat of lightning, safety measures discussed above);

fire (wind generator is mainly located in the steppe, where a fire is likely during the dry season);

possible icing of the blades at low temperatures (-15... -20°C).

Protection against these factors is provided by the design: the turbine is installed at a height of 8 - 10 meters on a steel support, or on the roof of buildings, which protects against fire.

Strong winds or icing can destroy parts or the structure as a whole, which can result in personal or animal injury, as additional protection can be used with a mesh fence that restricts access to the danger zone.

5.3. Characteristics Of Air And Meteorological Conditions

5.3.1 Characteristics Of Air And Meteorological Conditions In The Working Area Of The Project Developer, As A Factor That Determines The Choice Of Methods And Means Of Their Normalization

Work area - a room with a computer and VDT. The area of the working area of the project developer is 16m². The air of the working area is characterized by the following parameters:

- microclimate;
- dustiness;
- gassiness;
- ionization.

There is one computer operator's workstation in the work area, so it is necessary to consider protection against dust and air pollution and harmful levels of ionized air, and determine the optimal values of meteorological parameters.

Basically, meteorological parameters that affect performance are air temperature, air velocity (important because the speed of air movement depends on the rate of heat exchange with the environment) and humidity.

Therefore, to exclude the negative impact of meteorological factors, it is necessary to measure them and determine how to normalize for the comfortable operation of the computer operator. Measurements were performed at a height of 1 m from the floor, in four different places. Temperature, humidity, air velocity in warm and cold seasons were measured and are 30 °C, 70%, 0.2 m/s and 10 °C, 70%, 0.2m/s, respectively.

To determine the optimal characteristics of air and meteorological conditions, it is necessary to determine the category of work. Lightweight physical work (1a) includes work that is performed while sitting and does not require physical exertion, or work (1b) that is performed while sitting, standing, and that involves walking.

Measures to normalize the meteorological characteristics of the air in the work area: the use of natural and artificial general ventilation, the use of air conditioning with individual regulation of temperature, relative humidity and volume of air supplied, heat supply to the room through the water heating system in the cold season .

Laboratory analytical gas analyzers, express methods using indicator tubes and automatic gas analyzers can be used to determine gassiness, ionization of air and amount of dust in the air, but this is impractical for this case, as there is only one computer, and therefore to protect against these negative natural and artificial ventilation will suffice.

5.3.2 Determining The Category Of Visual Work Of The Computer User, Choosing The Optimal Distance From The Computer To The User's Eyes

Table 5.2. Appendix B, the dependence of the category of visual work on the ratio of the size of the object to the distance to it

The category of visual works	he limits of the d / l ratio
I	ess than $0.3 \cdot 10^{-3}$

II	from $0.3 \cdot 10^{-3}$ to $0.6 \cdot 10^{-3}$
III	st. $0.6 \cdot 10^{-3}$ to $1 \cdot 10^{-3}$
IV	st. $1 \cdot 10^{-3}$ to $2 \cdot 10^{-3}$
V	st. $2 \cdot 10^{-3}$ to 10^{-2}
VI	st. 10^{-2}

d-size of the object of distinction, l is the distance from the screen to the eyes.

$$d/l = 10^{-2}, d = 5\text{mm}, \text{whence } l = 500\text{mm}$$

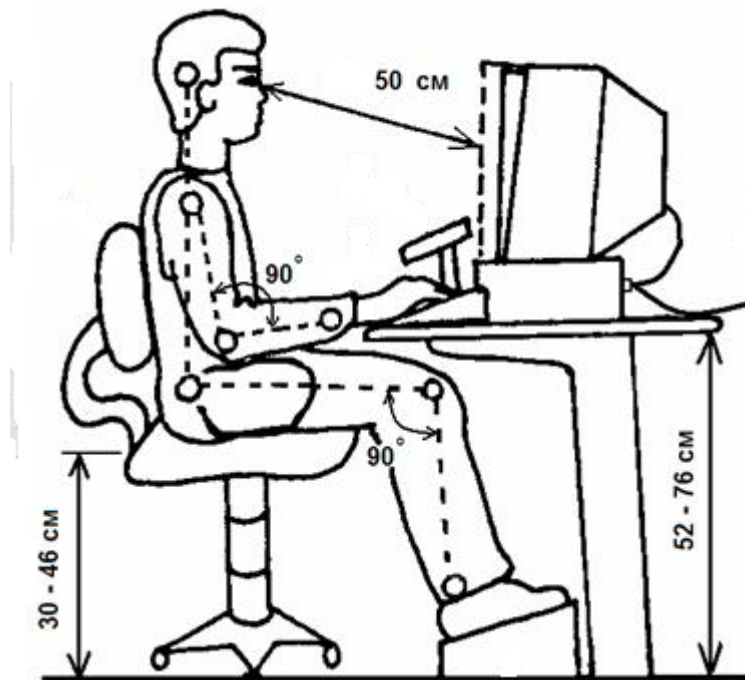


Figure 74 computer user positions

5.4. Conclusion

Potentially dangerous and harmful production factors that can occur during the operation of the wind turbine and can endanger human health and life have been identified.

An analysis of these factors was carried out, and in accordance with the regulations on labor protection, measures to neutralize dangerous factors were proposed. These measures are a number of technical solutions that will be taken into account when designing a product.